PL-TR-96-2023
Environmental Research Papers, No. 1184

THE AN/FPS-118 OTH RADAR:
Chapter 5, OTH Handbook

B.S. Dandekar
J. Buchau

11 January 1996

19980102 167

APPROVED FOR PUBLIC RELEASE; DISTRIBUTION UNLIMITED.

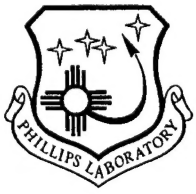

PHILLIPS LABORATORY
Directorate of Geophysics
AIR FORCE MATERIEL COMMAND
HANSCOM AIR FORCE BASE, MA 01731-3010

DTIC QUALITY INSPECTED 4

"This technical report has been reviewed and is approved for publication."

Maj Edward Berghorn, Chief
Ionospheric Application Branch

WILLIAM K. VICKERY, Director
Ionospheric Effects Division

This report has been reviewed by the ESC Public Affairs Office (PA) and is releasable to the National Technical Information Service (NTIS).

Qualified requestors may obtain additional copies from the Defense Technical Information Center (DTIC). All others should apply to the National Technical Information Service (NTIS).

If your address has changed, or if you wish to be removed from the mailing list, or if the addressee is no longer employed by your organization, please notify PL/TSI, 29 Randolph Road, Hanscom AFB, MA 01731-3010. This will assist us in maintaining a current mailing list.

Do not return copies of this report unless contractual obligations or notices on a specific document requires that it be returned.

REPORT DOCUMENTATION PAGE

Form Approved
OMB No. 0704-0188

Public reporting burden for this collection of information is estimated to average 1 hour per response, including the time for reviewing instructions, searching existing data sources, gathering and maintaining the data needed, and completing and reviewing the collection of information. Send comments regarding this burden estimate or any other aspect of this collection of information, including suggestions for reducing this burden, to Washington Headquarters Services, Directorate for Information Operations and Reports, 1215 Jefferson Davis Highway, Suite 1204, Arlington, VA 22202-4302, and to the Office of Management and Budget, Paperwork Reduction Project (0704-0188), Washington, DC 20503.

1. AGENCY USE ONLY *(Leave blank)*	2. REPORT DATE	3. REPORT TYPE AND DATES COVERED
	11 January 1996	Scientific Interim

4. TITLE AND SUBTITLE

The AN/FPS-118 OTH Radar: Chapter 5, OTH Handbook

5. FUNDING NUMBERS

PE 62101F
Pr 4643
TA GH WU01

6. AUTHOR(S)

B. S. Dandekar and J. Buchau

7. PERFORMING ORGANIZATION NAME(S) AND ADDRESS(ES)

Phillips Laboratory (GPIA)
29 Randolph Road
Hancsom AFB, MA 01731-3010

8. PERFORMING ORGANIZATION REPORT NUMBER

PL-TR-96-2023
ERP, No 1184

9. SPONSORING/MONITORING AGENCY NAME(S) AND ADDRESS(ES)

10. SPONSORING/MONITORING AGENCY REPORT NUMBER

11. SUPPLEMENTARY NOTES

This report will be of interest to Air Weather Service and the OTH radar controllers for prediction/ specification of ionospheric models, and to OTH radar operators for the description of AN/FPS-118.

12a. DISTRIBUTION/AVAILABILITY STATEMENT

Approved for Public release;
Distribution Unlimited

12b. DISTRIBUTION CODE

13. ABSTRACT *(Maximum 200 words)*

This report familiarizes the radar operators with the radar features used in the daily operation of the radar. These consist of the radar layout, its sector-segment arrangement, the barrier and interrogation beams, the ionospheric model residing in the radar system, and various displays available in the important missions of Correlation and Identification, and Detection and Tracking of the targets in the coverage illuminated by the radar.

14. SUBJECT TERMS

Ionospheric model, OTH radar operation;
OTH radar description

15. NUMBER OF PAGES

106

16. PRICE CODE

17. SECURITY CLASSIFICATION OF REPORT	18. SECURITY CLASSIFICATION OF THIS PAGE	19. SECURITY CLASSIFICATION OF ABSTRACT	20. LIMITATION OF ABSTRACT
Unclassified	Unclassified	Unclassified	SAR

Contents

1. INTRODUCTION 1

2. RADAR STRUCTURE 3

2.1 The East Coast Radar System (ECRS) 7
2.2 The AN/FPS-118 Radar's Segment/Sector/Beam Structure 7

3. RADAR OPERATION 12

3.1 The Barrier Sectors 12
3.2 The Interrogate Sectors 14
3.3 Environmental Assessment Support Sectors (SIR, SQR, SIS, SIM, SQS) 15

4. GEOPHYSICAL ENVIRONMENT OF THE CONUS OTH RADARS 16

4.1 East Coast Radar System 17
4.2 West Coast Radar System 21

5. THE ENVIRONMENTAL ASSESSMENT FUNCTION 24

5.1 Introduction 24
5.2 EA Tools and Procedures 25
5.2.1 The Backscatter Sounder and Frequency Management 25
5.2.2 Assessment of Radar Performance 30
5.2.3 Vertical Incidence Sounding 36
5.3 Coordinate Registration 39
5.3.1 Introduction 39
5.3.2 Background: Necessity of an Ionospheric Model 40
5.3.2.1 Oblique Ray Path 40
5.3.2.2 Vertical Incidence Ionogram 42
5.3.2.3 The Ionospheric Parameters 44
5.3.2.4 Skip Distance and Range 46
5.3.2.5 Variability of the Ionosphere 48
5.3.2.6 Using Backscatter Ionograms 51
5.3.2.7 Radar Operation Frequency Using Overlays on Ionogram 54
5.3.3 The AN/FPS-118 Ionospheric Model 54

Preceding Page Blank

6. THE RADAR CONTROL FUNCTION 62

6.1 Frequency Selection 62
6.2 Tools and Procedures 63

7. THE DETECTION AND TRACKING (DT) FUNCTION 68

7.1 Overview 68
7.2 Signal Processor (SP) 76
7.3 Peak Association 78
7.4 Initiation, Maintenance, and Termination of Tracks 79
7.5 Other DT Functions 82
7.6 Track Definitions 82

8. CORRELATION-IDENTIFICATION 84

References 90

Bibliography 92

Illustrations

1. Coverage Areas of ECRS and WCRS with locations of DISS stations in their vicinity. 5
2. ECRS coverage area with segment (1-3), sector (1-8),and beam (B-barrier, I-interrogate) structures. Segment 1 shows a uniform barrier, Segment 2 shows steps-like barrier with superposition of Interrogate beams, Segment 3 shows a deeper barrier. 8
3 Aerial view of the ECRS receiver site at Columbia Falls, ME; Segment 1-North EOS is on the left, Segment 3-South EOS is in the center and Segment 2-EOS is on the far right. 9
4. Aerial view of the ECRS transmitter site at Moscow, ME; Segment 3-South EOS is in the foreground, Segment 1-North EOS is on Moxie Mountain seen to the left of the center at the top, and Segment 2-EOS is behind the mountain. The large antenna structures are barely visible as small white lines in Segment 1. 11
5. ECRS coverage area of various beams in a geographic coordinate system. 18
6. The back lobes of the ECRS coverage area of various beams in a geographic system of coordinates. 20
7. WCRS coverage area of various beams in a geographic coordinate system. 22
8. The back lobes of the WCRS coverage area of various beams a in geographic system of coordinates. 23
9. Sounder control Menu (for producing Backscatter Ionograms). 27
10. 2000 nmi range Backscatter Ionogram. 28
11. 2000 nmi range Backscatter Ionogram showing the manually traced leading edge of the ground scatter and the location of the barrier B162 for a radar operating at a frequency of 19.2 MHz. 29
12. Menu of clear channel list versus bandwidth for selection of the radar operation frequency. 31
13. 2000 nmi range Backscatter Ionogram showing the manually traced leading edges of different reflection modes, and the locations of the interrogate I32 and the barrier B362 with selected radar operating frequencies of 17.9 and 22.7 MHz respectively. 32

14. Sector amplitude -Range plot of the clutter signal: the top is for WBW=10 kHz and the bottom for WBW= 5 kHz. Note that number of clutter peaks is proportional to WBW. 33
15. Graphical presentation of clutter and noise versus range for Sector Illumination Routine (SIR) and Sector Quiet Routine (SQR). 35
16. Quantitative plot of Normalized Clutter to Noise Ratio (NCNR) for segment 1 of ECRS for all 8 sectors showing acceptable radar performance. 37
17. Quantitative plot of Normalized Clutter to Noise Ratio (NCNR) for segment 3 of ECRS for all 8 sectors showing degraded radar performance due to equatorial clutter. 38
18. Geometry of the oblique Ray path. 41
19. Vertical Incidence Ionogram , Ionospheric Layer Parameters (IONOS) and Observed Virtual Height (IONHT) codes from DISS system at Bermuda. 43
20. Ionospheric Layers 45
21. Ionospheric Raytracing 47
22. Monthly Median contours of f_oF_2 for low sunspot activity (SSN=14) for Goose Bay. 49
23. Monthly Median contours of f_oF_2 for high sunspot activity (SSN=160) for Goose Bay. 50
24. Percent increase in f_oF_2 during morning hours for low sunspot activity. 52
25. Percent increase in f_oF_2 during morning hours for high sunspot activity. 53
26. Range frequency overlay on vertical incidence ionogram for estimating best elevation angle for the selected barrier distance from the transmitter. 55
27. High latitude auroral and trough features and their effect on ionospheric spread. 57
28. f_oF_2 map for the ECRS coverage area. 61
29. Radar Control, Status, and Environmental assessment Functional Flow Diagram. 64
30. Radar Control Functional Flow Diagram. 65
31. Clear Channel Selection Functional Flow Diagram. 66
32. Console assignment List Display Selection. 67
33. Simplified Block diagram of Detection and Tracking Function. 69
34. Example of a Single Amplitude-Range-Doppler Display. 71

35. Example of a Three-Beam Range-time Display. 73
36. Example of an Amplitude analysis Display. 75
37. Example of a Three-Beam Doppler-Time Display. 77
38. Simplified Block diagram of Procedure for Initiating, Maintaining and Terminating Tracks. 81
39. Simplified Block Diagram of the Correlation and Identification Function. 85
40. Example of CI Operator's Three-Beam Range-Time Display. 87
41. Example of CI operator's Single-Beam Range-time Display. 89

Tables

1. Location and Geographic Coordinates of the ECRS and WCRS. 6
2. VI Update Sites for East Coast Radar System (ECRS). 62

Acknowledgments

The authors thank Major Edward Berghorn for his valuable comments and interest in the work. The authors also thank Major Azzarelli and Mr. Carl Bowser (Martin Marietta) for their valuable comments, and especially Dr. J. Leon Poirier for his tremendous help for the sections on Detection and Tracking and Correlation and Identification in this report.

Preface

This report provides the radar operators with a description of the radar, its layout, its operating environment with respect to ionospheric phenomena, the ionospheric model residing in the radar system, Detection and Tracking and the various displays that are available to aid the operators in operating the radar.

We have made an effort to include most of the display features very commonly encountered in the OTH operation. However the use of this information, may show that there is a need 1) to include additional radar features and 2) provide more clarification of some features already discussed here. Therefore we would encourage a feedback and /or comments. Please feel free to contact:

Dr. B. S. Dandekar
Phillips Laboratory /GPIA
29 Randolph Road
Hanscom AFB, MA 01731-3010.

With the deployment of the OTH radars, the OTH community recognized a need for an OTH Handbook that would provide a basic understanding of the OTH operation, the general layout of the radar structure, and the basic geophysics background. With the help of the OTH community, Jurgen Buchau took the lead and accepted the responsibility for producing the OTH Handbook. The planned handbook has six chapters. These are 1) Introduction, 2) OTH Radar System: System Summary, 3) Physics of the Ionosphere for the OTH Operation, 4) High Frequency (HF) Radiowave Propagation, 5)The OTH Radar Operation and 6) Glossary for OTH Radars. Chapters 2 and 4 have been published by Dr. Gary Sales as technical reports (see reference). Chapters 3 and 6 of this handbook have been published by Dr. Balkrishna S. Dandekar and Jurgen Buchau. This report forms the fifth chapter of the OTH handbook.

The AN/FPS-118 OTH Radar
Chapter 5, OTH Handbook

1. INTRODUCTION

Several published reports (G. Sales PL-TR-92-2123 and 2124, Dandekar and Buchau PL-TR-95-2127, Dandekar et al PL-TR-95-2149) have provided the information necessary to understand the operation of an Over-the-Horizon Backscatter (OTH) radar, discussing the basic concepts on which the design of the US OTH radars is based. Emphasis is placed on the structure and controlling factors of the ionosphere, which through its refractive properties provides the basis of OTH radar operation. The discussion of the complex issue of HF radio propagation in the ionosphere provides an understanding of how the operational frequency and the related radar parameters are selected, and how to derive the target ground coordinates from the radar measurements (radar range and radar azimuth). The report on radio propagation (G. Sales PL-TR-92-2123) also explained the generation and application of the radar's most important frequency management tool, the backscatter ionogram.

The following sections describe the operation of the AN/FPS-118 Ionospheric model[1], drawing on the previously introduced concepts and material in reports mentioned above. Section 2 discusses the sector-beam structure of the individual 60° radar segment, and the deployment of two 180° coverage radars, consisting of three 60° segments each, at the East and West coasts. Section 3 provides an overview on the use of the eleven surveillance sectors available in each segment to form a barrier and to support interrogation requirements. The specific geophysical environment of the two radars is addressed in Section 4.

Received for publication 21 December 1995

Drawing heavily on the displays available to the radar operator, Sections 5 to 8 then provide a general description of the full radar process, which makes it possible to identify targets/aircraft observed in the barrier or in the active interrogate sectors. The close interaction of the Environmental Assessment (EA) and Radar Control (RC) operators with the Detection and Tracking (DT) and Correlation and Identification (CI, called Track Correlation (TC) by the Air Force operators) required for successful operation of the radar is also described.

Proper operation of the radar is a complex task, primarily due to the dynamic nature of the ionosphere, which must be considered as an essential and at times unreliable component of the radar. The initial step in the operation of the radar is therefore the assessment of the state of the ionosphere by the EA operators, resulting in the automated selection of nominal frequency bands, which will provide the required coverage. A second essential input provided by the EA operators is the reflection height or Coordinate Registration (CR) tables required to convert radar range/azimuth into ground coordinates.

To deal with the complexities of the propagation, clutter, and noise environment the Radar Control (RC) function is equipped with a spectrum analyzer, a large range of displays of the radar data, and a high degree of flexibility in selecting radar operating frequencies, Waveform Repetition Frequencies (WRF), Coherent and noncoherent Integration Times (CIT, NCIT), and Waveform Bandwidth (WBW). The rationale for choosing a specific set will be discussed. The desired end result of the EA - RC cooperation is the illumination of the barrier or of an interrogate sector with an operating frequency that provides sufficient signal to noise over a barrier wide enough (beam selection) and deep enough (operating frequency selection) to detect and track aircraft.

With the selected set of radar controlling instructions, the radar is operated and radar data are processed. The radar data are displayed at the Detection and Tracking (DT) consoles, where time histories of radar data including the target returns are automatically or manually joined into tracks. The track data are then displayed at the co-located Correlation and Identification (CI) consoles, where they are compared to the air traffic flight plans and actual flight route data provided by the Federal Aviation Agency (FAA) and the Oceanic Control and Air Route Traffic

Control centers (ARTCC). The desired end result of the CI process is to associate and identify the observed tracks with planned flight tracks. The result of this association process is correlated or OTH -uncorrelated tracks.

Constant interaction between the Correlation and Identification (CI), Detection and Tracking (DT), Radar Control (RC) and Environmental Assessment (EA) functions is required to adjust the radar parameters to the continually changing ionospheric and noise environment and thereby optimize radar performance. Feedback from DT and CI are especially important to alert EA and RC of problems with Coordinate Registration (CR), and deteriorating radar performance, and to initiate corrective actions.

Finally Sections 7 and 8 outline how the various sets of radar data are used to assess the current performance of the radar in terms of actual or inferred Probability of Track Establishment (or Probability of Detection). This information and the unconfirmed aircraft tracks are reported to the North American Air Defense Command (NORAD) in Cheyenne Mountain, as an input to determining the national air defense situation.

2. RADAR STRUCTURE

The Air Force OTH Backscatter Radar System, the AN/FPS-118, was designed, built and delivered by the General Electric Company based on specifications developed by the US Air Force. All major concepts had been tested in 1980-81 with the Experimental Radar System (ERS), which also had been built by General Electric Company. The ERS had been deployed and operated with transmit facilities at Moscow, ME and receive and operations facilities at Columbia Falls, ME, at the same locations as the transmit and receive sites of the current East Coast Radar System (ECRS). Using the same general design as the AN/FPS-118 Radar, the prototype ERS provided the coverage as Segment 1 of the ECRS. The Design Test and Evaluation (DT&E) of the ECRS AN/FPS-118 Radar took place in the fall and winter of 1989-1990, with delivery of the ECRS to the Air Force by the spring of 1990.

The basic unit of the AN/FPS-118 Radar is an OTH radar providing coverage over 60° in azimuth and 2000 nmi in ground range. The coverage area of a basic unit is called a segment.

Two radar systems have been delivered to the Air Force, each consisting of three basic AN/FPS-118 Radar units, and providing 180° coverage at the East coast (ECRS) and the West coast (WCRS) respectively. The coverage of these two radars is shown in Figure 1. The ECRS provides a surveillance capability for the central and western North Atlantic and the Eastern Caribbean Sea, while the WCRS covers the Eastern Pacific from Alaska to off the coast of Mexico. The segments for each radar are numbered Segments 1, 2, and 3 in clockwise sequence. Shown in addition to the nominal radar coverage are the locations of the Air Weather Service Digital Ionospheric Sounding System (DISS) net, which support the radar operations and which will be discussed in Section 4 (The EA Function).

(By directive of the Secretary of the Air Force, the WCRS has been mothballed as of 1 July 1991, and the ECRS is being operated on a limited operations schedule, providing coverage in one segment per day (8 hour operation) for 40 hours or five days per week. The operations of the ECRS were planned to be shifted from a military to a contract effort on 1 October 1992 but have not yet been shifted.)

As discussed later in Section 2, the transmit and receive antennas of an FM/CW radar have to be separated to prevent the transmit signal from saturating the receivers and thereby disabling the radar. Since large areas of land are required for both the transmit and receive arrays, both systems have deployed these facilities in rather remote locations, and near the coastal lines, for which they are to provide air approach surveillance. The operations centers have been located in the general area of the radar's deployment, at US Air Force bases most suitable for the housing and general support of the operations personnel and their families, since they do not have to be co-located with either of these facilities, and since they require substantial numbers of personnel for their operations. The following table provides the site names, the geographic co-ordinates, and relevant distances for the two radars.

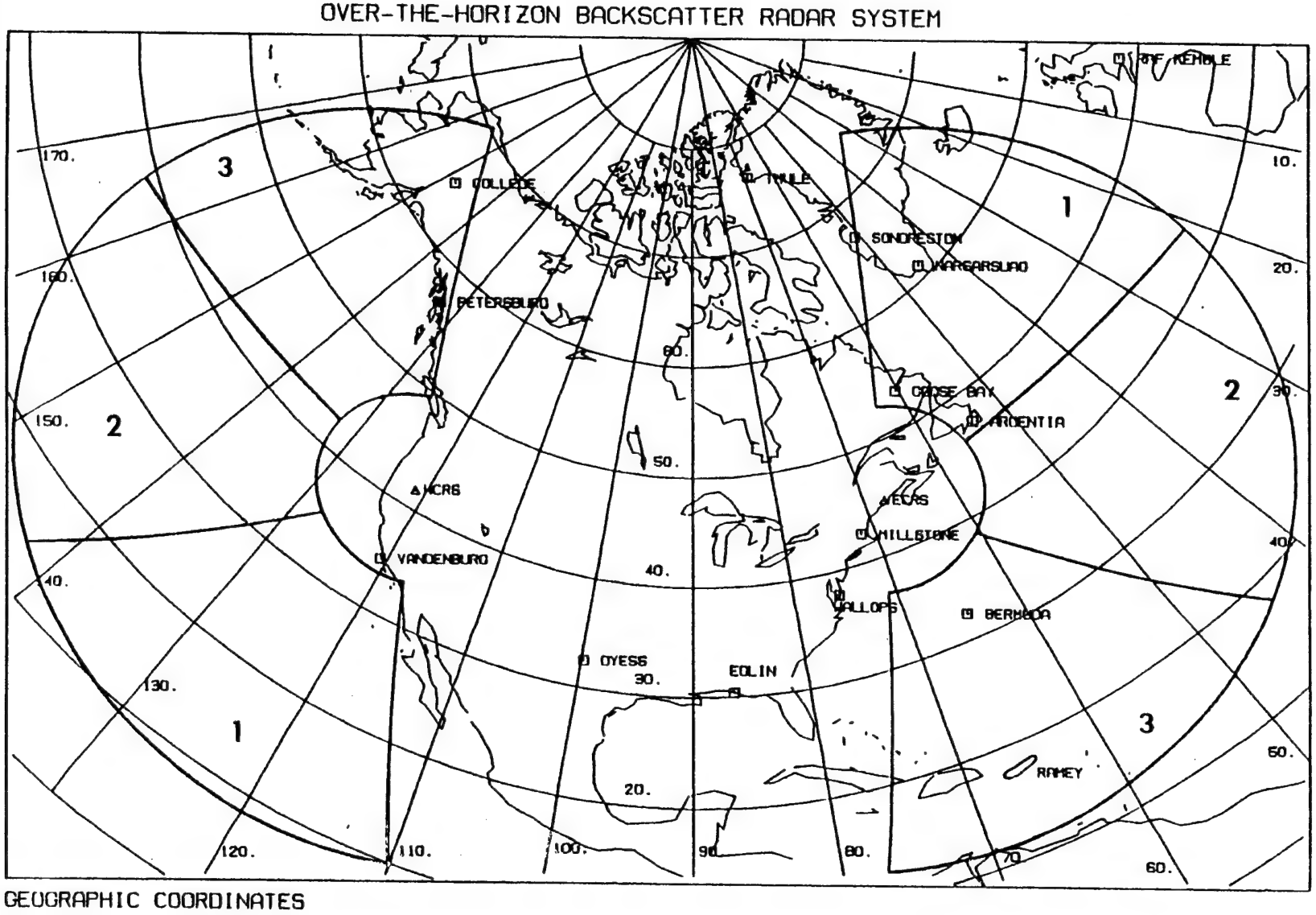

Figure 1. Coverage Areas of ECRS and WCRS with locations of DISS stations in their vicinity.

Table 1

Locations and Geographic Co-ordinates of the ECRS and WCRS

East Coast Radar System

Facility	Location	Latitude N	Longitude W	Distance (to Ops Ctr)
Operations	Bangor, ME	44° 48'	68° 50'	
Transmit	Moscow, ME	45° 09'	69° 51'	48.1 nmi
Receive	Columbia Falls, ME	44° 48'	67° 48'	43.9 nmi
Distance transmit to receive site				91.9 nmi.

West Coast Radar System

Facility	Location	Latitude N	Longitude W	Distance (to Ops Ctr)
Operations	Mountain Home, ID	43° 03'	115° 52'	
Transmit	Rimrock Lake, OR	41° 42'	121° 10'	248.6 nmi
Receive	Buffalo Flat, CA	43° 17'	120° 22'	197.5 nmi
Distance transmit to receive site				101.2 nmi

Since all segments of the two AN/FPS-118 Radars as well as their method of operations are identical, we will discuss the details of the radar lay-out and of the operations using the ECRS as the example. Differences are typically related to the geographic location and especially the geophysical/ionospheric environment, and will be discussed in section 3 (Geophysical Environment of the AN/FPS-118 Radars).

2.1 The East Coast Radar System (ECRS)

Three transmit facilities and transmit antenna arrays are located at Moscow ME, while three receive facilities and receive antenna arrays are located in the blueberry fields of eastern Maine near Columbia Falls. The ECRS Operations Center at the Bangor Air National Guard Base (ANGB) at Bangor ME provides surveillance from three arrays of the air routes to and from the East Coast of the United States from Labrador to beyond Puerto Rico.

Figure 2 shows the coverage of the ECRS on a geographic map. The ECRS consists of three basic component radars, which provide coverage, in three 60° segments, for a full 180°. The radar coverage starts at a ground range of 500 nmi and extends out to 2000 nmi ground range (Note that range of ECRS has been extended to 3000 nmi at all azimuths since March 1993). In its current configuration the AN/FPS-118 Radar cannot process radar/target data from inside 500 nmi or from longer (unambiguous) ranges than 2000 nmi, even if propagation conditions would provide for adequate performance at these distances. (We will show in Section 5, how using a radar property called range folding, the AN/FPS-118 Radar under favorable propagation conditions can be used to detect and to some extent even track aircraft at ranges beyond the basic 1800 nmi limit. Track correlation however cannot be performed beyond the primary 3000 nmi range). Note that in Figure 2 the coverage range is 2000 nmi. The automatic track mode is from 500-3000 nmi.

2.2 The AN/FPS-118 Radar's Segment/Sector/Beam Structure

Segment 1 of the ECRS, on a boresight (central azimuth of the segment coverage) of 46.5° (True or East of North), covers the azimuth range from 16.5° to 76.5°, Segment 2, on a boresight of 106.5°, covers from 76.5° to 136.5° and Segment 3, on a boresight of 166.5°, covers from 136.5° to 196.5°. The digital beam formers form the required transmit and receive beams over an azimuth range of ± 30° from the boresight of the respective segment (Note that ECRS was electronically rotated by 15° in 1993 so that the coverage now is 31.5° to 211.5°). Figures 3 and 4 show aerial views of the receive and transmit sites, respectively.

In Figure 3 the view of the ECRS receive site located at Columbia Falls, ME, looks to the southeast in the general direction of the ocean. The segment 1, North East Operating Sector

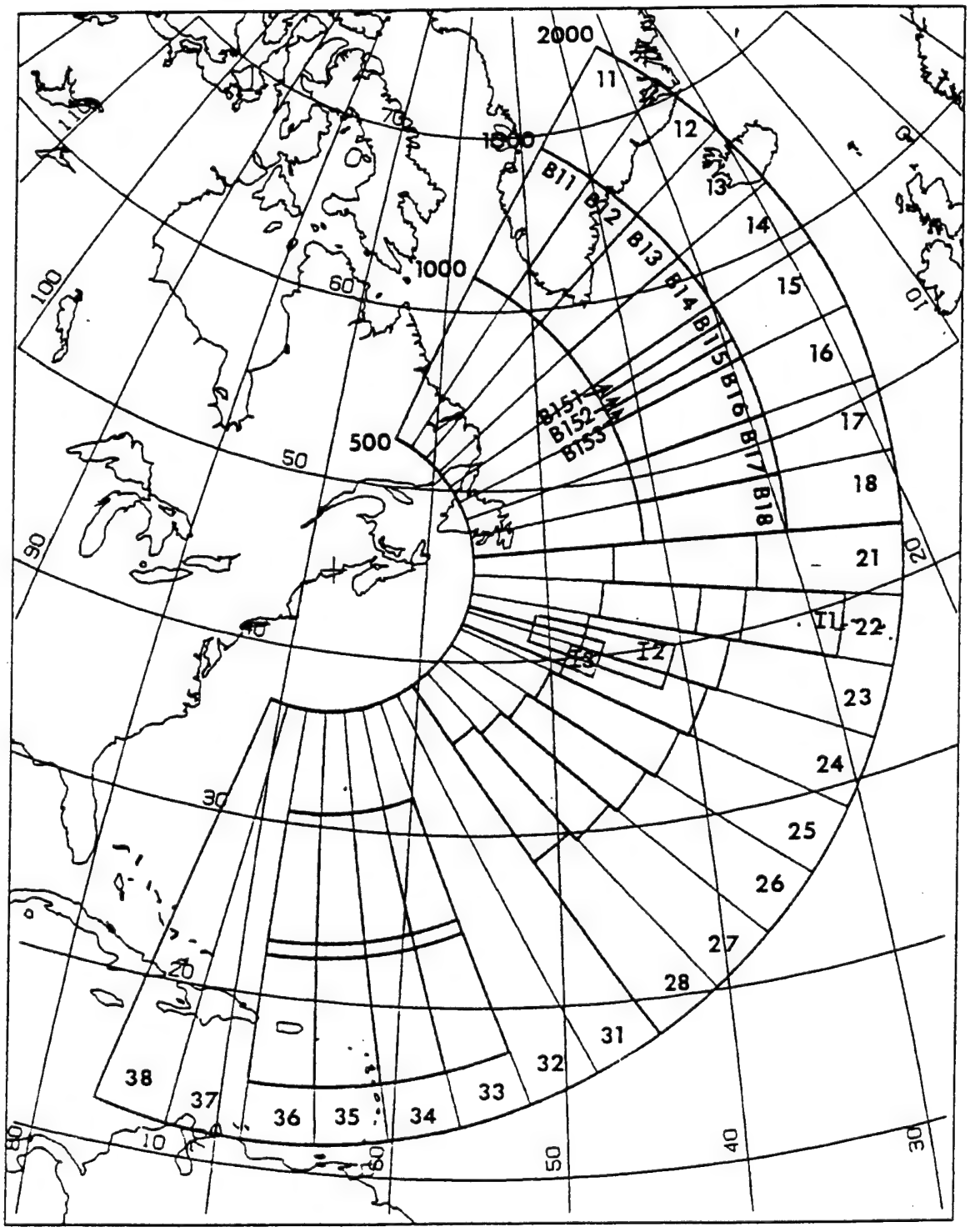

Figure 2. ECRS coverage area with segment (1-3), sector (1-8),and beam (B-barrier, I-interrogate) structures. Segment 1 shows uniform barrier, Segment 2 shows steps-like barrier with superposition of Interrogate beams, Segment 3 shows a deeper barrier.

Figure 3. Aerial view of the ECRS receiver site at Columbia Falls, ME; Segment 1-North EOS is on the left, Segment 3-South EOS is in the center and Segment 2-EOS is on the far right.

(NEOS) is on the left, segment 3, South East Operating Sector (SEOS) is in the center and segment 2, East Operating Sector (EOS) in on the far right. The segment placement is so arranged to reduce interference between the three receive sites.

The ECRS transmit site shown in Figure 4, is located at Moscow, ME, is in the Appalachian mountains some 30 miles northeast of the Sugarloaf ski area. Segment 3 SEOS is in the foreground of the picture. Segment 2 EOS is located behind and segment 1 NEOS is almost on the Moxie mountain peak slightly left of the center at the top of the picture. The large antenna structures are barely visible as small white lines in segment 1.

Azimuthal subdivisions of the segments shown in Figure 2 represent the basic organization of the radar: each component Radar segment is divided into eight contiguous 7.5° sectors, which are labeled in clockwise sequence Sectors 1 through 8.

To illuminate all or a sub-set of the eight sectors, the AN/FPS-118 Radar has as its basic operational unit a total of eleven frequency independent 7.5° transmit/receive sectors, which are used in various combinations to form contiguous barriers (using eight transmit/receive sectors) while leaving three independent sectors for the interrogate function. These eleven sectors can form partial and even broken barriers, providing for a larger number of interrogate sectors. As many as eight transmit/receive sectors may be assigned to the interrogate function. For each sector, the transmit antenna array forms a 7.5° wide transmit beam, using the transmit array appropriate for the chosen frequency band. The receive array at the same time forms five contiguous 2.5° receive beams, overlaying the same azimuth sector. Of these five beams only the inner beams are used for track processing. (Due to the separation of transmit and receive sites a parallax correction depending on the selected surveillance distance is automatically provided by the system. This parallax correction is transparent to the operator). For each receive sector, the radar provides a 512 (or 256 or 128) nmi deep window, in which the receiver digitizes and processes the signals received. The start ranges of the eleven receive sectors are selected from 500 to 2488 nmi (nominal, for a 512 nmi range window).

At this point we want to introduce the numbering and identification of the three times eleven potentially active sectors of the ECRS (eleven sectors per segment). The segments are numbered 1 through 3, the sectors in each segment 1 through 8, and the three receive beams in

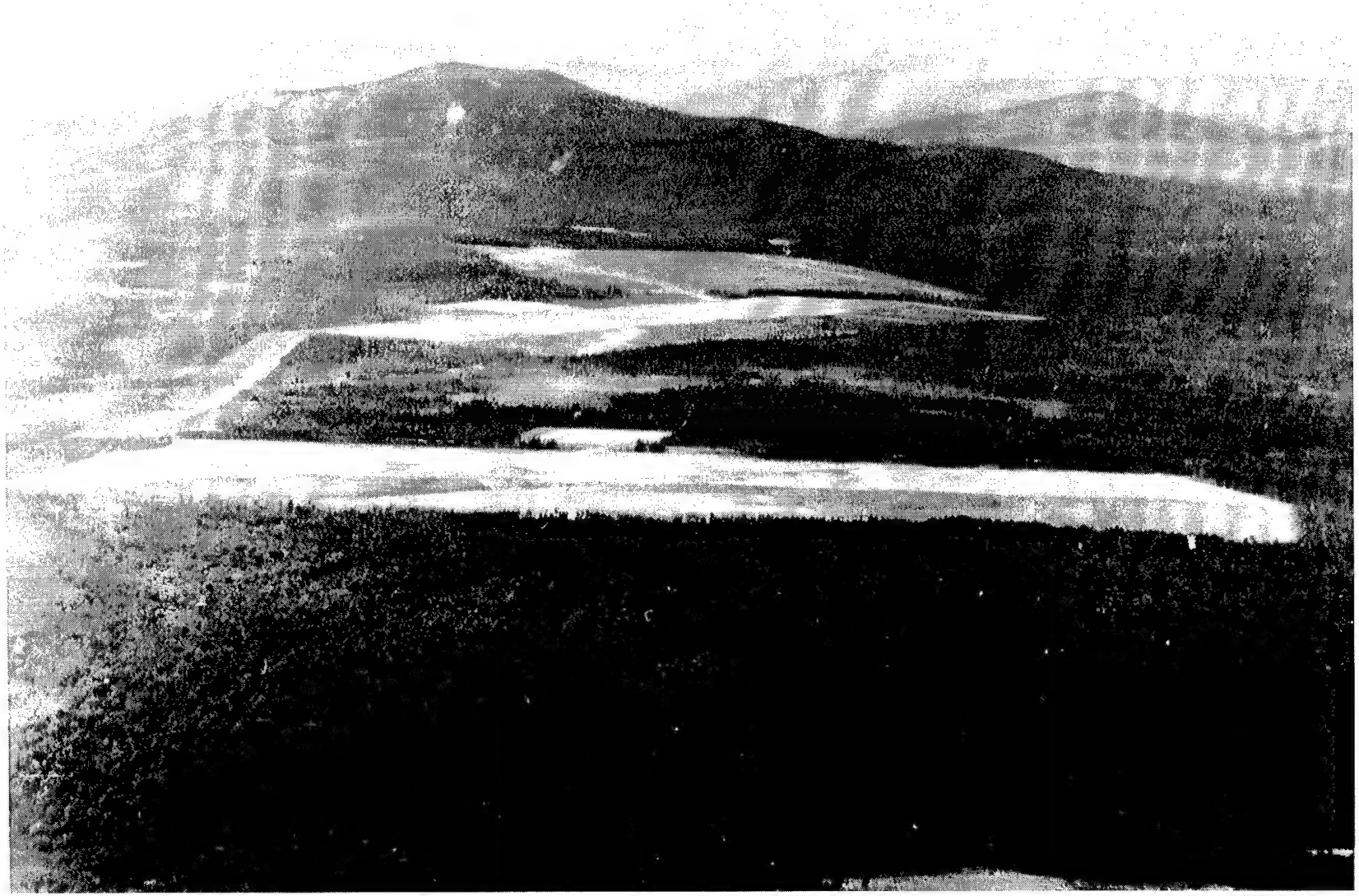

Figure 4. Aerial view of the ECRS transmitter site at Moscow, ME; Segment 3-South EOS is in the foreground, Segment 1-North EOS is on Moxie Mountain seen to the left of the center at the top, and Segment 2-EOS is behind the mountain. The large antenna structures are barely visible as small white lines in Segment 1.

each sector 1 through 3. All numbering is in a clockwise sequence, starting from the North at the ECRS, and from the south-eastern most sector at the WCRS.

The sectors are identified by their segment and sequential sector number as 11, 12, ... 18, 21, 22, ... 38, as shown in Figure 2. Active barrier sectors are always aligned with the basic sector structure and carry the identifiers of the respective sector after the designator B for barrier. A barrier sector activated in sector 23 therefore carries the designation B23 and is centered along the azimuth of 95.25°. As an example the three receive beams for barrier sector B15 have been identified. The three receive beams in B15 are labeled in clockwise sequence B151, B152, and B153. Inactivity of a specific barrier sector does not affect the identification of the other (active) sectors, that is, their numbering sequence is tied to the basic segment/sector structure and numbering.

Interrogate sectors can be lined up with any barrier beam, that is, in 2.5° increments, for a total of 22 increments, because the outer beams cannot exceed ±30.° There are therefore for each segment, 8 sectors x 3 beams = 24 directions possible, which can be selected as an interrogate sector boresight or azimuth. The boresight of an interrogate sector is the direction of its central beam: beam 2. The interrogate sector/beam labeling starts with an I for interrogate, followed by 1 through a maximum of 8 for the number of interrogate sectors activated. Obviously, since only a total of eleven transmit/receive sectors are available, if eight interrogate sectors are activated, only three sectors are available for barrier duty, or vice versa. (Note an additional High Azimuth Resolution Mode is available for interrogation that uses 3.75° wide footprint with 1.25° receive beams which are centered on a left or right half of the 2.5° normal beam).

3. RADAR OPERATION

3.1 The Barrier Sectors

The radar was designed to provide, in its normal mode of operation, a surveillance barrier, which friendly or hostile air traffic approaching or departing the US coast line would have to cross, and during which time they would be detected, tracked, and identified as a known (friendly) or unknown (potentially hostile) aircraft. The position of the start range of a barrier depends on strategic, tactical, and geophysical/ionospheric considerations.

For example, for strategic purposes the United States is interested in knowing about a potential threat early enough to allow it to be identified and neutralized before it reaches the coast or other positions from which it could launch a preemptive attack. For these purposes, the radar would be tasked to establish a barrier nominally 1100 nmi from the radar, allowing surveillance from 1100 to 1600 nmi in range. Since under good propagation conditions the full 500 nmi wide barrier allows detection and tracking of aircraft, typical jet aircraft flying at nominal 450 knots (830 km/h) traverse the barrier in about an hour, ample time for track and identity establishment. After crossing a barrier with a start range of 1100 nmi., the unknown targets are still approximately 2 hours away from the Continental United States (CONUS), sufficient time for necessary action.

In Segment 1 of Figure 2 a complete barrier has been set up using all eight barrier sectors, with a uniform start range of 1100 nmi. This is a very typical initial setup of the radar in its normal mode of operation, and under normal ionospheric conditions.

In Segment 2 of Figure 2 we show the AN/FPS-118 Radar in full operation: all eleven sectors are active (heavy outlines), with eight sectors forming a 500 nmi wide barrier across the radar segment's coverage, and three interrogate sectors positioned for specific interrogate purposes. In the selected example the three interrogate sectors are positioned to provide coverage into and out of the barrier, overlapping with each other and the barrier in azimuth and/or range.

All eight barrier sectors may be set up at a common start range, as shown in Segment 1, or at staggered start ranges as in Segment 2. As the operational setup for Segment 3 indicates, the radar operating menus also permit deactivation of Barrier Sectors for reassignment as interrogate sectors. In the example selected, the outer barrier consists of 4 sectors, with a start range of 1200 nmi, while 4 interrogate sectors initiated on the same azimuths as the barrier sectors provide with a start range of the inner barrier of 750 nmi. thus total coverage over 950 nmi. The inner barrier is from 750 to 1262 nmi and the outer barrier is from 1200 to 1712 nmi thus overlapping the respective barrier sectors by 62 nmi. It is also possible to choose eight Interrogate Sectors to provide the coverage shown in Segment 3, in which case they individually or as a block could be shifted in azimuth in 2.5° increments (or 1.25° for High Azimuth Resolution Sector).

3.2 The Interrogate Sectors

Interrogate sectors serve several purposes. They provide a capability, without interfering with the routine operation of the barrier, to support the following requirements (for example):

a. Interrogate Sectors allow aircraft detected within the barrier to be tracked for extended ranges and for an extended time as they approach the United States. This in effect extends the barrier depth in selected areas.

b. US surveillance or fighter aircraft can be vectored towards an unknown target in the barrier or in another interrogate sector. This vectoring is important. If the indicated position of an unknown target is in error, and both target and interceptor are observed in the same range/azimuth sector, then the interceptor could be vectored relative to the observed nominal target position.

c. Under conditions where the ionosphere does not support a deep barrier, it is possible to use the second frequency available, with an additional interrogate sector to generate an effectively deeper barrier in a specific barrier direction. This approach may be used under poor propagation conditions, when the barrier is very narrow and only marginally suitable for detection, tracking, and correlation.

d. Specific targets within the barrier can be checked for specific characteristics. For example, the system can determine if more than one aircraft is associated with a single radar return, if the aircraft is of a certain type, or if the target is a helicopter. The multiple aircraft test can also be done using a flight size check, which is a form of single sector measurement under the direct control of the Radar Control (RC) operator. The flight size check uses a distinct high resolution waveform and does not affect interrogate sectors.

The three Interrogate Sectors shown in Segment 2 of Figure 2 have been set up in a configuration that together with barrier sectors B23 and B24 provides surveillance of specific aircraft or general air traffic flying on a southwesterly course out of the Azores toward Washington DC. over a 1300 nmi distance (or for approximately three hours).

The setup of the Interrogate Sectors in Segment 3 of Figure 2, in conjunction with the four barrier sectors, provides for surveillance of a large contiguous coverage area, in this case focused on the air traffic from the northeastern coast of South America. This type of operation is

being used by the ECRS in support of drug traffic interdiction efforts of the U.S. government. It permits tracking over this large area over extended times, while at the same time enabling the vectoring of interceptor aircraft for inspection and action.

3.3 Environmental Assessment Support Sectors (SIR, SQR, SIS, SIM, SQS).

One of the best tools the EA operator has to assess the environmental situation, and to determine how the radar performs or may perform on a selected prospective operational frequency, is the radar itself. For this purpose the EA operator has access to a suite of support sector modes. Their use by the EA operators will be discussed in detail in Section 4. Since they are part of the overall radar structure, share the same transmitters and antennas with the barrier and interrogate beams, and need their own time slot in the sequential operation of the radars transmissions, they are also discussed here.

The Sector Illumination Routine (SIR) allows for a coarse assessment of the quality of frequency management and radar performance for each sector that the EA operator has activated. The SIR provides one sector at a time for radar transmission on the frequency of a respective barrier sector once every scan of the complete segment. Every other revisit cycle, the respective SIR time slot can be allocated to the Sector Quiet Routine, discussed below. It therefore takes the radar 16 full segment scans (that is revisit cycles) to accumulate a complete set of SIR/SQR data for eight barrier sectors in a segment. The total range window for which the ground clutter and the noise levels are acquired is nominally 1000 nmi; the ground range start is selected from 500 nmi to 1000 nmi. The SIR data permit for example, the assessment of the barrier location for the specific frequency in the context of the overall propagation conditions (skip distance, range folding), clutter conditions, and support decisions (such as the need for frequency or range change).

The Sector Quiet Routine (SQR), if activated, provides for data on the RFI (radio frequency interference) conditions for the barrier sectors for which it has been activated. It operates the receivers with the transmitters off, collecting noise data with the standard barrier operating parameters. This permits the operators to differentiate between radio frequency

interference (additive noise) measured by the SQR and ionospheric and auroral Doppler spread clutter (multiplicative noise) measured by the SIR, information important to the frequency management of the radar.

To gain information on how a new frequency, a range change, or any other change of the radar's operating parameters would affect radar performance, the EA operator can initiate a Sector Illumination Special (SIS). This provides for a single dwell operation of the radar in a selected sector (that is, for the duration of the selected Coherent (CIT) and noncoherent Integration Time (NCIT)), with all parameters available to the RC for selection. This permits investigation (for example under marginal performance conditions), of the impact of frequency or other parameter change to improve (or worsen) the situation, without interfering with a potentially tenuous detection and tracking situation.

Similarly, a single dwell operation of the Sector Quiet Special (SQS) provides information on noise conditions on a potential frequency for a specified sector.

4. GEOPHYSICAL ENVIRONMENT OF THE CONUS OTH RADARS

The impact of ionospheric and auroral irregularities on OTH radar operation in general has been presented in detail in Section 3.3.2. Here these problems are briefly discussed in the context of the specific location of the ECRS and WCRS as related to the specific orientations of their sectors. Irregularity regions affect the radar not only if they occur within the coverage area, but also if these irregularities are illuminated at large ranges. Whenever the propagation path of a radar transmit/receive sector intersects an irregularity region at large distances beyond the unambiguous range of the selected wave form, spread clutter from these regions may be range folded back into the radar's primary radar range window. If strong enough, this range folded clutter will adversely affect radar operation and performance. The orientation of the back lobes of the individual sectors to the auroral oval is also of significance. At night the oval is often close to the radars. The impact of the global irregularity regions on the two radars is therefore discussed in the context of the great circle paths in the forward and back lobe directions from the radars to their respective antipodes.

4.1 East Coast Radar System

Figure 5 presents, in a Mercator projection, the global propagation path for the ECRS in the forward or operations direction. The great circle paths bounding the individual sectors are shown. The great circle paths at the segment boundaries are enhanced. All great circle paths cross the equator and converge at the antipode. The plus (+) signs indicate 1000 nmi range marks.

The important irregularity regions of the global ionosphere are the auroral/polar cap regions (found at night and for moderately active conditions to the north (south) of the 65° (-65°) CG Latitude), the night time F layer trough, which lies equatorward of the auroral oval and the equatorial anomaly or disturbance region, which is nominally found from just after local sunset to sunrise in the latitude region between ± 20° CG latitude. These CG latitude curves are marked on the map. Also shown is the geomagnetic equator, near which the irregularities at the equator develop initially, before they fully develop to extend over the full 40° latitude range.

It should be understood that the locations of the disturbance boundaries are only nominal, for average magnetic conditions. Under quiet magnetic conditions the auroral irregularity region may not reach down to the 65° CG latitude of the respective hemisphere, while under very active conditions auroral irregularities may be found much further south (north for the southern hemisphere). In daytime the auroral clutter boundary is found approximately 10° to the north (south in the southern hemisphere) of indicated 65° CG latitude, however auroral absorption events may occur down to 65° CG latitude at all times. The equatorial irregularities exhibit a strong seasonal dependence, which is different for the respective equatorial regions observed by either radar (for details see Section 3.3.2).

Figure 5 shows that every sector, the more northerly at large distances, crosses the equatorial day/night disturbance region, before it reaches the radar's antipode. It can therefore be expected that under certain (for the radar unfavorable) propagation conditions and certain periods of time, spread clutter may be observed in any specific sector. The currently available limited clutter data indicate, that at least Segments 2 and 3, due to proximity of the equatorial disturbance regions, are experiencing clutter effects consistent with the known occurrence patterns of equatorial irregularities.

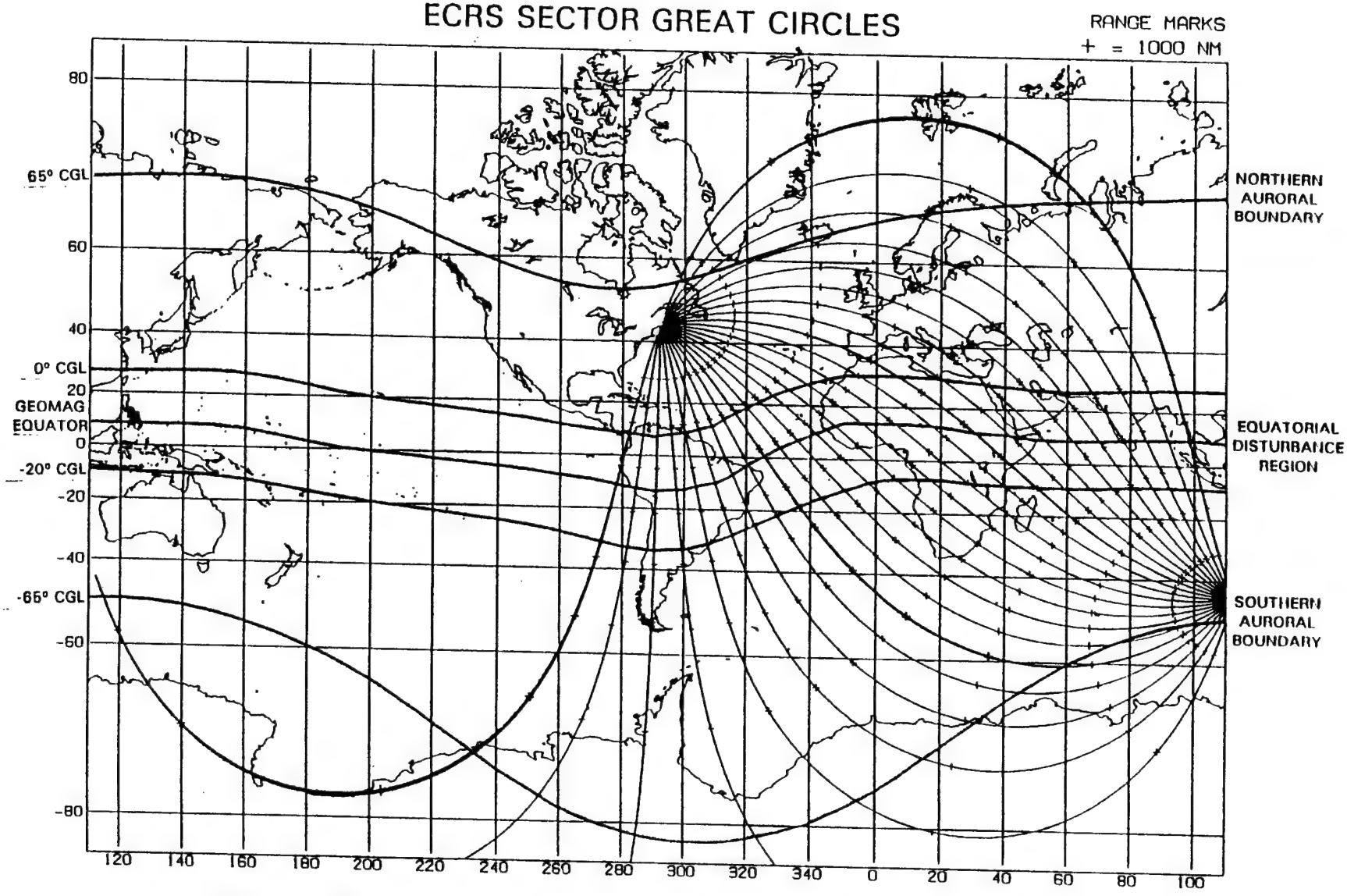

Figure 5. ECRS coverage area of various beams in geographic coordinate system.

The auroral clutter found at night to the north of the 65° CG latitude affects primarily segment 1 (typically sectors 11 though 13). The F-Layer trough with its weak ionosphere and enhanced irregularities is found at night to the south of the auroral band, and often extends the high latitude effects to include sectors down to 14 or 15. Since the Europe-to-America air traffic routes often skirt Iceland, the southern tip of Greenland, and cross Labrador, observation of this traffic is at times impeded by auroral and trough activity.

The southern auroral oval south of -65° CG latitude is typically at ranges greater than 7500 nmi from the ECRS. It may at times be a source of spread clutter, especially for Segments 2 and 3. For these segments, the local time situation along the great circle paths may be favorable for reaching this disturbance region with sufficient energy, so that backscattered energy may actually affect the radar. Since the unambiguous range for the lowest WRF (10 Hz) is 8000 nmi, and since the auroral disturbances may be rather extended both in azimuth and range, range unfolding may not always be successful. No specific observations of this problem have been made from the ECRS, but correlation of increased clutter with the preferred times has not occurred and its effects may be minor.

Figure 6 shows the back lobes of the ECRS radar beams. The OTH radar system uses a linear broadside antenna array that produces a second major lobe (back lobe) directed towards the rear of the radar coverage. A metallic mesh backscreen is used for both the transmit and receive antenna arrays to attenuate this back lobe by approximately 50dB. However, for a powerful system such as the OTH radar, this still represents potential signals in an undesired direction. It is possible to observe a large target (20 to 30dB larger than routine traffic) through this attenuated back lobe beam but such large targets (such as missile plumes) are rare events that do not result in false and unidentified target increases. The more serious complication arises from clutter sources in the auroral and equatorial regions illuminated and received via these back lobes of the antenna system. This clutter degrades system performance even when the radar's main beam is directed away from these sources since its largest size is 20 to 30dB greater than routine air traffic.

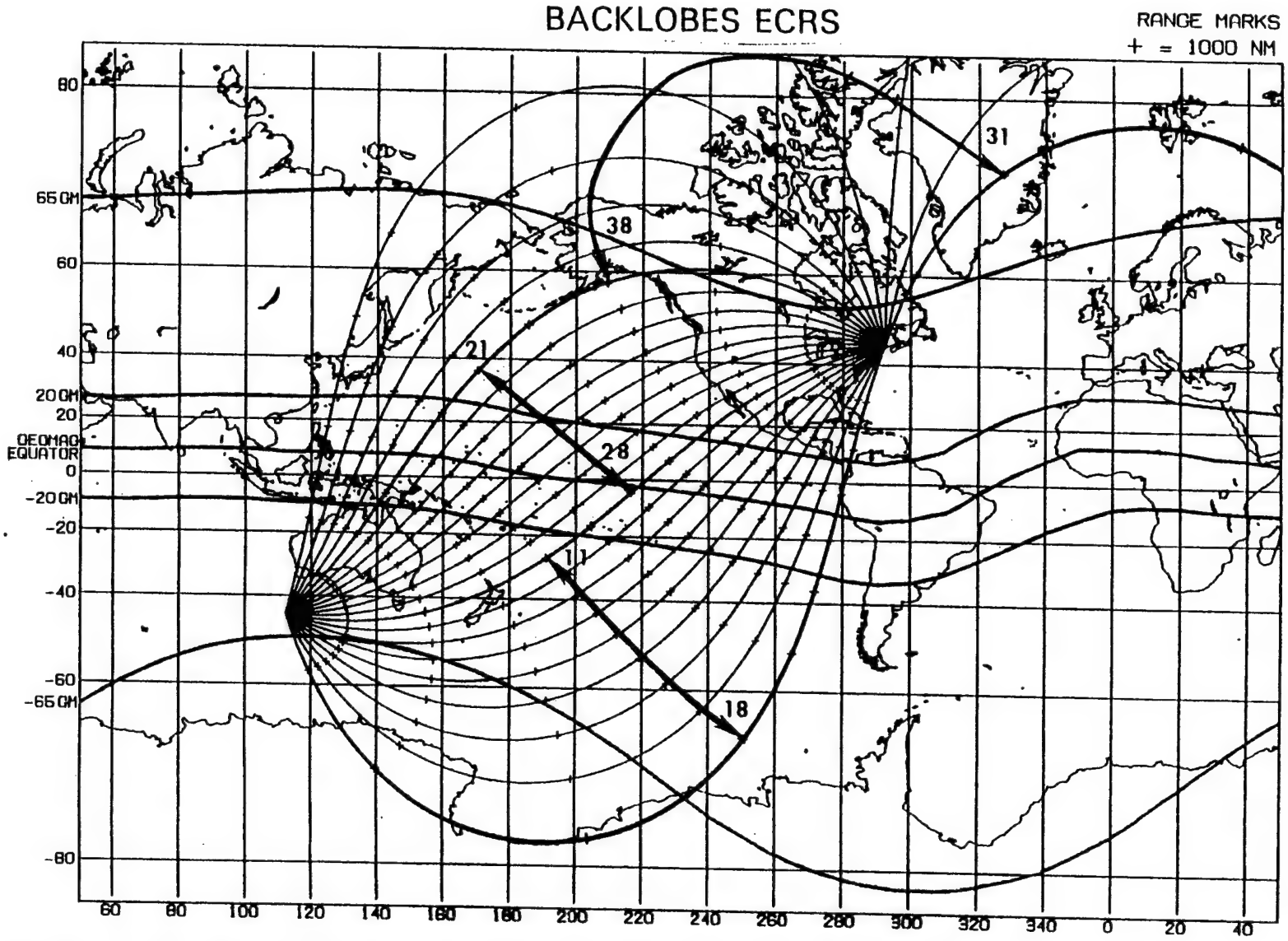

Figure 6. The back lobes of the ECRS coverage area of various beams in geographic system of coordinates.

4.2 West Coast Radar System (WCRS)

Figure 7 shows the WCRS sector great circles in relation to the global disturbance regions. While the auroral boundary typically comes to within a few hundred nmi of the ECRS, the WCRS is more favorably located, and experiences the auroral irregularities only at larger ranges in Sectors 37 and 38. Auroral effects, even though observed at the WCRS, are reportedly substantially weaker and less problematic than for Segment 1 of the ECRS. This is primarily because it is at lower corrected geomagnetic latitude, thus the midpoints to a typical 1100 nmi barrier at the WCRS are rarely affected by either trough or auroral oval.

The equatorial irregularity region is approximately 500 nmi closer at the WCRS than at the ECRS due to the slightly more southerly location of the WCRS and the location of the magnetic equator in this longitude sector. This, together with unresolved propagation and aspect related phenomena, may be responsible for the considerably more severe equatorial clutter problems experienced at WCRS. For details see Section 3.3.2. Extended observations of equatorial clutter, often throughout the whole night and into the morning hours have been reported from the WCRS Segments 1 and 2 when placing a barrier in the 500 to 1000 nmi interval, and clear evidence exists that equatorial clutter at times also affects Segment 3, including the most northerly Sector 38. Mitigation through the use of low WRF (range unfolding) has at times been successful.

The southern auroral oval especially for WCRS Segments 1 and 2 is almost 1000 nmi closer to the radar than in the ECRS situation. This may be one of the reasons why the southern oval has often been observed in 8000 nmi long range backscatter sounding of the WCRS, while it rarely has been reported from the ECRS. This may also account for the reported enhanced number of cases, when range unfolding with low WRF did not allow complete mitigation of the observed spread clutter at the WCRS.

Similar to Figure 6, Figure 8 shows the back lobes of the WCRS beams shown in Figure 7.

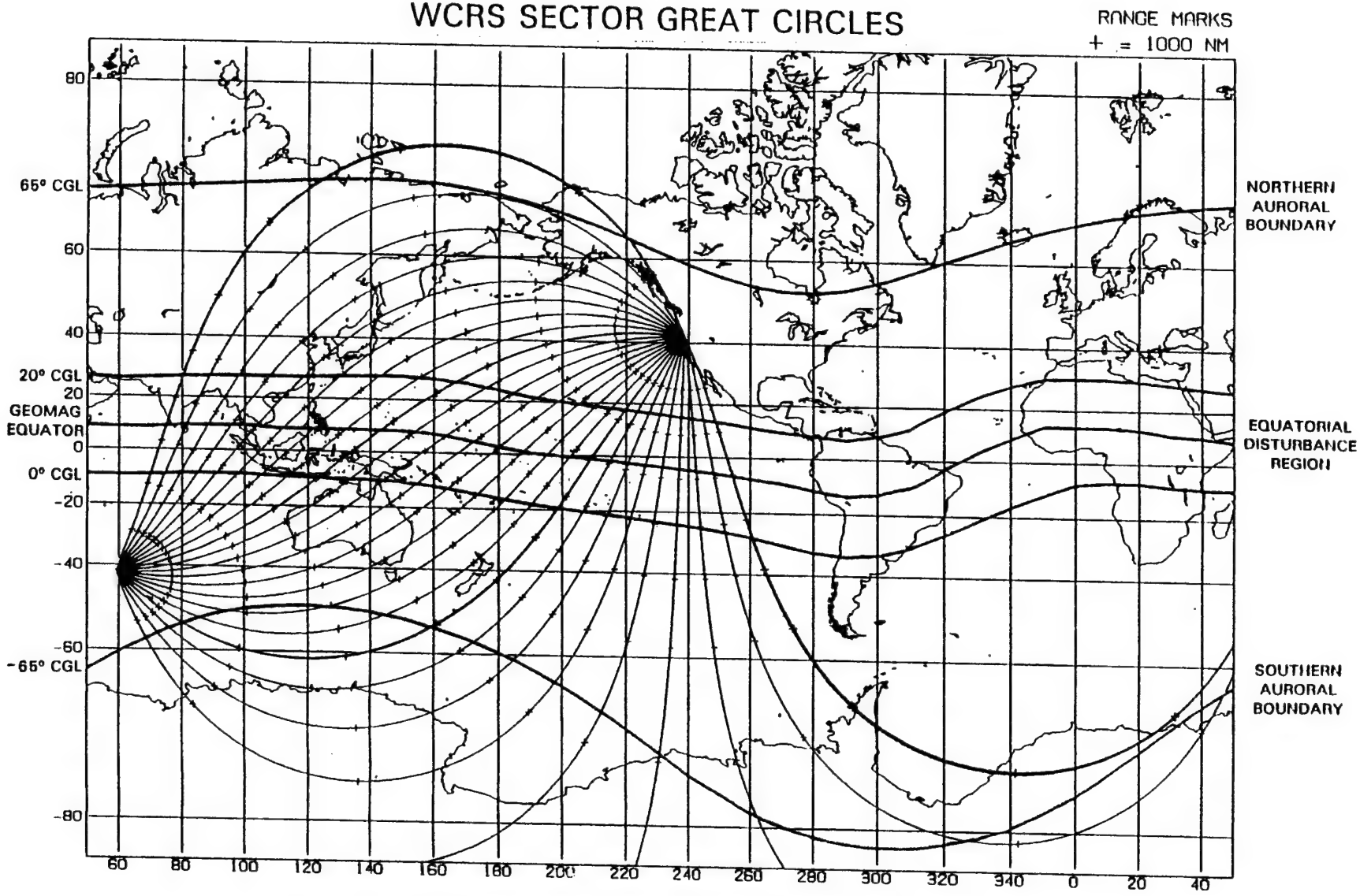

Figure 7. WCRS coverage area of various beams in geographic coordinate system.

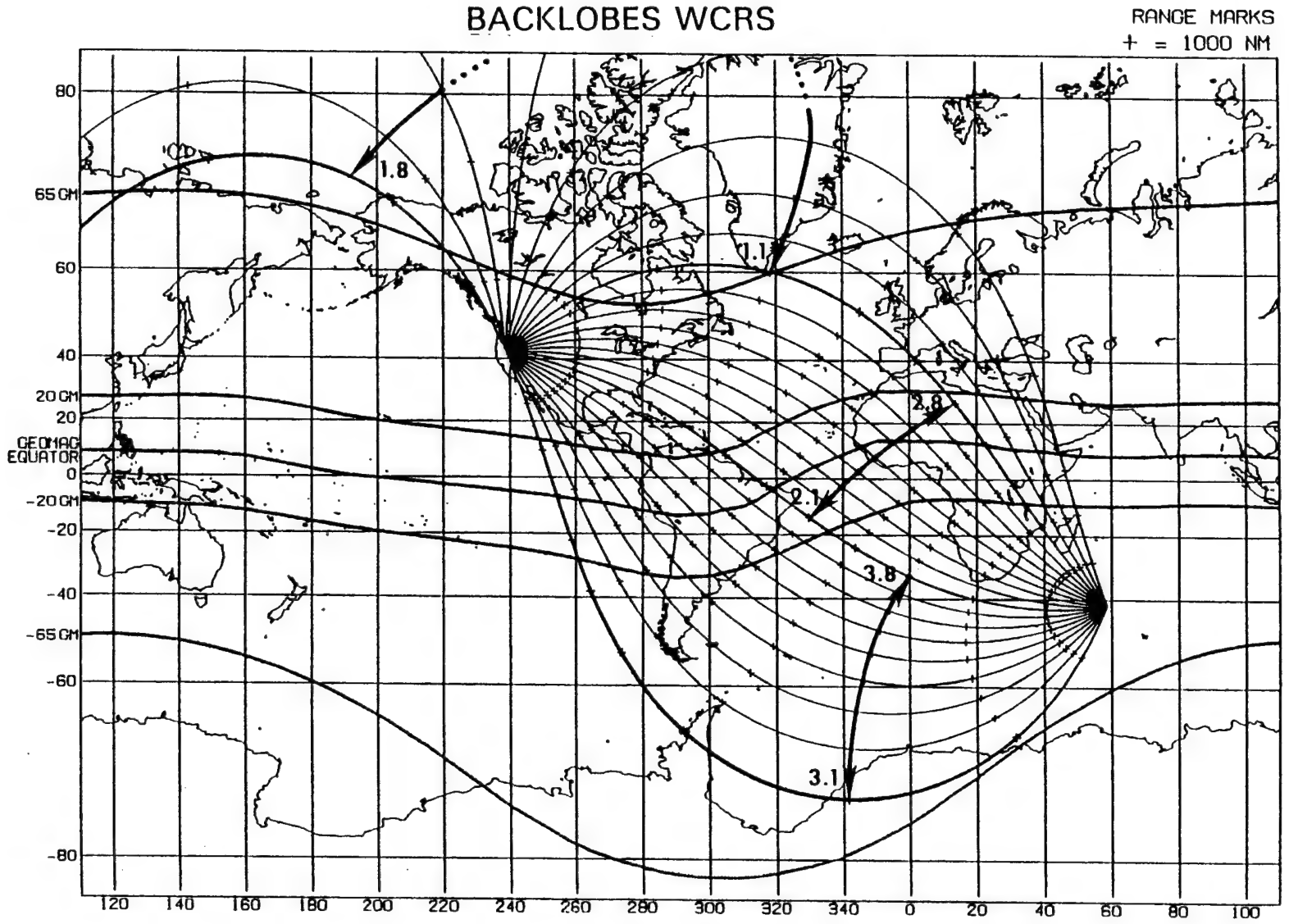

Figure 8. The back lobes of the WCRS coverage area of various beams in geographic system of coordinates.

5. THE ENVIRONMENTAL ASSESSMENT FUNCTION

5.1 Introduction

The OTH Radar System is unique because it requires not only transmitters, receivers, and appropriate antennas to operate properly, but also requires something external to its facilities and equipment, namely, the ionosphere. The reflection or refraction of the radar signals by the ionosphere permits the radar to bridge large distances; to look 'over the horizon'. The ionosphere is therefore an integral part of the radar that must be accounted for from its design to its minute by minute operation. The ionosphere varies substantially day to day and hour by hour, and its present state must be assessed for proper frequency selection and coordinate registration. Because coordinate registration, which is the conversion of radar range and azimuth of a target to its ground coordinates, is required for target location, a significant part of the radar system resources and a whole radar function (the Environmental Assessment Function)are devoted to characterizing the environment and its interaction with the radar.

If the ionosphere were simply a reflector, with a known height, the radar range and azimuth of a target could be converted into the corresponding ground coordinates using simple geometry. Under sporadic E (Es) conditions, this scenario is nearly applicable.

However, under the conditions typically encountered, the radar operators must deal with the regular E, the F_1, and the F_2 layers, and a more detailed knowledge of the ionospheric conditions along the ray path is required for radar operation and coordinate registration. All of the ionospheric parameters important to the radar operation vary continuously; the height of the different layer maxima, the thickness of the layers, and above all, the critical frequencies (maximum electron densities) of the layers. These parameters are combined to determine the frequency required to illuminate the ground at a desired range. For Coordinate Registration, the radar signal's reflection height must be known as a function of operating frequency and range. Deviations from a "typical" behavior due to solar and subsequent geomagnetic activity further complicate the radar operations. In addition to affecting the simple propagation scenario (often requiring rapid frequency changes), geomagnetic disturbances generate localized and global scale irregularities in the ionosphere. These ionospheric irregularities can cause Doppler spread radar clutter, a serious detriment to the performance of the radar.

To select the required frequencies, determine the reflection height to provide the basis for coordinate registration, and assess the impact of disturbances on radar performance, the EA operators have access at their consoles to a set of remote sensors, and use of computer tools. A large array of radar and environmental data displays for analysis of ionospheric and propagation conditions and radar performance are also available.

Section 5.2 discusses these EA tools and their applications. Section 5.3 contains a description of the ionospheric model, which is used in the EA process to provide the means of mapping the localized ionospheric sounding results over large areas. This process can generate a map that shows, for example, the radar signal reflection height for any desired azimuth and range. The model can also aid in frequency management, especially at times of rapid ionospheric changes, such as sunrise or sunset.

5.2 EA Tools and Procedures

5.2.1 THE BACKSCATTER SOUNDER AND FREQUENCY MANAGEMENT

The generation of a backscatter ionogram and its use in frequency management had previously been discussed by G. Sales (PL-TR-92-2123). The AN/FPS-118 Radar has one backscatter sounder associated with each 60° segment, except for Segment 1 of the ECRS, which, because of its very dynamic environment, is provided with two sounders. They can produce two backscatter soundings in coupled directions simultaneously, (Sectors 1 and 3, 2 and 4, 5 and 7 and 6 and 8), cutting the revisit time for one complete 60° azimuth sector in half. The transmit antenna for each sounder consists of two vertically polarized log-periodic curtains arranged in a "V" configuration to provide a nominal beam width of 60° overlaying the azimuthal coverage of the respective segment. Two out-of-coverage antennas provide for backscatter soundings in the nominal direction opposite to the segment's boresight. A 10 kW amplifier drives the sounder transmit antennas, transmitting an FM/CW sweep from 2 to 30 MHz, or sections of this sweep. The start and end frequencies of the sweep are selected in 1 MHz increments. Four sweep rates are available: 25, 50, 100, and 200 kHz/sec, providing for observable backscatter ranges of 8000, 4000, 2000, and 1000 nmi respectively.

The receive beam for the backscatter sounder is formed using an auxiliary beam former that takes its input from receive elements in the main receiver array. The beamformer uses 72 antennas of the receiver array, 24 for each of three receiver bands. The receive beams formed have a nominal beam width of 7.5° and overlay the eight sectors.

Figure 9 shows the menu for programming the backscatter soundings. Each of the sounding sectors (except as noted above for Segment 1) can be controlled individually in all parameters, allowing tailoring of the soundings to the need of the operator. However, it is possible to set all sectors to the same parameter with a single action.

Figure 10 shows a typical 2 to 30 MHz and 2000 nmi range extent backscatter ionogram. This range coverage is matched to the 2000 nmi coverage (in slant range) available to the radar itself, and is therefore the format most commonly used for frequency management by the EA operators. Since at a sweep rate of 100 kHz/sec a total of 280 sec (4 min 40 sec) is required for a full sweep, it would take the sounder over half an hour (15 minutes in segment 1) to complete a full scan of all eight sectors, a time that is long compared to the rapid ionospheric changes during transition times. For this reason the EA operator normally selects a frequency subrange or uses a different number of azimuth sectors to shorten the revisit time. The subrange selection depends on the operational scenario, but must display some minimum portion of the full ionogram so that the mode structure and other important features can be properly interpreted.

The first step in frequency management is the manual scaling of the leading edge of the ground backscatter by the EA operator. The result of such tracing is shown in Figure 11 as the fine line along the leading edge of the ground scatter. The Radar Control operator, whose console is co-located with the EA console, has in the mean time set the starting ground ranges for the sectors to be activated at the start of the required barrier location. The ground range selected for the start is scenario dependent, typically 1100 nmi. A frequency window, typically 1 MHz wide, is opened for the selection of a frequency that will provide the required coverage. This frequency window extends from the intersection of an imaginary horizontal line at the desired slant range start with the leading edge trace, and going to lower frequencies. This ensures that the barrier start is beyond the skip distance (the backscatter leading edge) for all potential frequencies. Such an initial frequency window is shown as the horizontal bracket inside the

SEGMENT 2 SOUNDER CONTROL MENU

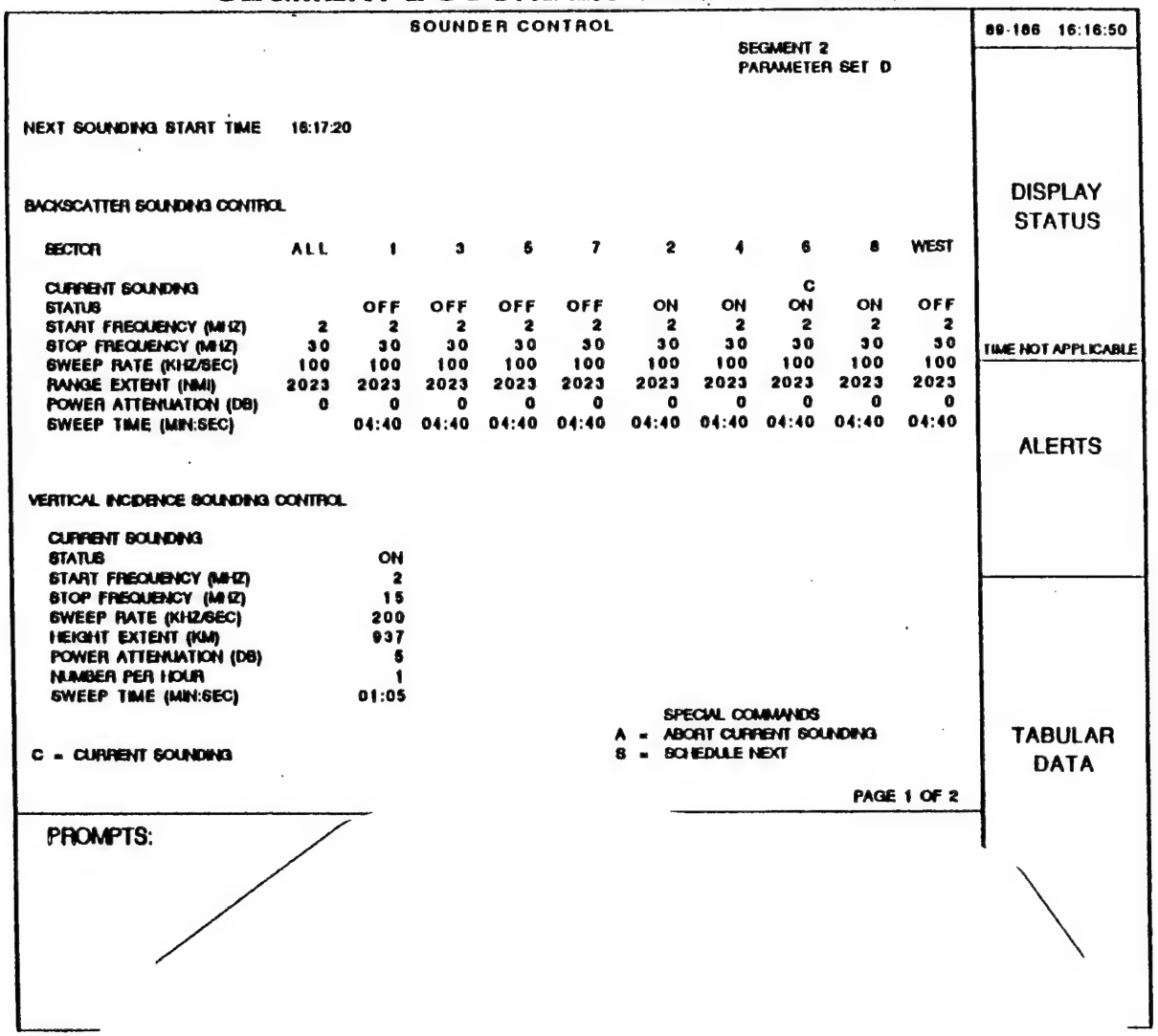

Figure 9. Sounder control Menu (for producing Backscatter Ionograms).

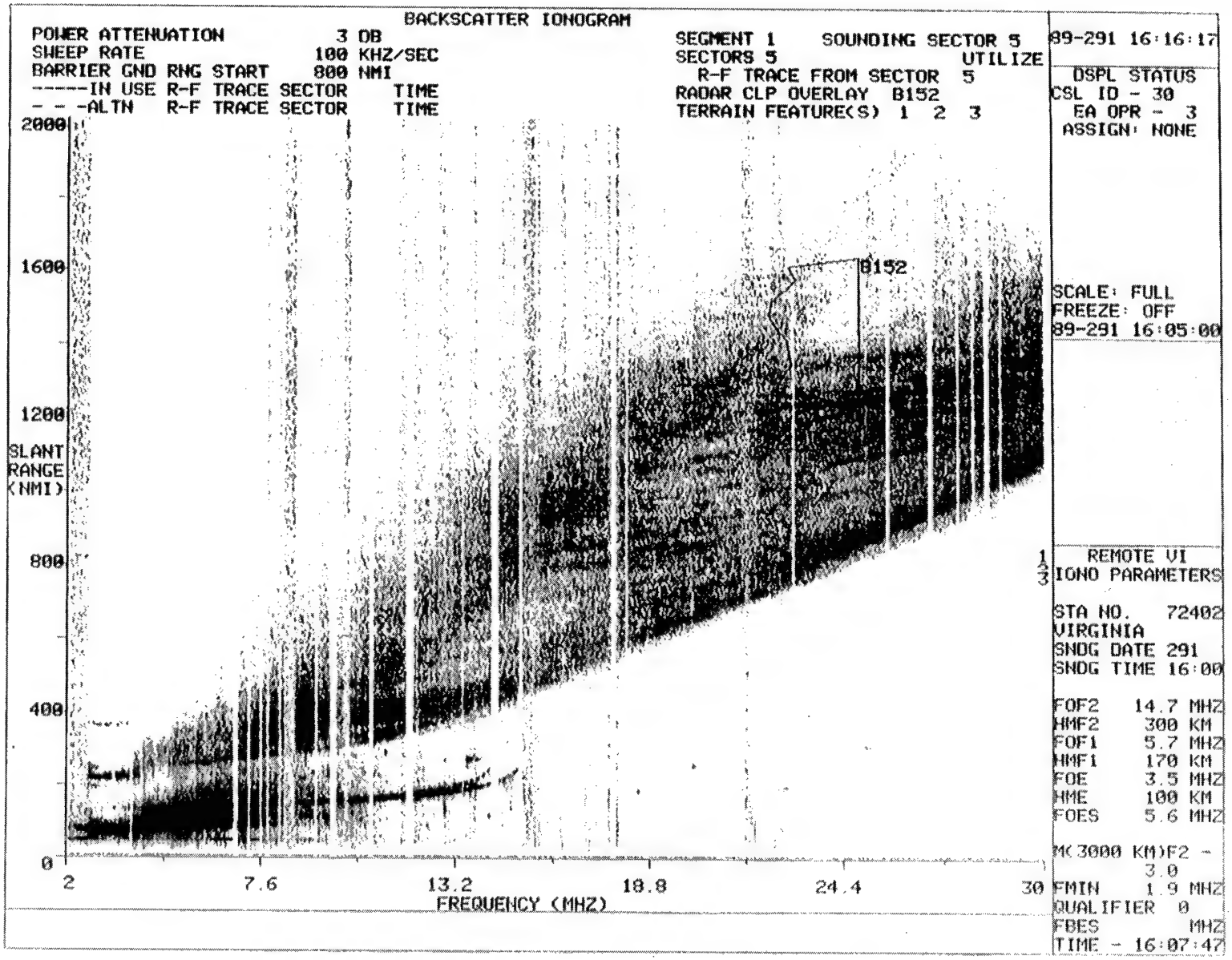

Figure 10. 2000 nmi range Backscatter Ionogram.

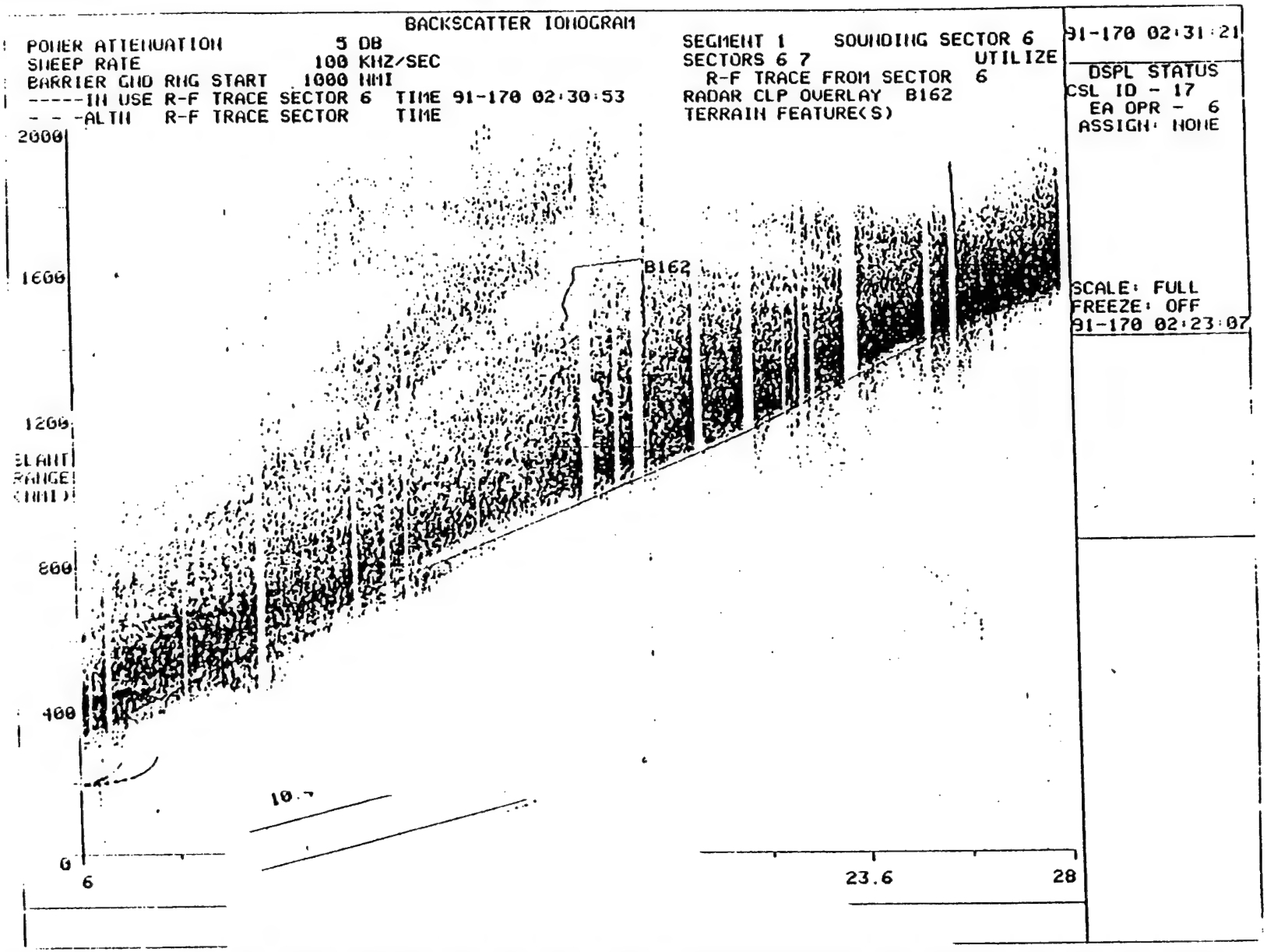

Figure 11. 2000 nmi range Backscatter Ionogram showing the manually traced leading edge of the ground scatter and the location of the barrier B162 for the radar operating frequency of 19.2 MHz.

ground clutter near 19.2 MHz. Over this frequency band a "Clear Channel Search" with the frequency monitor is initiated by the RC operator. This process provides the EA operator with a list of clear channels, grouped by bandwidth and noise level. An example of the clear channel list is presented in Figure 12. From this list the EA operator selects the frequency, which is then initiated by the RC operator, putting the radar into action. As soon as a frequency has been selected by the EA and RC operators, a vertical line appears at the appropriate location within the window bracket, indicating both frequency and barrier range extent (see Figure 13). After collection of the initial radar data on the newly selected frequency, the EA operator can display the average clutter peak level by calling up the overlay "clutter level peak" for the barrier frequency. As is done for the barrier frequency display, a horizontal line is plotted indicating the clutter levels over the barrier range extent. As seen also in Figure 13, the clutter peak level is plotted in the horizontal direction against the vertical barrier frequency line.

5.2.2 ASSESSMENT OF RADAR PERFORMANCE

Several displays are available to the EA operator to determine how good the frequency selection is, and to continuously monitor radar performance. The most detailed of these is the Sector Amplitude Range Display (ARD) shown in Figure 14. This is the typical display of range nested Doppler spectra, showing in each range cell the ground clutter at 0 Hz, and the unambiguous Doppler spectrum to ± ½ WRF (for details see report by G. Sales, PL-TR-92-2134). The ARD data are displayed with signatures of the incoming target (positive Doppler) on the left hand side of the zero Doppler line. The ARD permits assessment of the quality of the illumination (ground clutter amplitude) for the target detections, and the interference or spread clutter conditions, providing the best information to assess potential reasons for deteriorating radar performance. Figure 14 shows ARD data for two transmit beams: B14 in the upper and B15 in the lower panel. Note that each transmit beam has three simultaneous receive beams (1,2,3), marked on the upper right hand corner for each trace. The operating frequencies for the beams, 25.402 and 25.714 MHz respectively, are different at this time. The Wave Form Bandwidths (WBW) that determine the range resolution are 10 and 5 kHz respectively. Thus, the range resolution cells (spacing between successive ground clutter zero Doppler peaks) are 8

CLEAR CHANNEL LIST VERSUS BANDWIDTH

SEGMENT 3
SECTOR 15/85

91-338 22 06 14

SPECTRUM MONITOR CONTROL
TYPE A
CENTER FREQ 17.550 MHZ
EXTENT 1.020 MHZ
CELL BW 1.00 KHZ
ANTENNA SE

MISSION CONTROL
STATUS ON
WAVEFORM FM/CW
WBW (1) 20 KHZ
FREQ AA17.3030 MHZ

ACCUMULATIONS 12

WBW (KHZ)	POTENTIAL RADAR FREQUENCY (MHZ)	NOISE LEVEL (DBM/HZ)	PERCENT TIME CLEAR
5.	18.0400	-142	91
	18.0590	-142	83
	17.9510	-141	91
	17.9380	-141	75
	17.6520	-140	25
	17.1350	-140	75
	18.0190	-140	83
	17.9650	-139	100
	17.9190	-139	91
	17.1000	-139	91
10.	17.9460	-141	75
	17.1300	-139	83
	17.9120	-139	83
	18.0530	-139	91
	18.0130	-139	91
	17.0950	-139	91
	18.0330	-138	66
	17.1960	-138	25
	17.0580	-137	91
	17.8920	-137	33
20.	17.9510	-139	75
	18.0460	-139	75
	17.9040	-138	33
	17.2050	-137	8
	18.0060	-136	83
40.	17.9290	-137	25
	18.0260	-137	75

* EXCEEDS NOISE THRESHOLD

(1) 40. KHZ WBW CLEAR CHANNEL LIST IS USED FOR ALL FM/ICW WAVEFORM OPERATING FREQUENCY SELECTION, INDEPENDENT OF THE SPECIFIC WBW IDENTIFIED ON THE DETAILED BARRIER AND/OR INTERROGATE CONTROL MENUS

DSPL STATUS
CSL ID - 18
EA OPR - 8
ASSIGN: NONE

SCALE: FULL
FREEZE: OFF
91-338 22:06:00

REMOTE UI
IONO PARAMETERS

STA NO. 71816
GOOSE BAY
SNOG DATE 338
SNOG TIME 21:30

FOF2 8.0 MHZ
HMF2 280 KM
FOF1 MHZ
HMF1 KM
FOE 1.2 MHZ
HME 110 KM
FOES MHZ

MK 3000 KM)F2 -
3.0
FMIN 1.6 MHZ
QUALIFIER 0
FBES MHZ
TIME - 22:05:40

Figure 12. Menu of clear channel list versus bandwidth for selection of radar operation frequency.

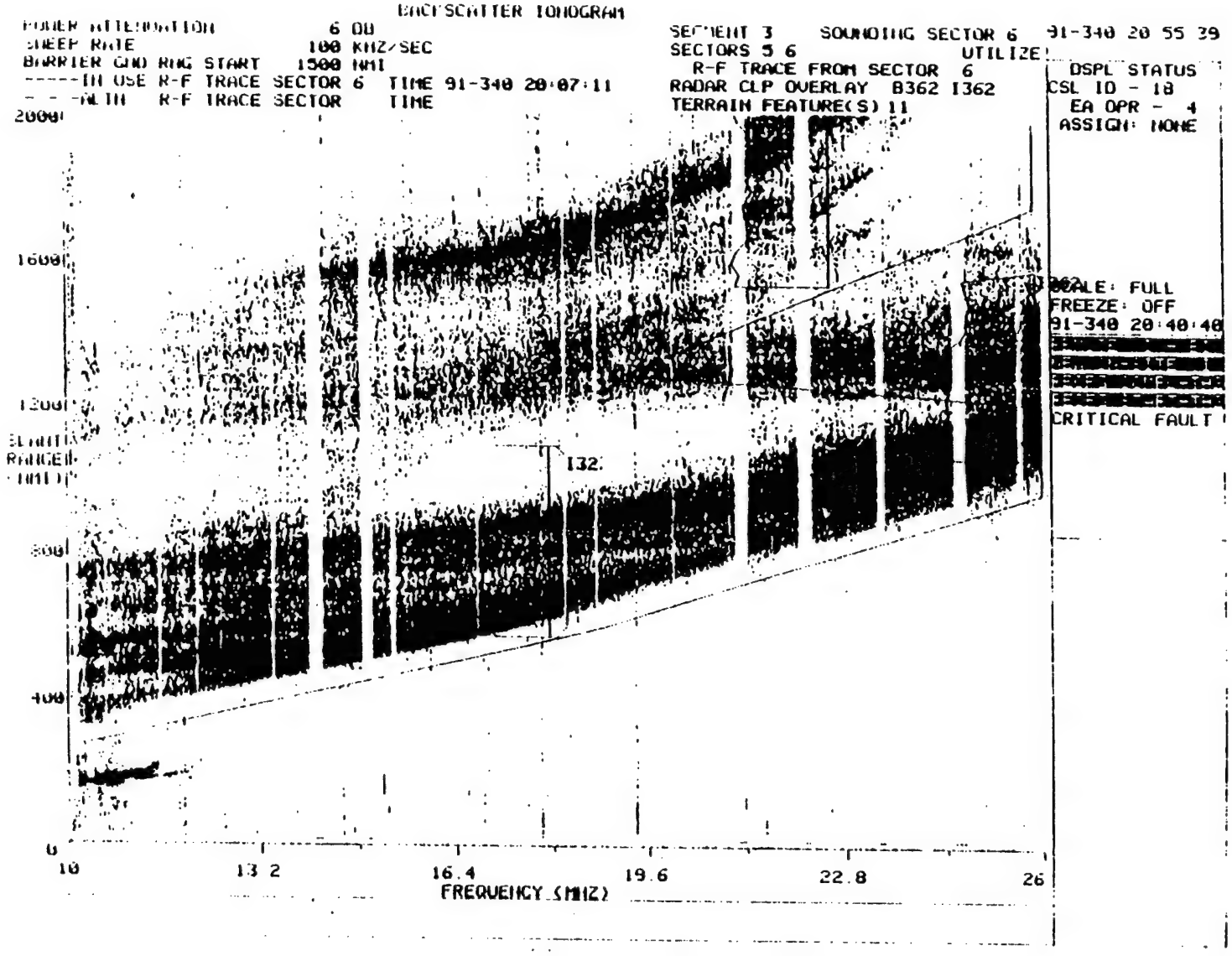

Figure 13. 2000 nmi range Backscatter Ionogram showing the manually traced leading edges of different reflection modes, and the locations of the interrogate I32 and the barrier B362 with selected radar operating frequencies of 17.9 and 22.7 MHz respectively.

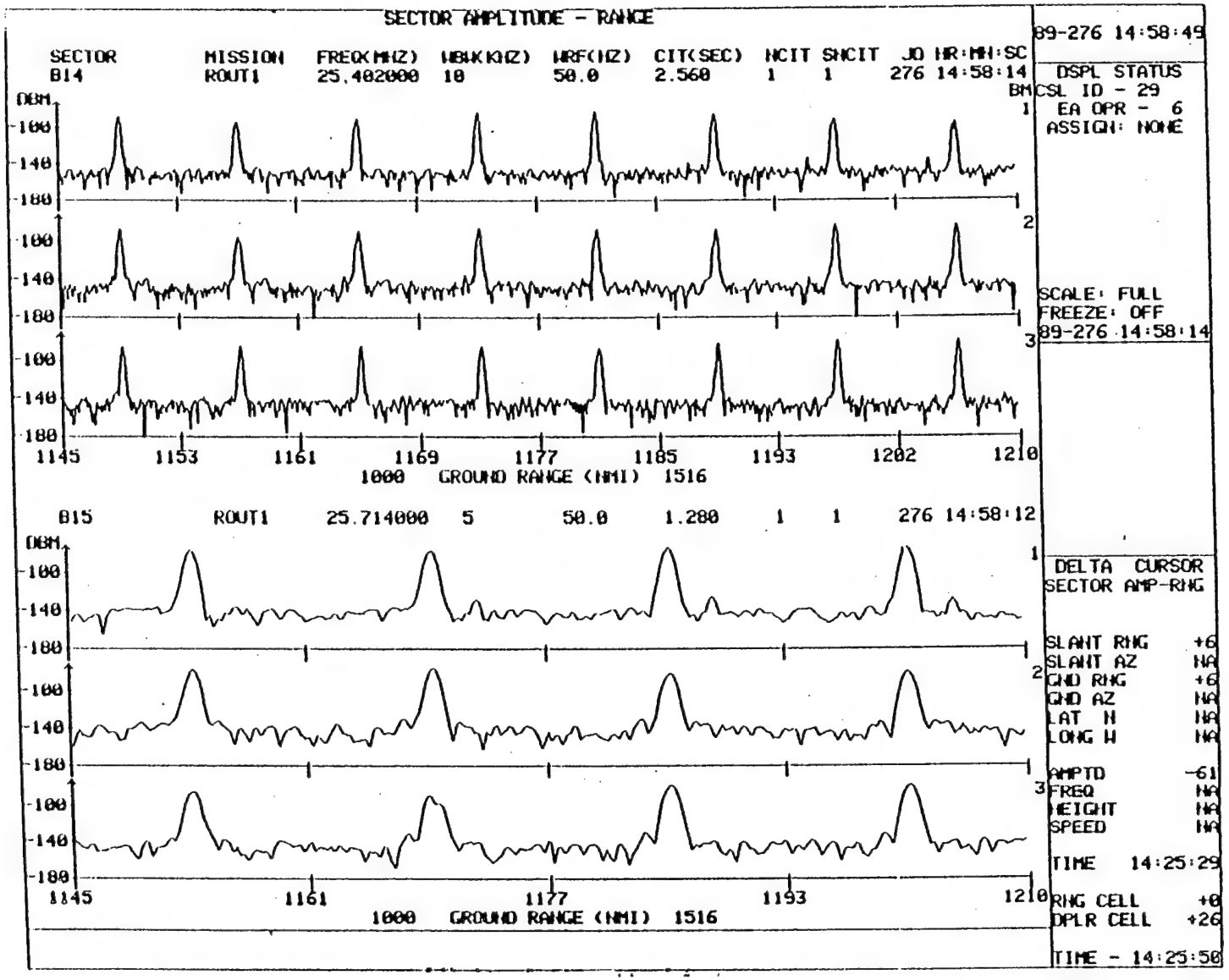

Figure 14. Sector Amplitude -Range plot of the clutter signal: the top is for WBW=10 kHz and the bottom for WBW= 5 kHz. Note that number of clutter peaks is proportional to WBW.

and 4 nmi respectively. The radar subclutter visibility for all this set of (-80 to -150) 70dB provides SNRs of 20 to 40dB on targets. No target signatures are seen on the ARD display at this time.

Generally the EA operator uses a summary of these data to get a quick overview. This summary is provided in the Clutter and Noise vs. Range (CNR) display, shown in Figure 15. The CNR display provides separate traces showing averages over 8 to 16 range cells of the clutter peak amplitudes and of the averaged spread Doppler noise. These data are provided for the full range extent of the barrier window, and also for the 1000 nmi range extent covered by the Sector Illumination Routine (SIR). Both barrier and SIR are operated on the same frequency, which permits the assessment of the placement of the maximum 500 nmi barrier in the larger context of the SIR range extent. Figure 15 shows (from nominal 900 nmi out to 1900 nmi) the average ground clutter levels (continuous traces) and spread clutter levels (dashed traces) measured by the SIR over the SIR range extent. Superimposed are the shorter 500 nmi traces of the ground and spread clutter levels obtained from the barrier data. Also displayed are the Sector Quiet Routine (SQR) data, which were collected with the radar transmitter off, measuring the Radio Frequency Interference (RFI) background for the respective sector. For identification the SQR data have been identified. At the operator's display, color is used to identify the various data types of the CNR display. In Figure 15 the skip distance for the selected frequency of 25.714 MHz is seen to be at approximately 850 nmi ground range. The barrier, which starts at a ground range of 1000 nmi is properly placed according to Figure 15, starting just behind the focusing edge of the ground clutter.

The difference between the clutter and noise level (in dB) is the clutter-to-noise ratio (CNR), an important measure of radar performance. The barrier noise floor in Figure 15 is slightly enhanced in the 1300 to 1500 nmi range; CNR is approximately 55 dB, providing good performance across the full 500 nmi of the barrier. The enhancement of the barrier/SIR noise level compared to SQR noise level indicates the presence of multiplicative clutter resulting from the radar transmissions, that is, the presence of ionospheric irregularities or meteor trails, or secondary focusing are indicated. It should be noted that Figures 14 and 15 were taken almost simultaneously; therefore the barrier ARD data can be directly compared with the averaged barrier CNR data.

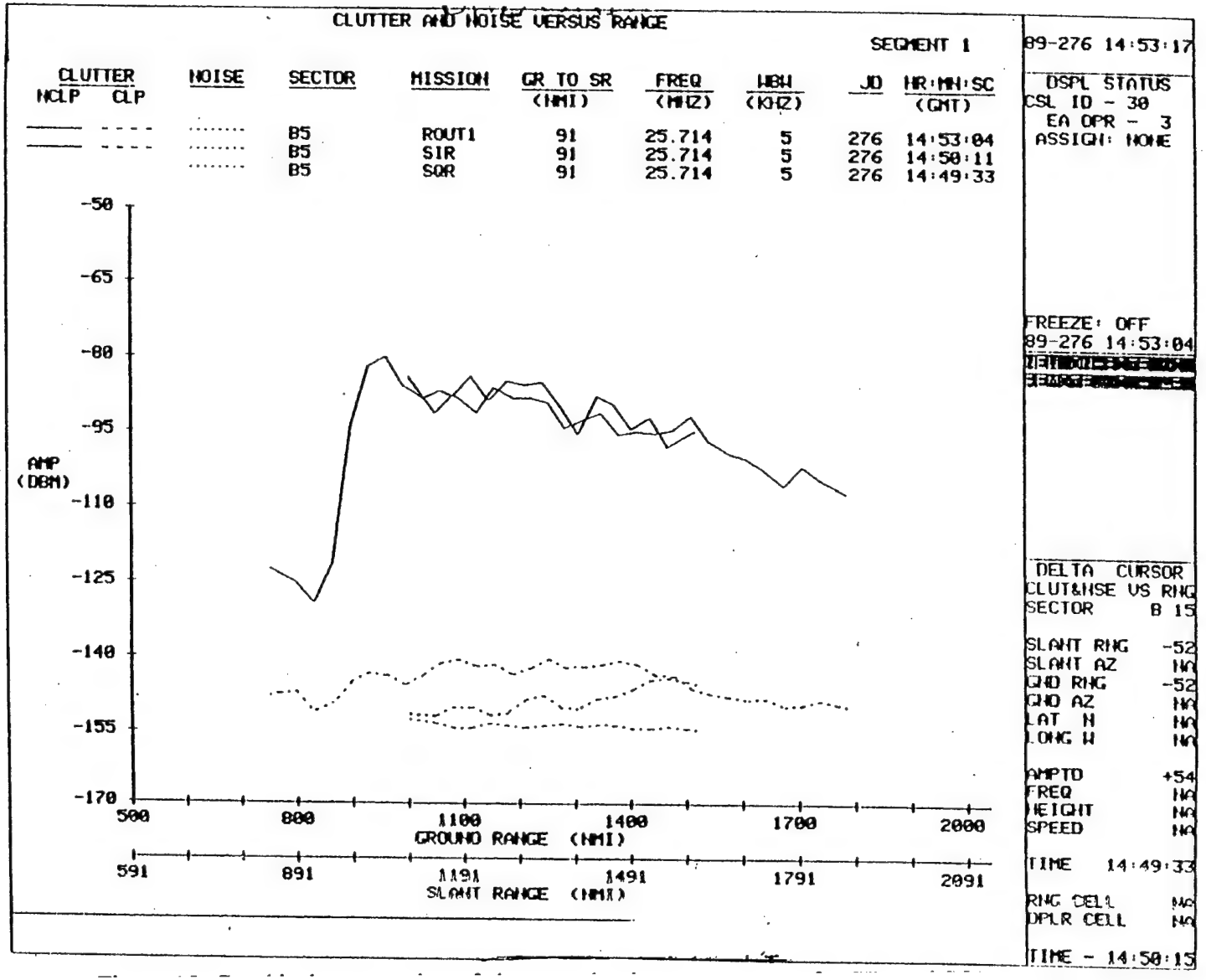

Figure 15. Graphical presentation of clutter and noise versus range for Sector Illumination Routine (SIR) and Sector Quiet Routine (SQR).

From the ARD data one computes the ratio of the clutter peak to the clutter base. The parameter is called Normalized Clutter to Noise Ratio (NCNR), which refers to the range cell normalized at 1000 nmi from the radar shown on the horizontal axis of the ARD display (Figure 15). A display of NCNR over the coverage area shows the level of performance (good, acceptable, not acceptable) of the Radar.

Radar performance over the full 180° coverage area or separately for the three segments can be assessed in the Qualitative (color coded radar display) or Quantitative (numerical and color coded radar display) Geographic Barrier NCNR (dB) maps. An example of a Quantitative Geographic Barrier NCNR map for Segment 1 of the ECRS is shown in Figure 16. The NCNR values (in dB) are clearly readable, indicating a CNR of 50 to 70 dB, which is excellent radar performance for this segment. Figure 17 shows an NCNR map for Segment 3 during the initial phase of equatorial clutter development. The pair of lines running almost vertically at the center of the map show the sunset terminator. The right side of the terminator is in darkness. Note that in beams B37 and B38, which are sunlit, NCNR is 60 dB, but the NCNR in beams B36 to B31 to the right of the terminator reduces steadily down to 35 dB due to the enhanced equatorial clutter returns, which are range folded into the primary coverage for the primary waveform selected.

5.2.3 VERTICAL INCIDENCE SOUNDING

While the backscatter sounder is the radar's best tool for frequency management, it does not provide information essential to the Coordinate Registration (CR) process, namely the reflection height of the radar signal as a function of operating frequency, range and azimuth. The skip distance for a specific operational frequency is a function of three quantities: layer critical frequency, layer height, and layer shape or half thickness. If the layer height goes up (down), or the critical frequency goes down (up), the skip distance increases (decreases). The layer shape (or half thickness) affects the skip distance too, albeit less severely. It is not possible to separate either variable directly from backscatter measurements, therefore measuring the skip distance does not (at least not without substantial modeling and assumptions) permit the determination of the reflection height. However, this information can be directly determined from the ionospheric

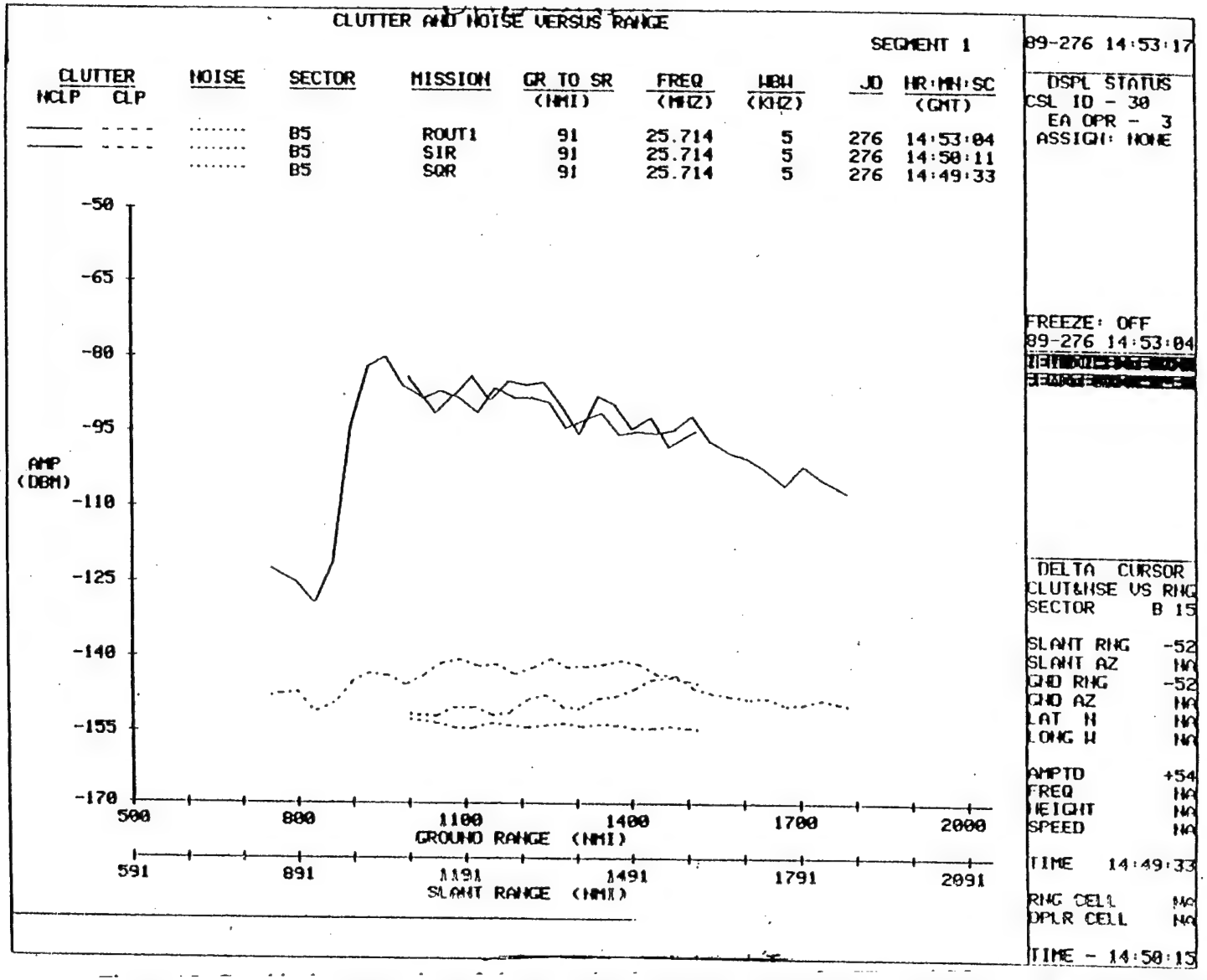

Figure 16. Quantitative plot of Normalized Clutter to Noise Ratio (NCNR) for segment 1 of ECRS for all 8 sectors showing acceptable radar performance.

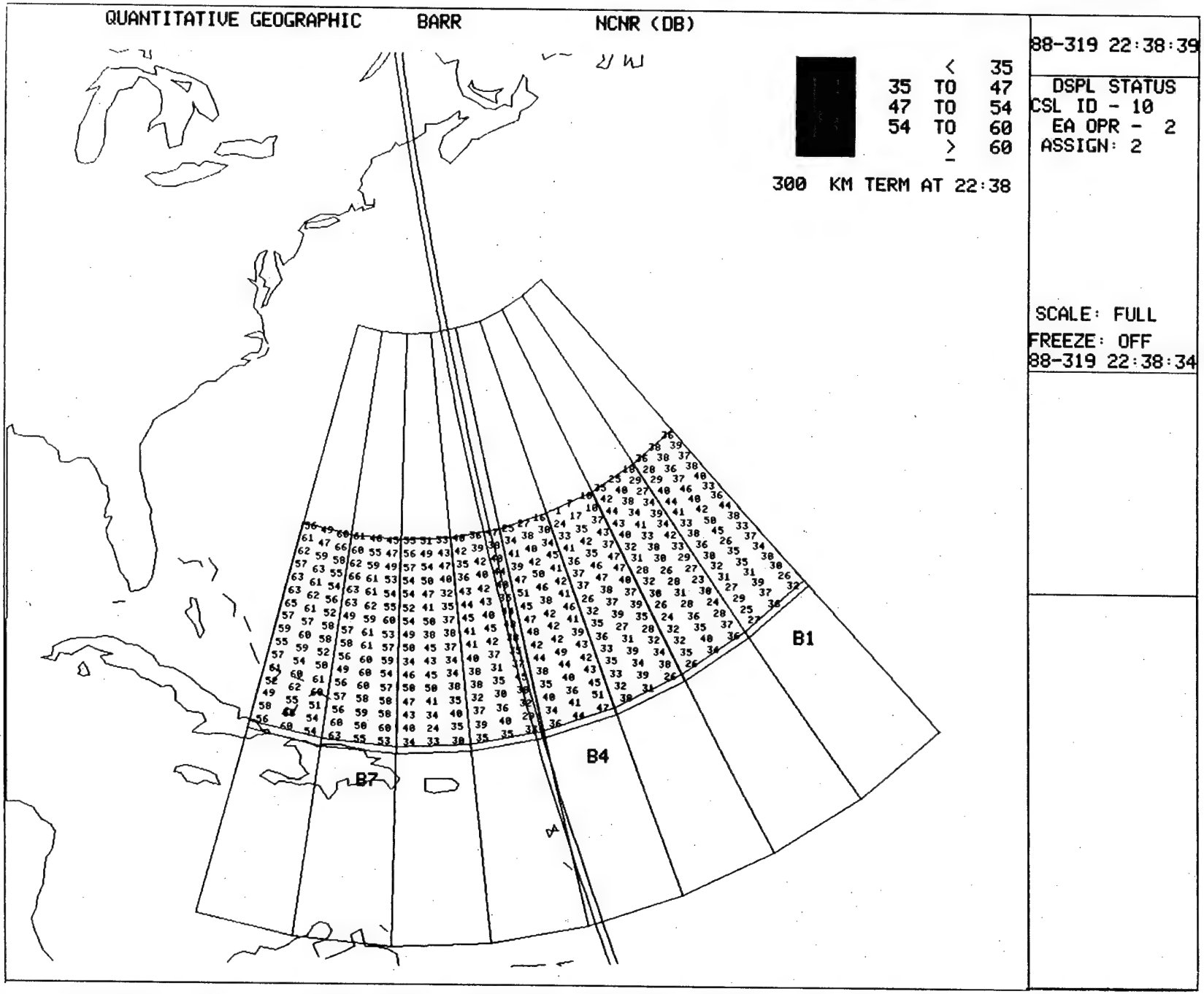

Figure 17. Quantitative plot of Normalized Clutter to Noise Ratio (NCNR) for segment 3 of ECRS for all 8 sectors showing degraded radar performance due to equatorial clutter.

profile measured by an ionospheric sounder at or near the mid or reflection point of the radar propagation path to the barrier. It is this midpoint ionosphere that controls operating frequency and reflection height.

It is fortunate that the midpoint ionospheric regions to barrier distances of 1100 nmi and greater can be monitored in Segment 1 from Goose Bay and Argentia, and for Segment 3 from Bermuda. To provide continuous ionospheric data, the Air Weather Service has deployed three Digital Ionospheric Sounding Systems (DISS) at these locations. These DISS provide, each quarter or half hour, ionospheric soundings or ionograms to the ARTIST^2 (Automated Real Time Ionogram Scaler with True height analysis) processor, which identifies the overhead trace, from which it derives the electron density profile and determines the major ionospheric parameters. In a later section we will show an example of an ionogram from a DISS Vertical Incidence (VI) Sounding.

The relation of oblique frequency and reflection height to the reflection area ionosphere have been discussed in detail by G. Sales (PL-TR-92-2123). Computer overlays are available at the Tactical Operations Room, EA console, which permit the determination of the reflection height as a function of range for the radar operational frequency or any other selected frequency.

5.3 Coordinate Registration

5.3.1 INTRODUCTION

Several successive actions are needed to operate the radar properly. First the operator selects a proper operating frequency (in the range 5-30 MHz) along with an appropriate elevation angle setting of the transmitting antenna for illuminating a selected ground region. The radar energy illuminating the ground is propagated through the ionosphere by refraction. The operating frequency selected and the elevation angle at which the beam is projected from the antennas depend upon the height at which the reflection would take place and on the effective vertical frequency fv (at the point of reflection), which is a function of the electron density and its altitude distribution. The return signal from the ground or targets reaches the receiver by ionospheric reflection. The time delay (Δt) measured from start of transmission to the time of received signal provides the slant path length ($R = 0.5 * C * \Delta t$ displayed along the y axis in the

vertical/backscatter ionogram) traversed by the ray in the ionosphere. Using the known ground feature(s) (displayed on the backscatter ionogram) at a known distance from the transmitter (ground range) and the time delay, the operator determines the mode of ionospheric propagation - single hop, double hop, or mixed modes, which enables him to determine the virtual height and the point of reflection. The range and virtual height (as a function of operating frequency) are the basis of the coordinate registration tables of the radar system. Knowing the beam azimuth, the CR table allows the operator to convert the observed time delays (measured in Δt) of the targets (such as aircraft identified by Doppler technique) in the illuminated region to geographic coordinates and flight tracks . Thus we see that the ionosphere is an integral part of the operation of the radar. So it is essential to have the ability to predict and specify ionospheric conditions to operate of the OTH radar system.

In the following section we will consider in detail the necessity of using the ionospheric model. Then we will describe the AN/FPS-118 Ionospheric model[1] developed by General Electric (GE) for the support of the OTH radar operation. We will see how this model is applied to the functioning of the OTH radar system through the use of the coordinate registration system.

5.3.2 BACKGROUND: NECESSITY OF AN IONOSPHERIC MODEL

5.3.2.1 Oblique Ray Path

The frequency chosen for radar operation depends on the electron density distribution with virtual height at the reflection point (for example from a model such as ITS78/IONCAP). The associated oblique path geometry is shown in Figure 18. The ray takes off at an elevation angle Δ. The ray path is close to horizontal while penetrating the E layer (the operating frequency is not much larger than f_oE) and the ray enters the F layer at an elevation angle comparable to Δ. Around the point of reflection the ray bends and has a symmetrical downgoing path (assuming a uniform horizontal distribution of electron density with altitude). In the example shown the ray is reflected from the ground and follows the same path back to the transmitter/receiver. The true height for the reflection of the ray is h, whereas the apparent virtual height at reflection measured from the time delay between transmitted and received signal is h′, and the apparent path traveled by the ray is AB′C - CB′A. The vertical frequency, fv, at

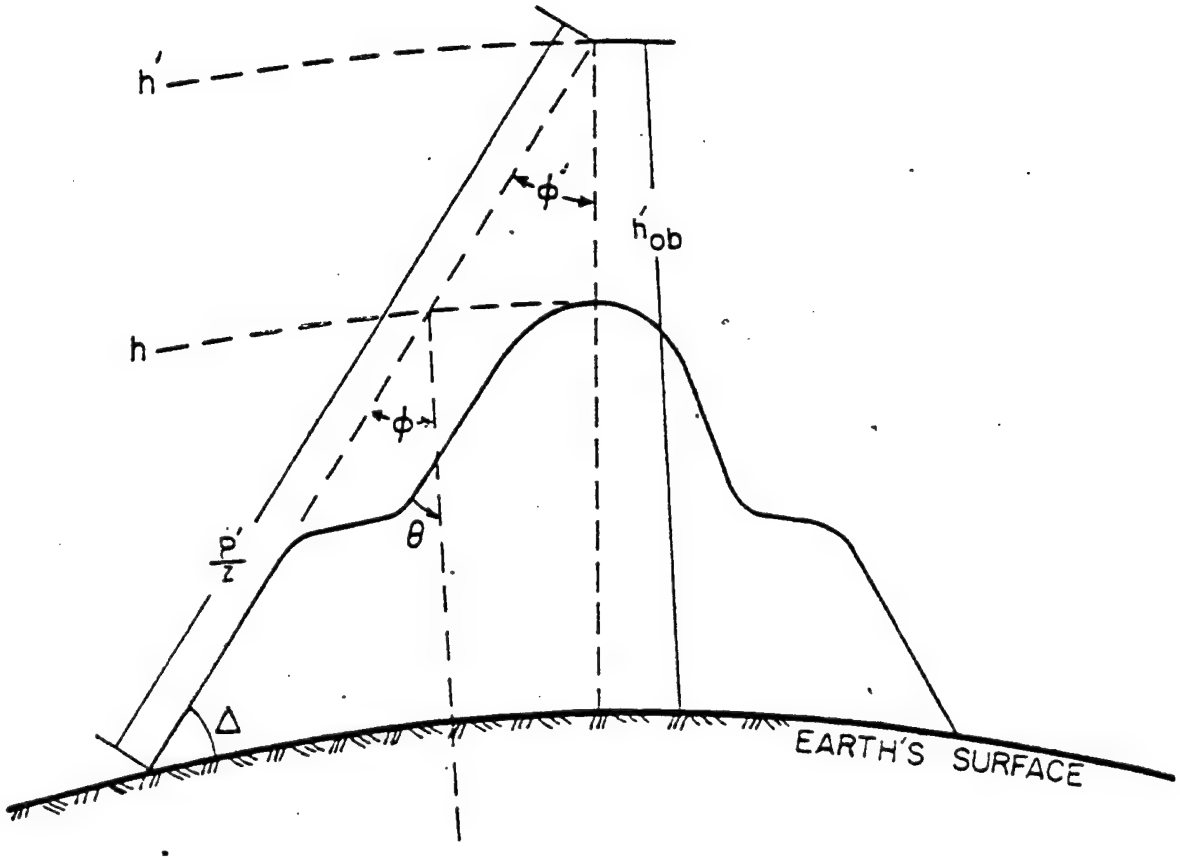

Figure 18. Geometry of the oblique Ray path.

true height h is related to the radar operating frequency F_{op} (operating/oblique) by the relation

$$F_{op} = f_v \sec \phi \quad (1)$$

where ϕ is the angle between the apparent ray path and the normal to the ionosphere at the true height of reflection. The virtual height h′ of the oblique path is related to Δ by the equation

$$\sin a \cos \Delta = \sin(a+h)/\sin\phi \quad (2)$$

where

Δ - is the takeoff angle of the ray,

a - is the radius of the earth,

h- is the true height,

h′ - is the virtual height of the oblique path and

ϕ - is the angle between the virtual ray and normal to the earth at h′.

Therefore, it is essential to know the electron density distribution at the expected point of reflection to select an operating frequency. The needed ionospheric parameters are measured using a technique called Vertical Incidence (VI) Sounding.

5.3.2.2 Vertical Incidence Ionogram

Figure 19 shows a Vertical Incidence Ionogram from Bermuda, which is in the Air Weather Service network. Using the computer software that is an integral part of the system, the machine is able to extract the parameters from the ionogram. The software that extracts the parameters is called ARTIST[2] for Automatic Real Time Ionospheric Scaler with True Height. In the figure the horizontal axis is the probing frequency in MHz. The vertical axis is the virtual height at which the signal is reflected and returned to the ground. The virtual height is given by h′=(C*Δt)/2. In this example the signal trace starts at 2.5 MHz. This starting frequency is called f_{min}. The E layer is seen around the virtual height of 120 km. The sudden jump in the trace around 4.1 MHz indicates the start of the F_1 layer. E and F_1 are typical daytime features and are absent at the night time. Another break in the curve around 6.7 MHz is due to reflection coming from the F_2 layer. Note the two traces in the ionogram. The left hand side trace is due to the ordinary ray. The other trace displaced to the right is due to splitting of the ray due to earth's magnetic field. This trace is called the extraordinary ray. Around 9.2 MHz the ordinary ray

FOF2	FOF1	M'F	M'F2	M3000	FMIN	FOES	MUF	FMINF
9.1	***	210.	****	2.58	2.5	3.7	23.5	4.1

FXI	FMINE	FOE	M'E	M'ES	QF	QE	FF	FE
9.9	2.5	3.7	100.	100.	***	***	***	.2

AUTOSCALED TRACES [KM]:

4.	*****	215.	210.	211.	216.	221.	226.	236.	241.	251.
5.	261.	266.	276.	281.	286.	296.	301.	311.	316.	326.
6.	331.	341.	346.	351.	356.	361.	366.	371.	376.	381.
7.	381.	386.	391.	391.	396.	401.	406.	411.	416.	421.
8.	426.	436.	446.	456.	466.	481.	496.	516.	536.	566.
9.	596.	641.								
2.	*****	*****	*****	*****	*****	100.	100.	100.	100.	100.
3.	105.	105.	105.	110.	110.	115.	120.	130.		

NORMALIZED AMPLITUDE AS AT REFLECTION HEIGHT 100KM IN [DB]

	TOPF	3	4	5	6	7	8	9 [MHz]
F	32	0	51	63	63	56	50	
E	22	51						
ES	22	51						

PROFILE - ULCAR

W = .0 KM

	FSTART [MHZ]	PEAK HT [KM]	A0 [KM]	A1 [KM]	A2 [KM]	A3 [KM]	A4 [KM]	DEV [KM]/PT	ROOTS
E	.199	101.417	-17.844	1.233	.172			2.2	-
F1									
F2	3.710	330.500	-197.429	-37.918	8.863	-.141	-2.467	9.3	-

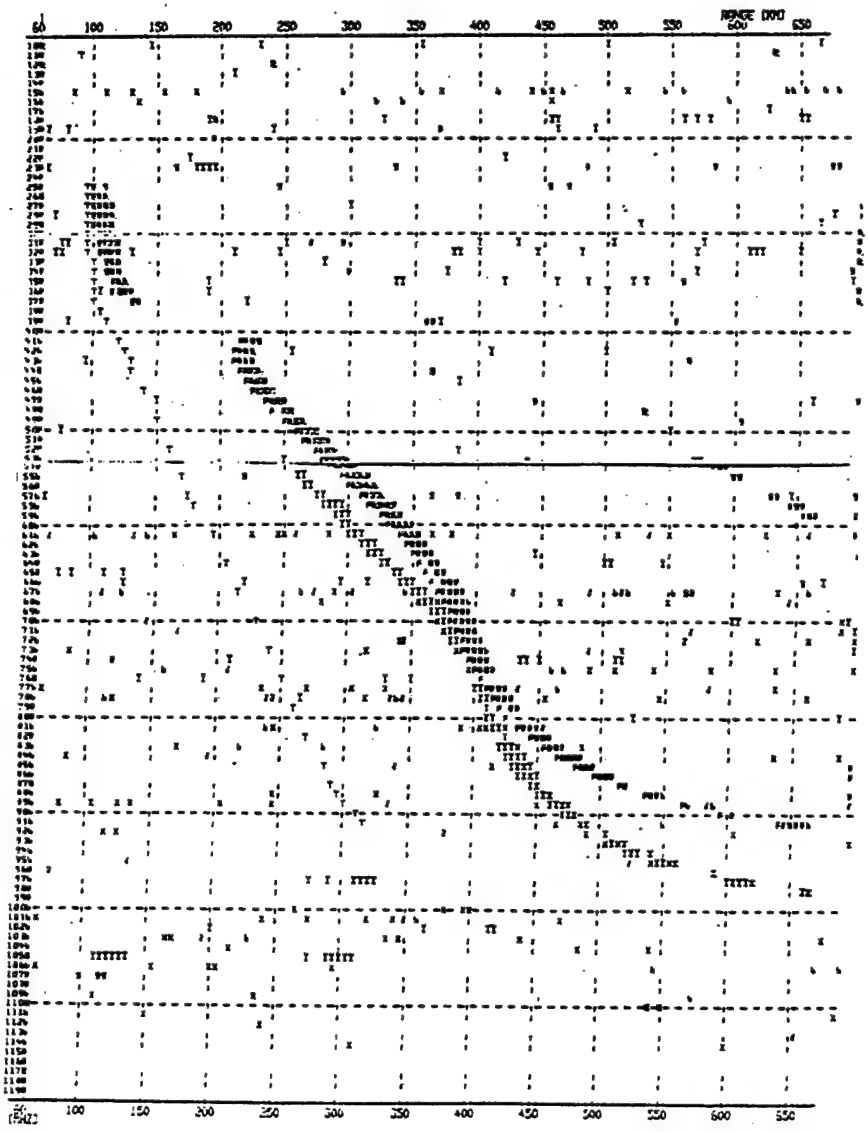

Figure 19. Vertical Incidence Ionogram , Ionospheric Layer Parameters (IONOS) and Observed Virtual Height (IONHT) codes from DISS system at Bermuda.

trace is vertical. The ray penetrates the ionosphere with no reflection received at the ground. The penetration frequency of the extraordinary ray is 9.8 MHz. The parameters extracted by ARTIST from this ionogram are tabulated in the figure. Note the curve plotted by letter T's - which is the true height determined for the signal trace of the probing frequency. The virtual height is greater than the trace height because the ray suffers retardation during its propagation through the ionosphere. The higher the frequency, the deeper it penetrates into the ionosphere, and the more it is retarded. Thus, the difference between true height and virtual height increases with increasing frequency. The ARTIST software of the DISS system extracts two forms of parameters: IONOS (ionospheric layer parameters) and IONHT (the observed virtual height trace). These are printed, starting at the left hand side of the figure. These codes (ionospheric parameters) are sent in real time via dedicated communication lines to the radar operations center to support the ionospheric model residing in the radar system. Such routine measurements are useful for determining the statistical variability of the ionosphere. These data form the basis for the development of the ionospheric models. To the operator the real time data display is important for determining the radar operating frequency by use of overlays (discussed later).

5 3.2.3 The Ionospheric Parameters

Because the ionosphere plays an important role in allowing (or not allowing) a certain radar operating frequency to illuminate the ground (range larger than the skip distance) let us take a brief look at the ionospheric parameters. The ionospheric layers are shown schematically in Figure 20. The horizontal axis shows the critical frequencies for the three layers, E, F_1, and F_2. The vertical axis shows the extent of each layer. The layers are assumed to be parabolic in shape. The true altitudes for the peaks of the layers are marked by h_mE, h_mF_1, and h_mF_2. The semi-thickness of each layer is shown by y_mE, y_mF_1, and y_mF_2. E and F_1 layers are solar controlled layers. Both these layers decay very rapidly after sunset. The F_1 layer is more of a midlatitude phenomenon. The F_2 layer, although solar controlled, has more complex behavior. In the midlatitudes the strongest feature at night is the slowly decaying F_2 layer. The parameters: critical frequency, true height of the peak electron density, and the semi-thickness for the three layers E, F_1, and F_2 are modeled for a statistical presentation of the ionosphere (empirical model)

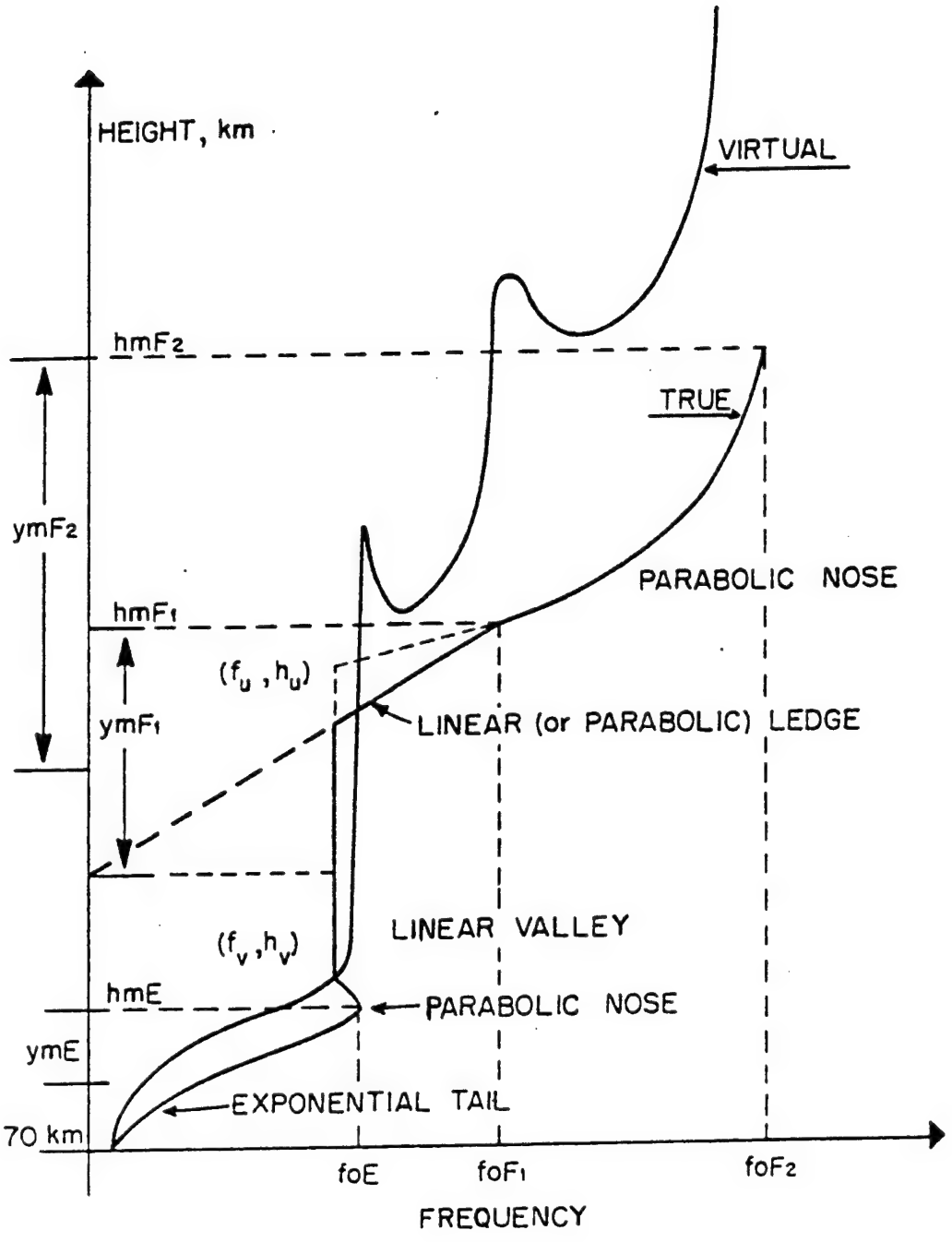

Figure 20. Ionospheric Layers

as a function of sunspot number (or solar flux at 10.7 cm), geographic latitude, longitude, diurnal and seasonal variations. An additional parameter commonly modeled is the Maximum Usable Frequency (MUF) for a standard distance of 3000 km. This is experimentally obtained by using a frequency-distance overlay on the ionogram. We will later see an example of the overlay technique. Most of these parameters and the virtual digital ionogram for the DISS stations deployed in support of ECRS (and WCRS) are displayed at the control panels. Let us see how the ionosphere controls the radar operation.

5.3.2.4 Skip Distance and Range

The importance of the ionosphere in the selection of operating frequency for illumination of a selected ground region is shown in Figure 21 by use of the ray-trace[3] technique. With a given ionosphere the ray-trace technique computes the ground range, group path (true height), phase path (virtual height) and the signal strength for a given ray (elevation angle and operating frequency). The ray-trace technique allows one to determine if a given ray will reach the ground (reflection) or will penetrate the ionosphere. The OTH radar cannot use any ray that does not reach (reflect back to) the ground. The figure is divided into six sections. The operating frequency is shown by the bold number in the left-hand top corner of each section. The elevation angles of the respective rays are shown along the line at the top of the section. The ray paths for the respective elevations are shown in each section. The horizontal axis is the ground range of the ray and the vertical axis shows the (true) height of reflection. Note that for a given operating frequency the ray travels to higher altitudes, but the ground range decreases as the elevation angle is increased. As the operating frequency increases the ground range increases. Note that in this example, for an operating frequency of 15 MHz the ray with a 19° elevation angle penetrates the ionosphere and does not reach the ground (no reflection possible). An additional point to be noted is the shortest distance (skip distance). For an operating frequency of 5 MHz and an elevation angle of 17° the skip distance is 530 km, whereas with this ionosphere the maximum skip distance is 2930 km for the operating frequency of 21 MHz with an elevation angle of 3°. Also note that for the same operating frequency, rays with elevation angles of 5° and 7° have larger range than rays with 3° elevation angles.

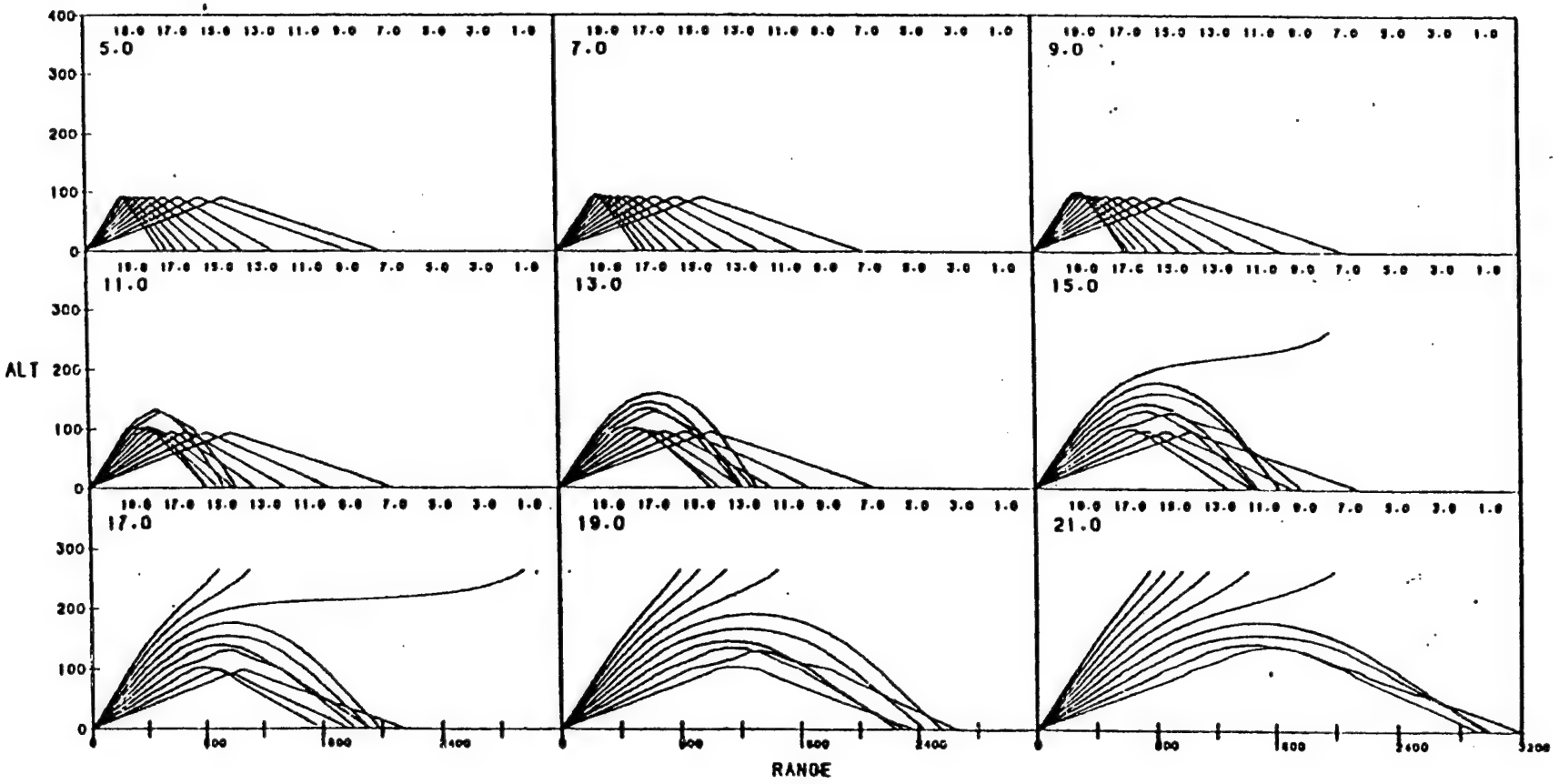

Figure 21. Ionospheric Raytracing

Thus we see that operating frequency and the ground range strongly depend upon the ionospheric distribution of electron density. The elevation and operating frequency are combined for reaching the selected ground range. Ranges less than the skip distance cannot be reached because the ray penetrates the ionosphere and cannot be used for ground illumination. Thus, the ionosphere with given (existing) electron density and its altitude distribution is critical for the success of the radar operation. One may wish to rely on some kind of ionospheric model for specifying the ionosphere at a given location and time, to ensure successful radar operation. Note that setting the barrier (that is, illuminating a certain region of a given width (500 nmi) along the radial direction from the transmitter) cannot be guaranteed due to a lack of suitable operating frequency and elevation angle which would enable the radar energy to reach that region, at the given time. Also note that in Figure 21 a given operating frequency (17.0 MHz) may reach the same ground region (≈1800 km) by reflection at E layer (E - mode) and/or reflection at F_2 layer (F_2 mode). This is called multimode. Also, the mode may switch, with the signal traveling over the forward path from the transmitter to ground by one mode and the return path from ground to transmitter by a different mode, which results in a mixed mode. In multimode operation the path length corresponding to each mode is different. As a result the signal strength of the received signal varies due to losses along the respective paths. Also, the multiple modes can generate multiple signatures for the same single target. For accurate location of the target the operator must isolate and identify the modes. For this purpose the specification of the ionosphere, that is, some realistic ionospheric model or real time measurement, is essential.

The widely varying ionospheric environment that will be experienced by the radar is shown in the following.

5.3.2.5 Variability of the Ionosphere

Large variations in the ionosphere are shown in Figures[4] 22 and 23 from observations at Goose Bay. Figure 22 shows the observed median hourly values of f_0F_2 for the calendar year 1976 with low sunspot activity (SSN = 14). The local time is along the horizontal and the month is along the vertical. The observed f_0F_2 contours are shown by dashes. Note that the highest f_0F_2 of 6 MHz occurred at 1400 L.T. in November. The lowest f_0F_2 of 2 MHz is seen for practically

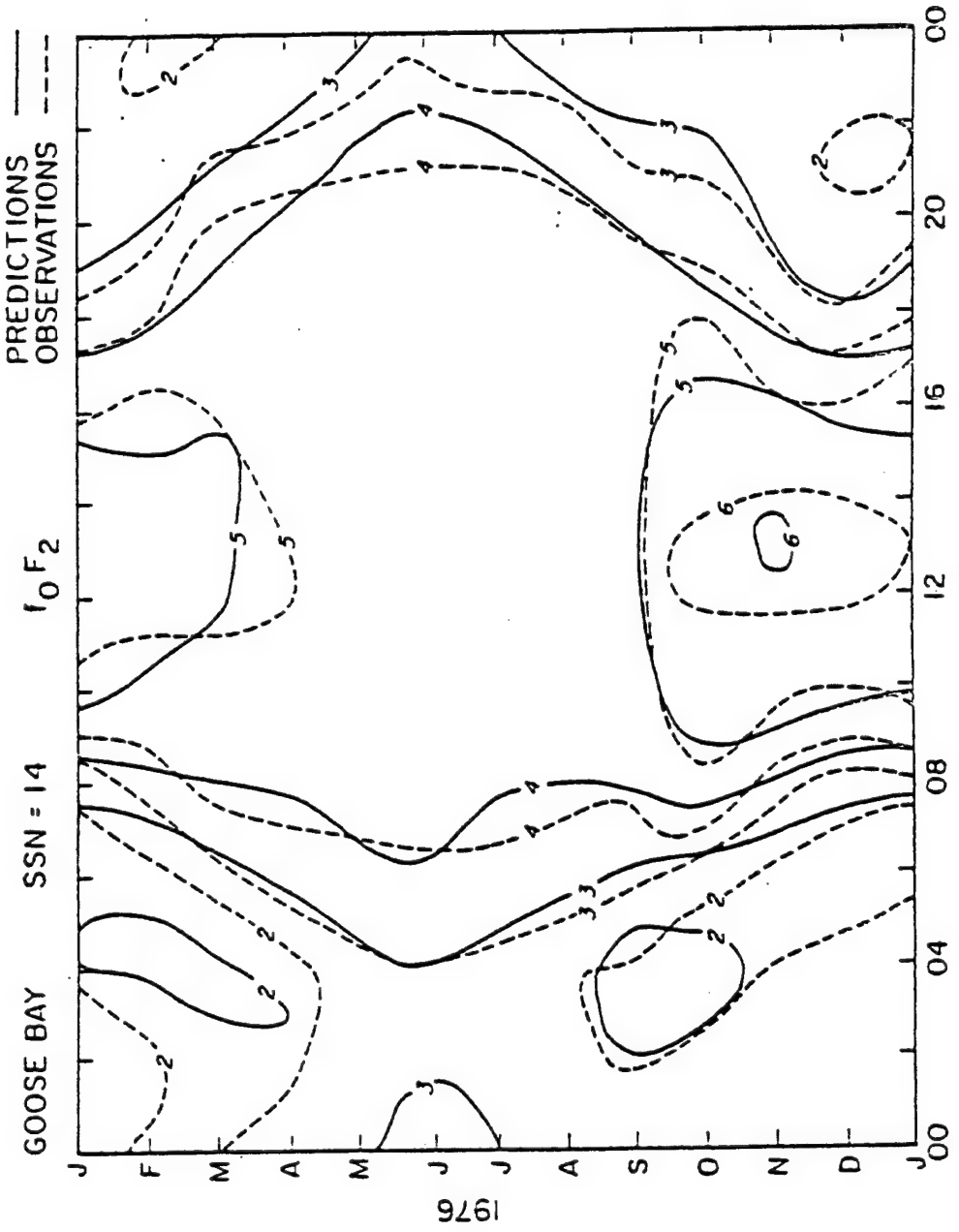

Figure 22. Monthly Median contours of f_0F_2 for low sunspot activity (SSN=14) for Goose Bay.

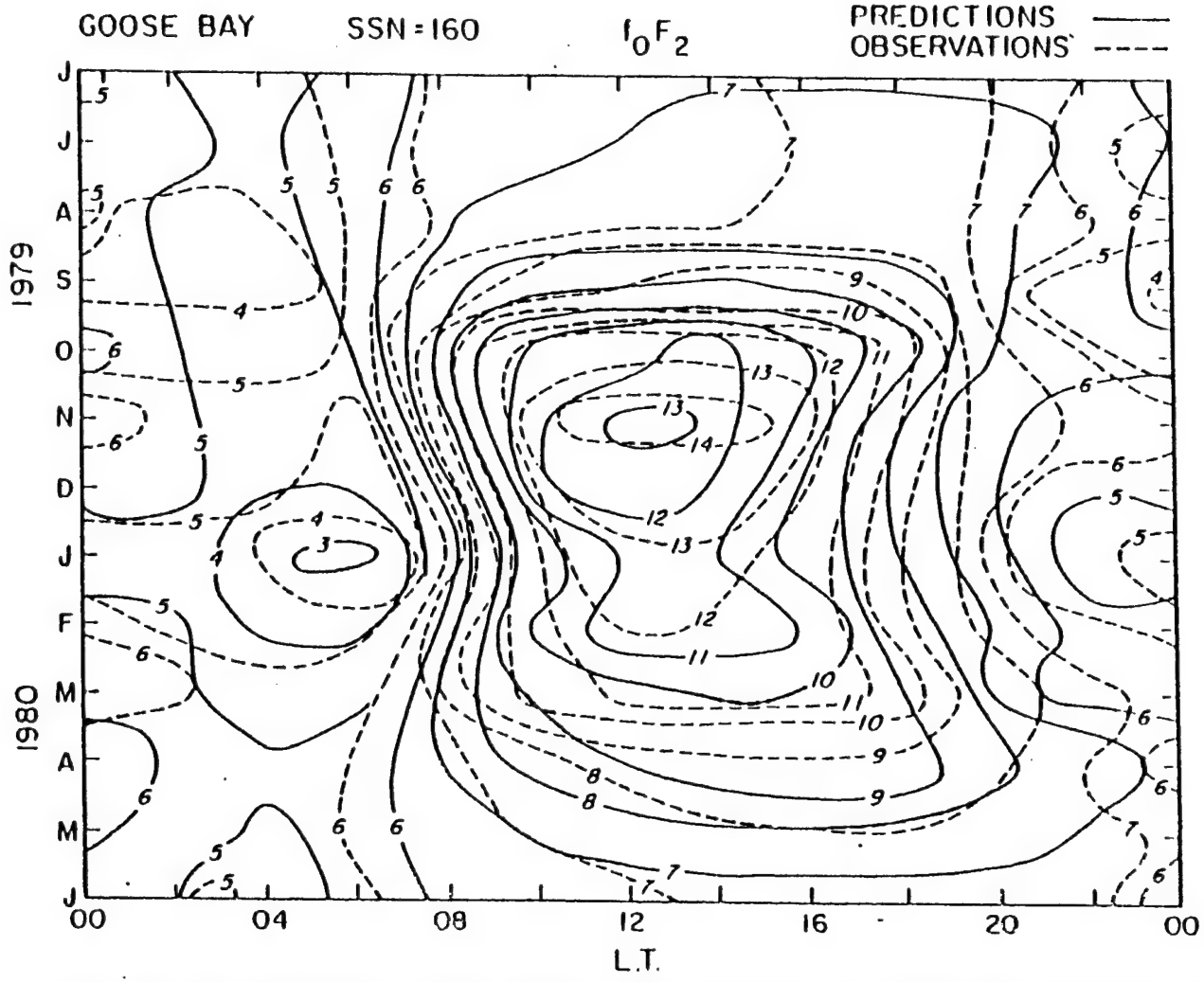

Figure 23. Monthly Median contours of f_oF_2 for high sunspot activity (SSN=160) for Goose Bay.

half the year during night hours. Thus a diurnal variation by a factor 2-3 is seen. The seasonal variation is 4 to 6 MHz during post noon hours.

Figure 23 shows the contours at the same station for 1979-80, a period of high sunspot activity of SSN = 160. Note that the diurnal variation has a factor of 2, and the solar cycle change between Figures 22 and 23 produces a change in f_0F_2 of a factor of 2. Also note that around morning and evening hours there is a rapid change in f_0F_2 as shown by the crowding of the f_0F_2 contours. Thus, for a given location, the diurnal change in f_0F_2 can be (14/2 = 7) a factor of 6-7.

The rapid variations in f_0F_2 during transition periods at sunrise are shown for four stations during a time of low sunspot number in Figure 24 and for five stations during a time of high sunspot number in Figure 25. Figure 24 shows percent change per hour in f_0F_2 for low sunspot (14) activity and Figure 25, for high sunspot activity (160). Note that the change per hour in f_0F_2 is quite large (50-60 percent) for a few hours. This rapid change is a regular phenomenon. For the radar it translates to frequent changes in the operating frequency. Our[4] estimates show that radar frequency may have to be adjusted every 8-10 minutes during the transition period. A good short period prediction/specification of the ionosphere during these periods will help the radar to keep in phase with the rapid changes.

5.3.2.6 Using Backscatter Ionograms

For frequency management, backscatter ionograms are used routinely. This approach is not successful at all times and for all regions. For example, in the northern section of the East Coast Radar System (ECRS), auroral activity produces unwanted spurious auroral clutter noise, which degrades the radar operation. Also, when the ionosphere is disturbed or weak (at night) the backscatter sounder is unable to identify the ground signatures that are essential for selecting the operating frequency for the proposed barrier. The ground signal could be weak for various reasons, such as increases in noise due to auroral clutter, which produces enhanced losses in the ground signal strength, or due to low electron density in the ionosphere, which reduces the reflection strength of the signal. Also, the midlatitude trough region, which is a night time high latitude (northern for both ECRS and WCRS) phenomenon, produces strong vertical gradients.

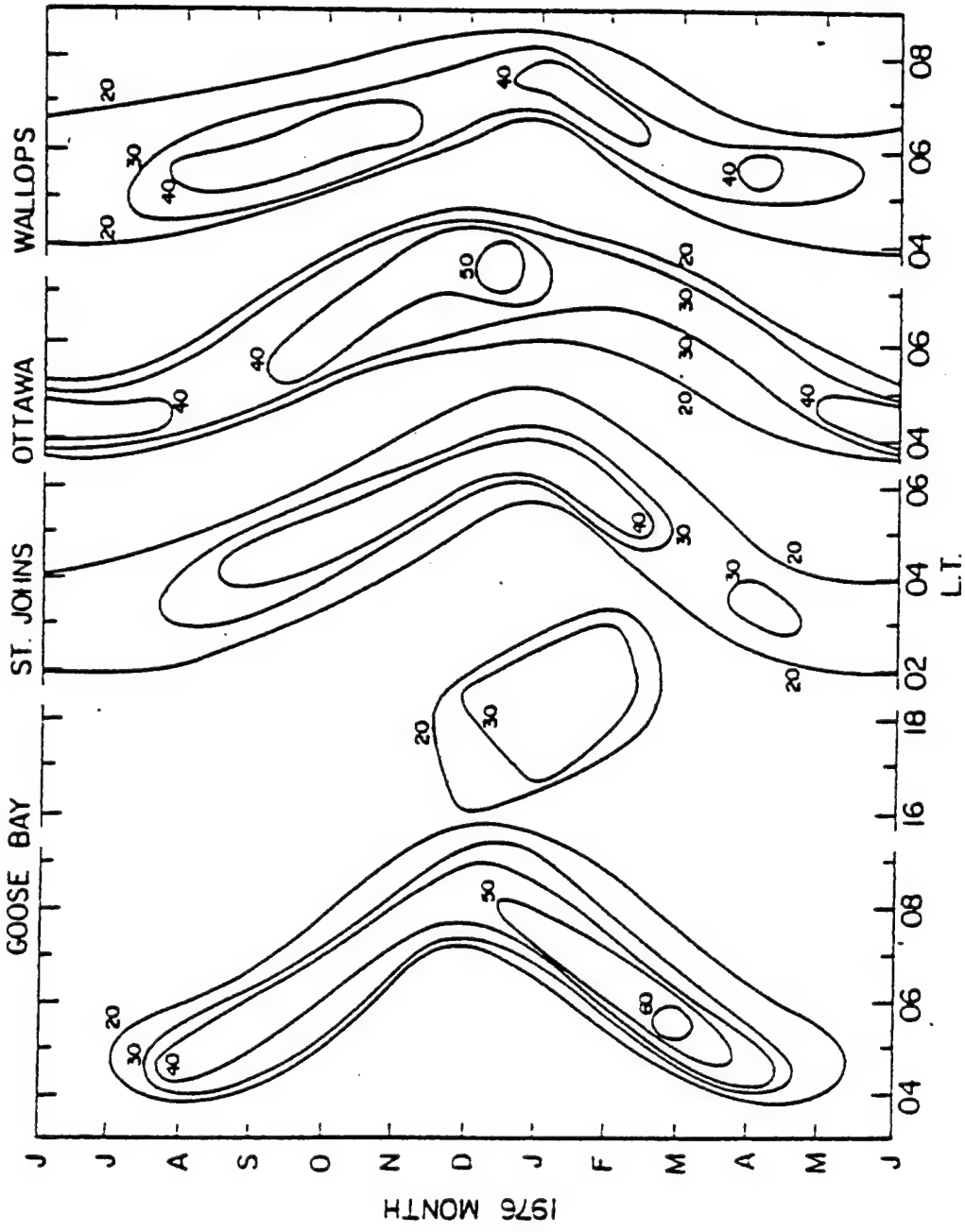

Figure 24. Percent increase in f_0F_2 during morning hours for low sunspot activity.

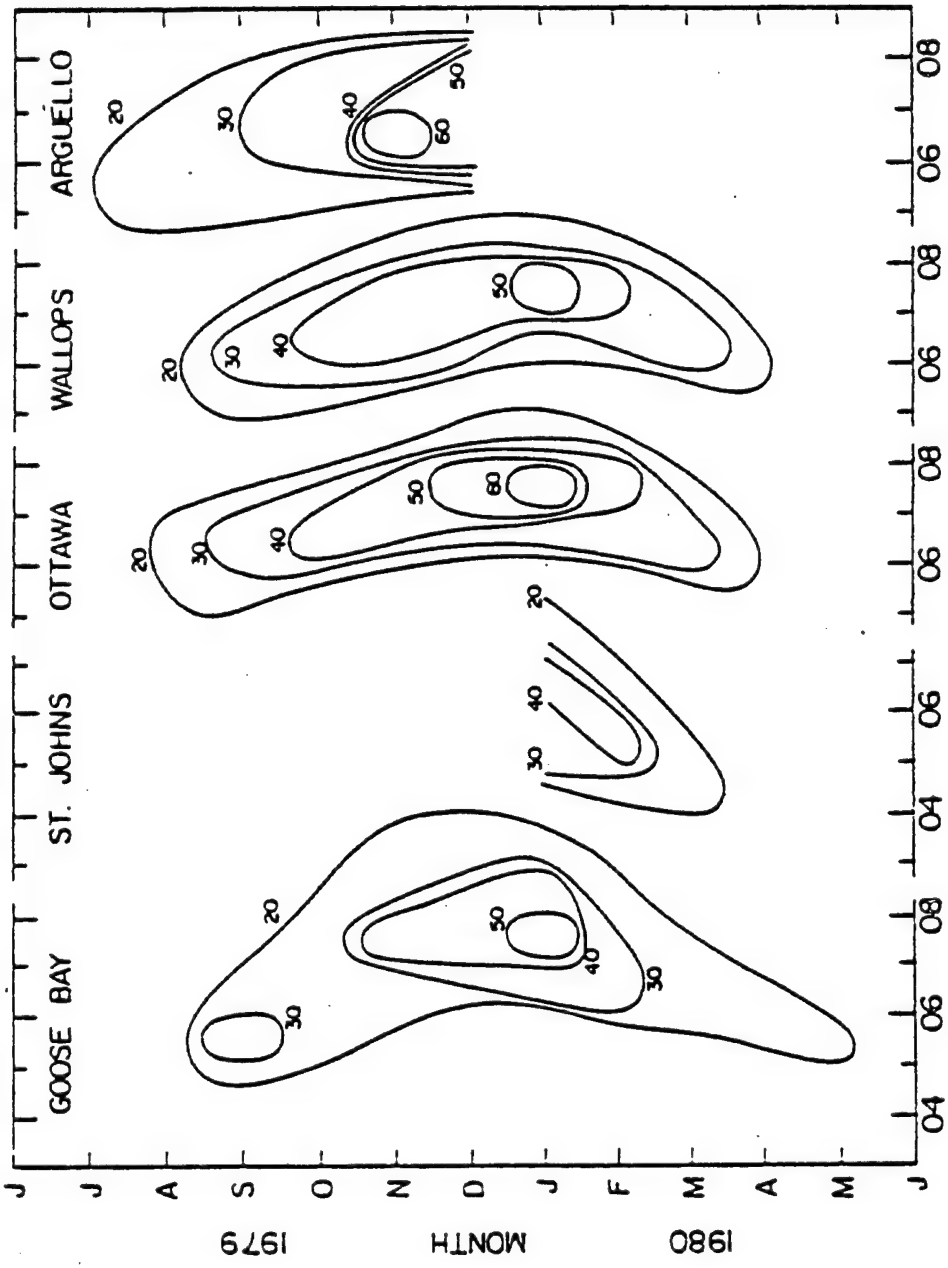

Figure 25. Percent increase in f_oF_2 during morning hours for high sunspot activity.

These strong gradients affect the expected ray paths. In the south looking section of ECRS one sees the folding over of long ranges from the equatorial anomaly. In unusable backscatter sounding cases, an alternate solution is to rely on some realistic ionospheric model for determining the operating frequency that will illuminate the selected ground range.

5.3.2.7 Radar Operation Frequency Using Overlays on Ionogram

One of the ways to select the radar frequency is to deploy a vertical incidence sounding system under the expected point of reflection and collect real-time data. An overlay of range versus elevation angle curves for a selected frequency is placed over the real time observation ionogram, and checks of overlays for different frequencies lets the operator determine the operating frequency. Figure 26 shows as an example, an operator panel display of the ionogram from the remote site Argentia, which is in the reflection region of part of segment 1 of the ECRS. The left-hand side curve marked by SE, PF_2 is the virtual height ionogram. The overlay (at 15 MHz) shows two variables. The slanting lines that are nearly horizontal show the ground range; 200 km to the right end and 1800 km to the left end. The nearly vertical curves are the elevation angles from 2° to 42°. The curve that is tangent to the ionogram indicates the focusing edge at the selected frequency and ground range. For the ionogram in Figure 26, the 15 MHz frequency provides F_2 mode illumination in the ground range interval of 1200 to 1600 km.

As it is impossible to conduct such measurements at each expected point of reflection for all radar coverage, an alternate is to synthesize an ionogram from layer parameters from a realistic model. This involves computations of the virtual height from true height layer parameters.

Thus, a reliable ionospheric model is very useful to help select the operating frequency, and finally to determine of the target location accurately. For this purpose General Electric Company (GE) developed the AN/FPS-118 model[1] in support of the OTH radar.

5.3.3 The AN/FPS-118 Ionospheric Model

This model is the updated version of the AFGWC polar model[5] developed by the US Air Force Global Weather Central (AFGWC), now called the Space Forecast Center (SFC). The

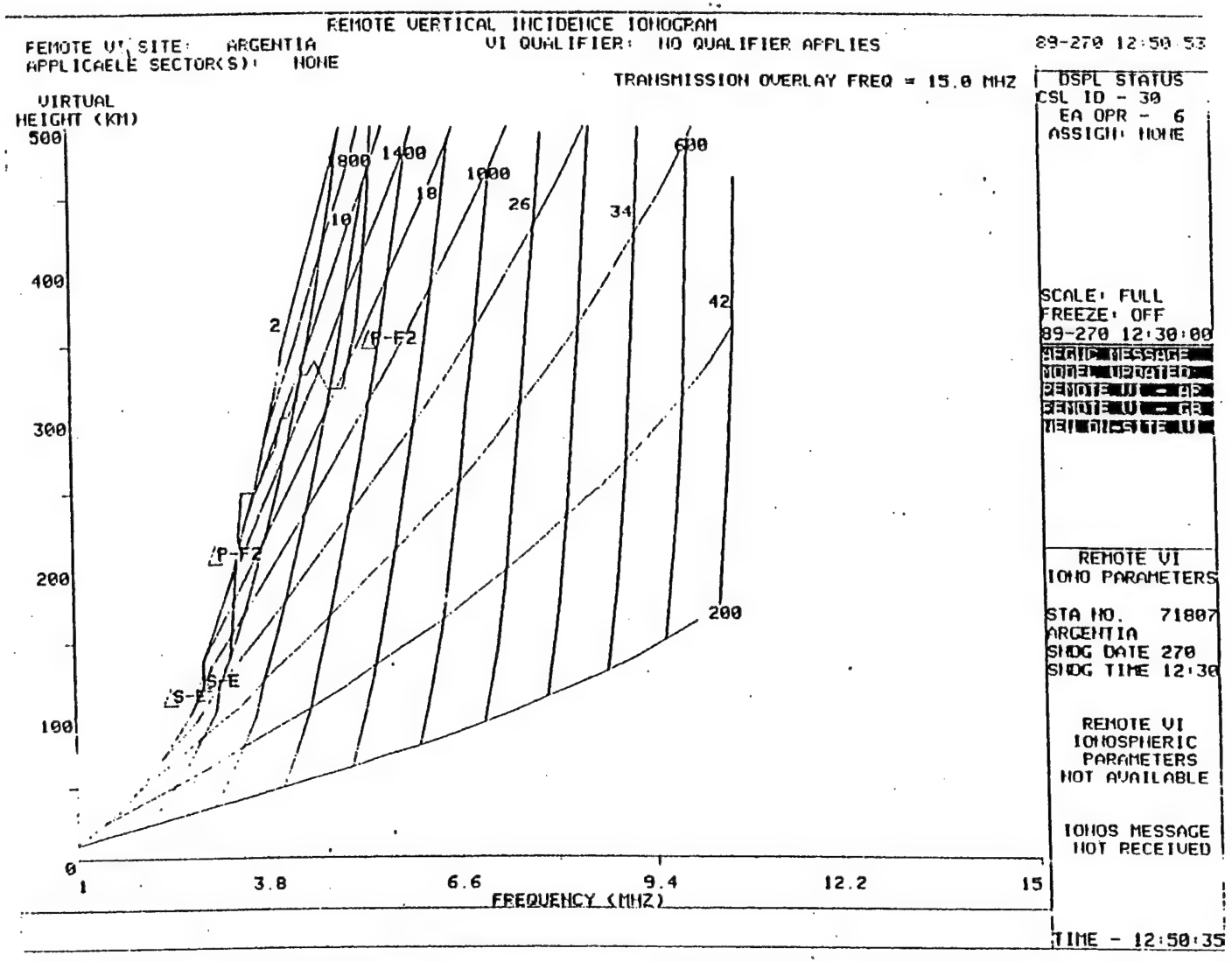

Figure 26. Range frequency overlay on vertical incidence ionogram for estimating best elevation angle for the selected barrier distance from the transmitter.

AFGWC Polar model uses the ITS-78 ionospheric model[6] as its starting point. (AFGWC model development started well before the evolution of the IONCAP[7] model). The basic model is driven by an effective sunspot number computed by AFGWC from f_0F_2 data for the past five days from a real-time or close to real-time network of up to 50 global ionospheric stations. From the study of Rush and Gibbs[8] the best prediction available for f_0F_2 was found to be a five day weighted average that is approximated by the least squared deviation fit of the ionospheric model to f_0F_2 of the past five days, averaged for each hour. The result is in an effective sunspot number. The effective sunspot number would naturally be different from the observed daily average sunspot number R_z issued from the solar data network. This effective sunspot number is used to predict the ionospheric state for the current day. The median model prediction (from ITS-78) would be one set of values for the entire month. It is known that the ITS-78 model does not properly predict the midlatitude trough depletions and the high latitude auroral enhancements. The general behavior and the ionospheric effect of these phenomena are shown schematically in Figure 27.

The top section of Figure 27 shows the auroral and trough features in a Corrected Geomagnetic Coordinate (CGMC) system. At the center of the 85° circle is the geomagnetic pole. The inner and outer boundaries of the auroral oval are shown in the figure. Note that the auroral oval is more equatorward and wider in the magnetic night sector (at the bottom). The auroral oval is both a day and night phenomenon. The optically-diffuse continuous aurora produces the diurnal E_a layer. The aurora is generated by precipitation of the charged particles originating from the sun. The midlatitude F-layer trough is a night feature terminating at 1800 and 0600 CGMT. The depletion is due to the loss of charged particles that move upwards along the magnetic field lines of the earth.

The corresponding ionospheric features and their behavior are shown in the lower section of Figure 27. At the bottom of the figure note the enhancement due to the Auroral E (E_a) layer. The middle section shows the F layer. The F layer is enhanced in the region corresponding to the auroral E_a layer. Equatorwards of the enhancement is the midlatitude trough, with steep walls (that is, rapidly decreasing f_0F_2 frequencies). The wall on the equatorward side is less steep than the wall on the poleward side. The top curve shows the combined effect of the high latitude features.

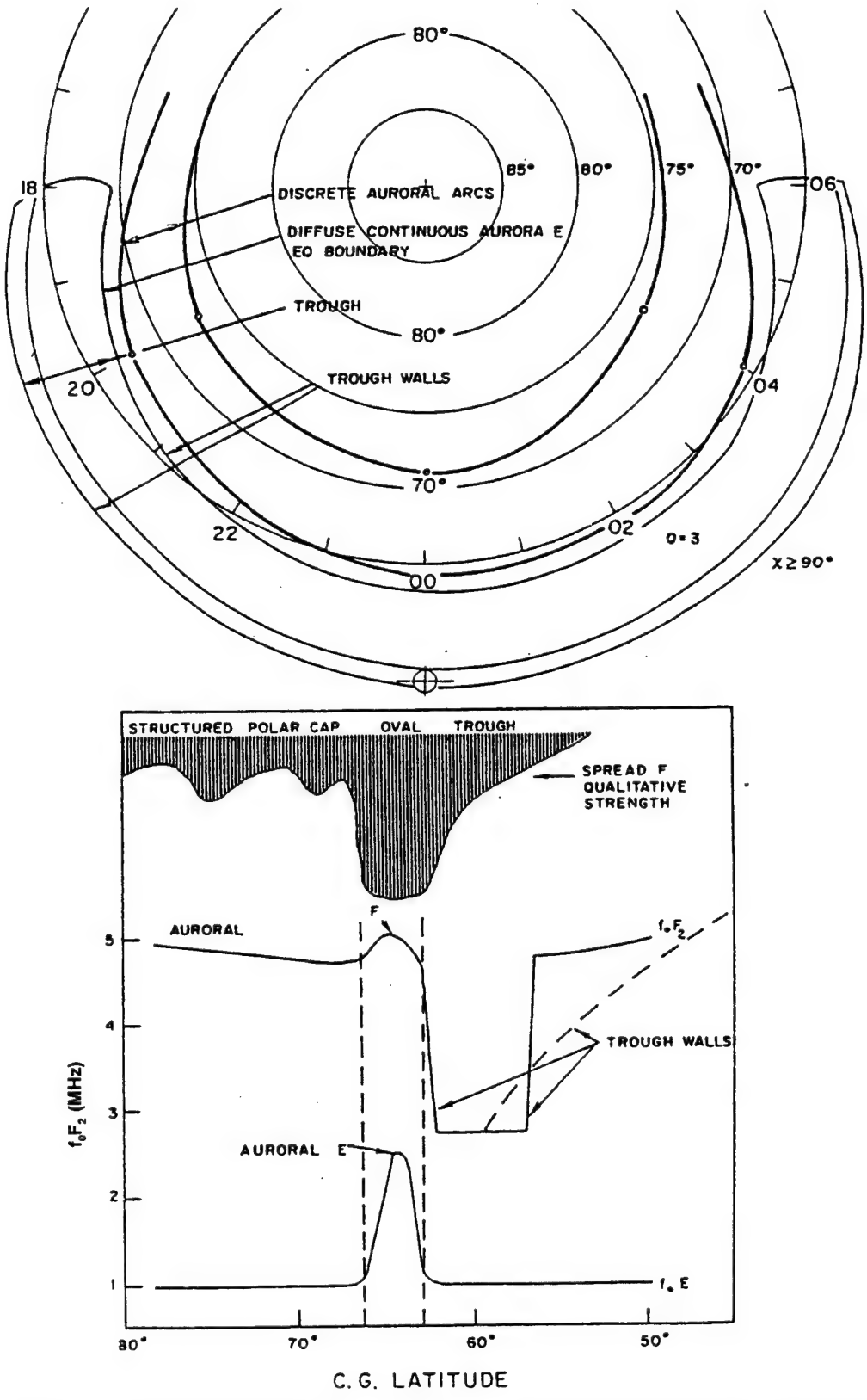

Figure 27. High latitude auroral and trough features and their effect on ionospheric spread.

This auroral feature was initially modeled by Wagner[9]. This version has been used by AFGWC in the polar model. According to this version, only the equatorward half-width of the auroral oval contributes to the auroral E_a layer.

The midlatitude F layer trough model by Miller and Gibbs[10] is used in the AFGWC polar model. This AFGWC Ionospheric Polar model is used by GE in support of the OTH radar operation. The additional feature introduced in the GE model is updating the predictions from the ionospheric model by using real-time data from several digisondes deployed in the OTH coverage area, introduction of a day time F_1 layer and provision for sporadic E blanketing input. In the following we will consider the GE approach in detail. The goal of the GE AN/FPS-118 model is to build a realistic real-time "virtual height ionogram" for grid points that are very likely to be the reflection points for the surveillance and barrier setting of the OTH coverage area. The surveillance range is from 500-3000 nmi. However the model is implemented over the 200 to 2200 nmi interval. The barrier width is 500 nmi and the start range can be set from 500 to 1500 nmi from the transmitter.

As stated before, the model is driven by the effective sunspot number determined from prior 5 day f_0F_2 observations from the AWS network of ionosonde stations. AWS computes the effective sunspot number and provides it to GE each day for running the model at the radar site. The trough part of the model is driven by the K-index of the magnetic activity. The K-index of magnetic activity, which is similar to K_p - the planetary index of magnetic activity, is computed every 90 minutes from the AWS chain of magnetometer stations (See Dandekar[11], 1982).

For driving the auroral oval, a part of the model needs the Q index. The ground-based Q index is presently available from a single station at Sodankyla, Finland. The Q index measured from a single station is good only in the midnight magnetic meridian of the station (see Dandekar[11]). Therefore AFGWC determines an effective K_p index from satellites making particle precipitation observations in the local midnight (or close) sector, and provides the value to GE. If the effective Q index is not available from satellite observations, it is determined from the Hardy equation using the K index. The Hardy equation (unpublished report)is given by $Q = 2\ K_p - 0.35$ (see Dandekar[13] for the modification to the Hardy equation, and Dandekar [12] for the assessment of the AN/FPS-118 Ionospheric model).

The ionospheric model is generated by using the effective sunspot number provided by the AWS, to compute the layer parameters: critical frequency, true height for the peak of the

layer, and the semi-thickness for the three layers and the M3000 factor for a given location and time. The trough and oval features driven respectively by K and Q are superimposed on the computed parameters. To make the model more realistic, real time data from several ionosondes located in the vicinity of the location are used for updating the model.

Figure 1 showed the OTH coverage area of the East Coast Radar System (ECRS). The names and geographic locations of the sites are listed in Table II. Of these sites, Patrick AFB, US has become operational, but the Azores site in not available, and Croughton, England has not yet become operational. Goose Bay, Argentia, and Bermuda are inside the OTH coverage area. Bangor, Wallops and Patrick AFB are on the border of the coverage. The closest grid point of the 2200 nmi extent of the coverage is 450 nmi away from the VI site Croughton. Thule is the polar station. Goose Bay is in the oval at high magnetic activity and is in the trough at low magnetic activity. Argentia is on the outside/southern edge of the trough. The real time data routed via the AWS net to the ECRS are displayed at the EA operator control panels.

The real time data update scheme compares the model prediction with the observation at the site and computes a multiplier which matches the model value with the observation. The multiplier is used for the other grid points with the condition that - midlatitude regions are updated by midlatitude VI sites, trough region grid points are updated by trough region VI sites, auroral oval region by oval VI sites and polar region grid points by polar region VI sites with no crossover between sites and the grid points which do not belong to regions with similar phenomena. Thus the model, with real-time data from the VI sites for update, should provide very realistic specification of the ionosphere in the coverage area.

With the inner-most and outer-most boundaries of the barrier at 1100 and 3000 nmi respectively, the corresponding reflection points range from 550 to 1500 nmi respectively for a single hop mode (for F_2 reflection) and for a barrier extending from 1100 and 2200 nmi, from 275 to 1650 nmi for a two hop mode for E or Es reflection. Thus, the range of grid points of major interest for model prediction for probable reflection points extend from 275 to 1650 nmi. Using the model parameters, which are in true height, one can construct a virtual height ionogram for each grid point, which provides a table of f_v vs. virtual height. Knowing the region to be illuminated (ground range and azimuth) from the transmitter, one can now use Equations 1

and 2 (Section 5.3.2.1) in conjunction with f_v-h^l tables to determine the operating frequency and elevation angle needed for illumination.

Figure 28 shows an example of an f_oF_2 prediction map available to the EA operator. In the figure the dots display the grid points and the numbers show the f_oF_2 values. Although these values are available for all the grid points, only a convenient number of values are displayed to avoid crowding in the display. The bold semicircle in the upper half of the figure is the equatorial boundary of the auroral oval, transmitted by the AWS to the OTH operations center. The double line (two colored lines on the screen allow the operator to determine the day and night sides) in the upper left hand corner shows the sunset terminator. The figure also shows the barrier settings as radial lines, joined by circular segments. For illuminating this barrier, the f_oF_2s at grid points midway between the radar and the barrier must be used, (fortunately the automated system handles all the operation). Three f_oF_2 maps are available to the operator for predictions up to 90 minutes ahead at intervals of 30 minutes. Similar maps are also available for the other ionospheric layer parameters (f_oE, f_oF_1, f_oF_2, h_mE, h_mF_1, h_mF_2, and MUF(3000)). The ionospheric parameters, in conjunction with operating frequency and ray trace technique[14,15], are used for generating the Coordinate Registration Tables. The CR tables are used to convert time delays of signals returned from the target(s) to geographic location in latitude and longitude of the targets.

One can also update the f_v-h^l tables by using the measurements available from aircraft flying under precision navigation. In effect, Precision Navigational (PNAV) instrumentation in an aircraft is equivalent to a known moving ground feature. Thus, knowing the range (location of the aircraft) and the time delay Δ^t between the transmitted and return signal from the aircraft with the antenna elevation and the operating frequency of the radar, provide the calibration at the f_v-h^l tables. PNAV aircraft provide ground coordinates with time to Oceanic Aircraft Control Centers (OACC) which are electronically reported in parallel to the AN/FPS-118 Operations Center.

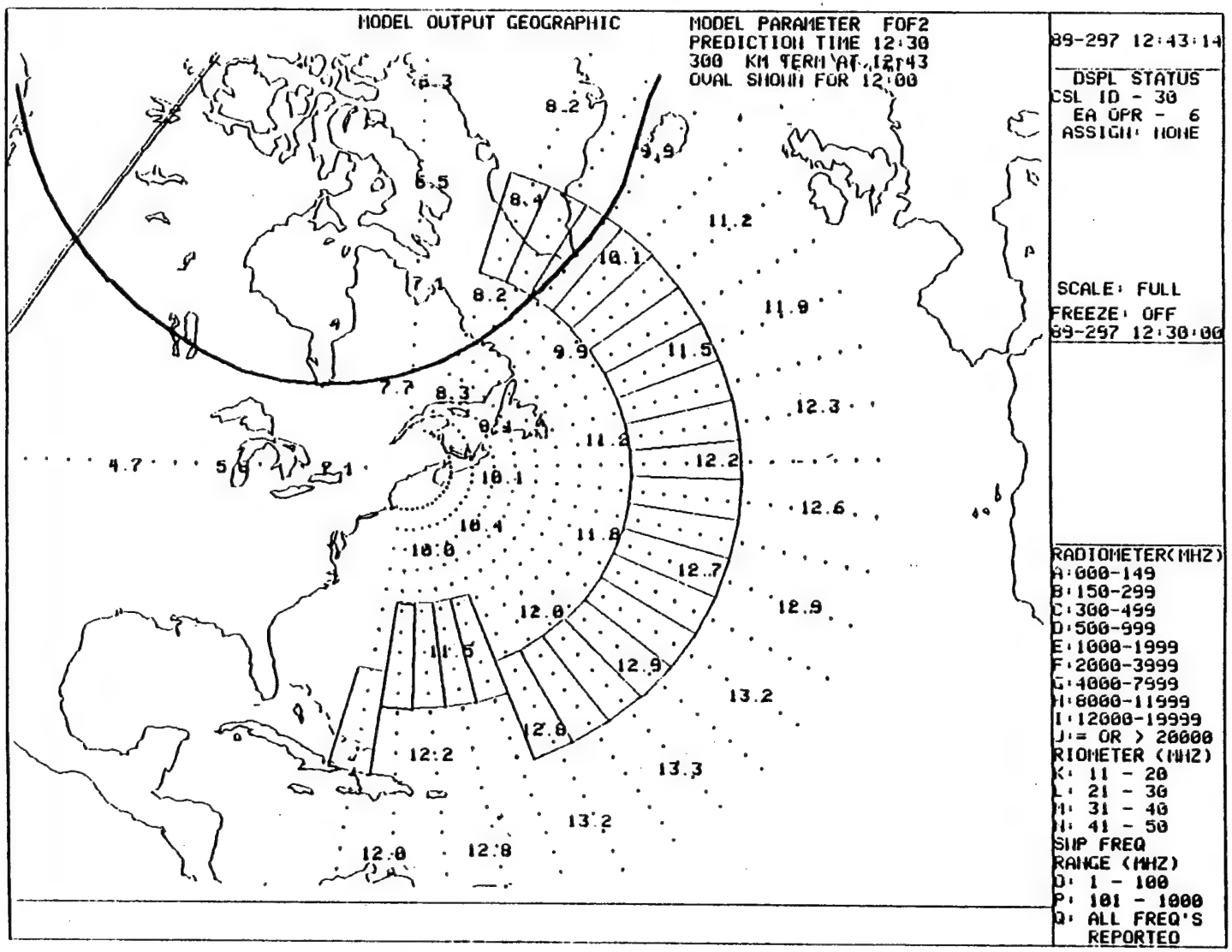

Figure 28. f_oF_2 map for the ECRS coverage area.

Table 2

VI Update Sites for

East Roast Radar System (ECRS)

Station No.	Station Name	Geographic Coordinates	
		Latitude (N)	Longitude (E)
0	Bangor, US	44.98°	291.18°
1	Thule, Greenland	76.50°	291.33°
2	Goose Bay, Canada	53.31°	299.52°
3	Croughton, England	52.00°	35.83°
4	Argentia, Canada	47.29°	306.03°
5	San Migual Island, Azores	37.50°	334.50°
6	Hamilton, Bermuda	32.33°	295.33°
7	Wallops Island, US	37.90°	284.50°
8	Patrick AFB, US	28.17°	279.33°

6 THE RADAR CONTROL FUNCTION

6.1 Frequency Selection

The principal task of the radar control function is to select an appropriate frequency to illuminate a selected area (range from the transmitter, and width), in a selected direction (azimuth) to identify and track targets (aircraft) in a barrier region. The use of vertical incidence and backscatter sounders in support of this function has already been discussed. An important external input to the radar is the AFGWC Space Environment message providing information of geophysical events that could affect the radar performance at present and in the immediate future. Another important external input is the flight plan and PNAV data from Oceanic Air Traffic Control.

A major portion of the radar operation involves monitoring the correct operation of a large number of equipment systems such as transmitters, receivers, antennas, and computer systems for control, data recording, status of display hardware, and real time analysis (automated) of some of these data. Operating the radar is really an engineering endeavor.

6.2 Tools and Procedures

The major control functions that are resident and integral parts of the radar system as a whole are overall radar control, scan sequence, backscatter and vertical incidence (VI) sounding, system performance assessment, equipment performance monitoring, coordinate registration, operation performance monitoring, Electronic Counter Measures and Electronic Counter-Counter Measures (ECM/ECCM), AFGWC space environment messages, display interface servicing, and System Maintenance and Console servicing. All these functions are inter-related in the sense that sequential iteration of these functions is a continuous cyclical process. Figure 29 is a flow diagram showing the inter-relation of these functions. Each of the major functions is divided into subfunctions. As an example, Figure 30 shows the flow of subfunctions of the radar control function, and Figure 31 shows the flow chart of the next level subfunction of clear channel selection. The lowest level of a subfunction process leads to calling for a keyboard entry from the Programmable Entry Panel (PEP) for a parameter selection, cursor entry on the screen, or from a display of a parameter on a screen.

Figure 32 shows an example of PEP for console assignment list display selection. It shows three PEPs. An operator selects an item (in this example TEXT DSPL) from the right PEP. This action changes the display in the middle PEP. With 24 keys on each of the 3 PEPs, and operator is provided a tremendous flexibility in controlling the radar functions and choices for calling various on-screen displays.

In controlling the radar, the operators can use displays on the screen, which can be either menus (text and tables with automatic and keyboard selection of control parameters), or graphical (color and black/white displays with options for selection of overlays and grids). Two sets of monitors (screens) with respective programmable entry panels allow displays and keyboard entries of parameters as shown in Figure 32. The PEP provides a very large number of options for the displays used to adjust the radar for successful performance. However, there can be ionospheric conditions that do not allow the radar to work in the desired fashion, no matter how the controls are adjusted.

Each console consists of a pair of monitors and PEPs. In addition each pair of consoles shares a hard copy printer, and a telephone hookup for voice communication. There are a large number of consoles provided so that operators and observers may conduct and monitor the operation in all segments.

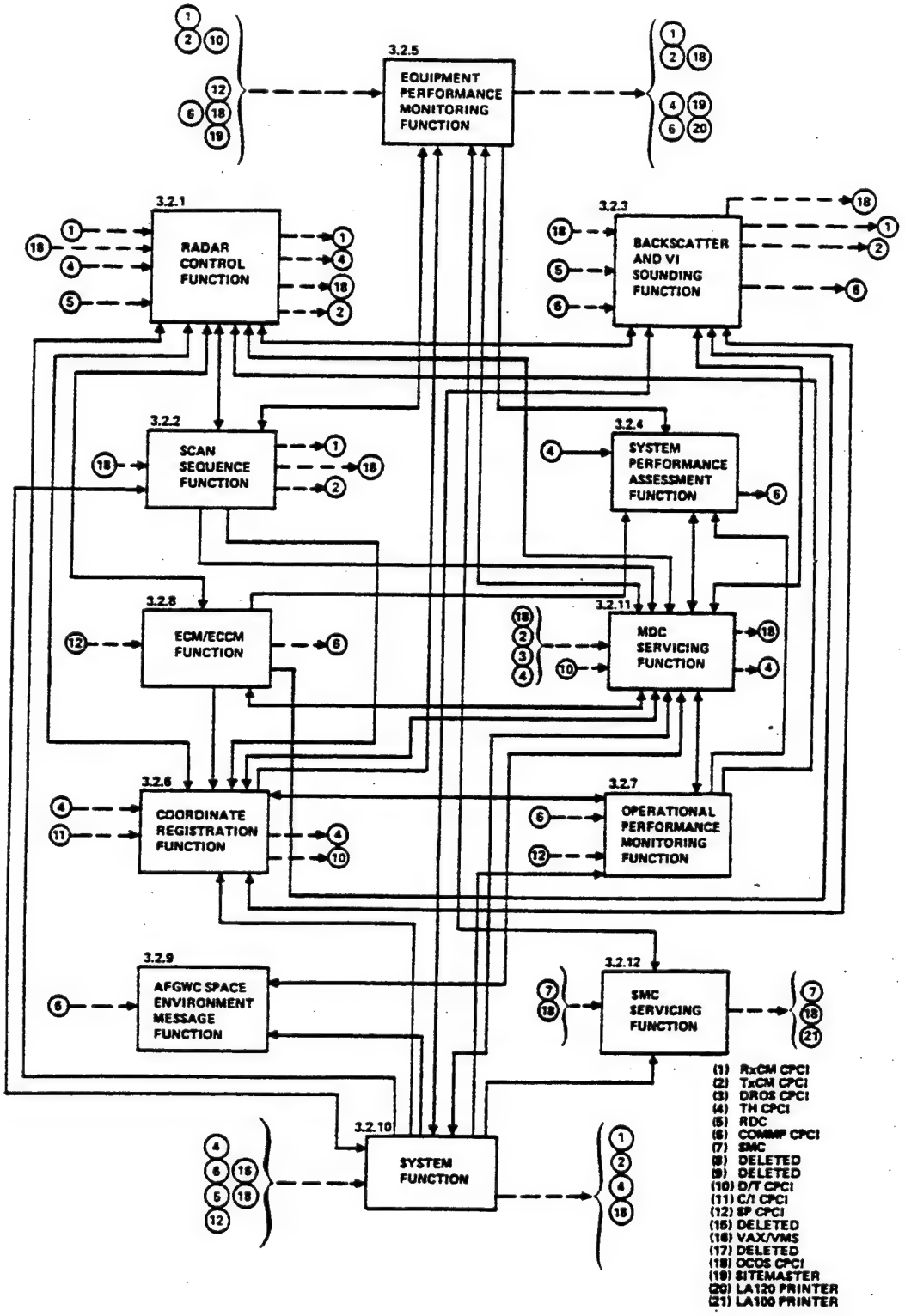

Figure 29. Radar Control, Status, and Environmental assessment Functional Flow Diagram.

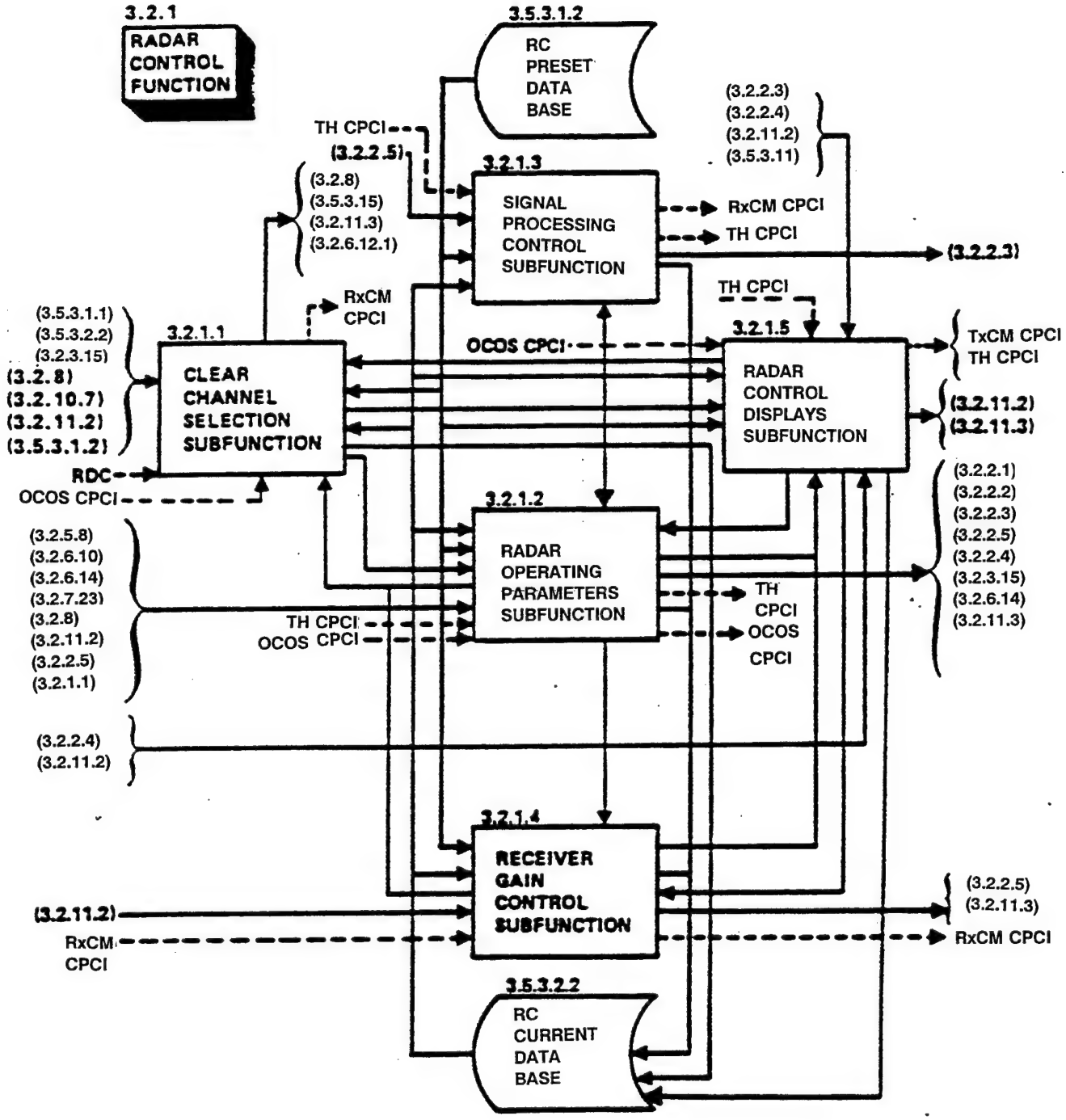

Figure 30. Radar Control Functional Flow Diagram.

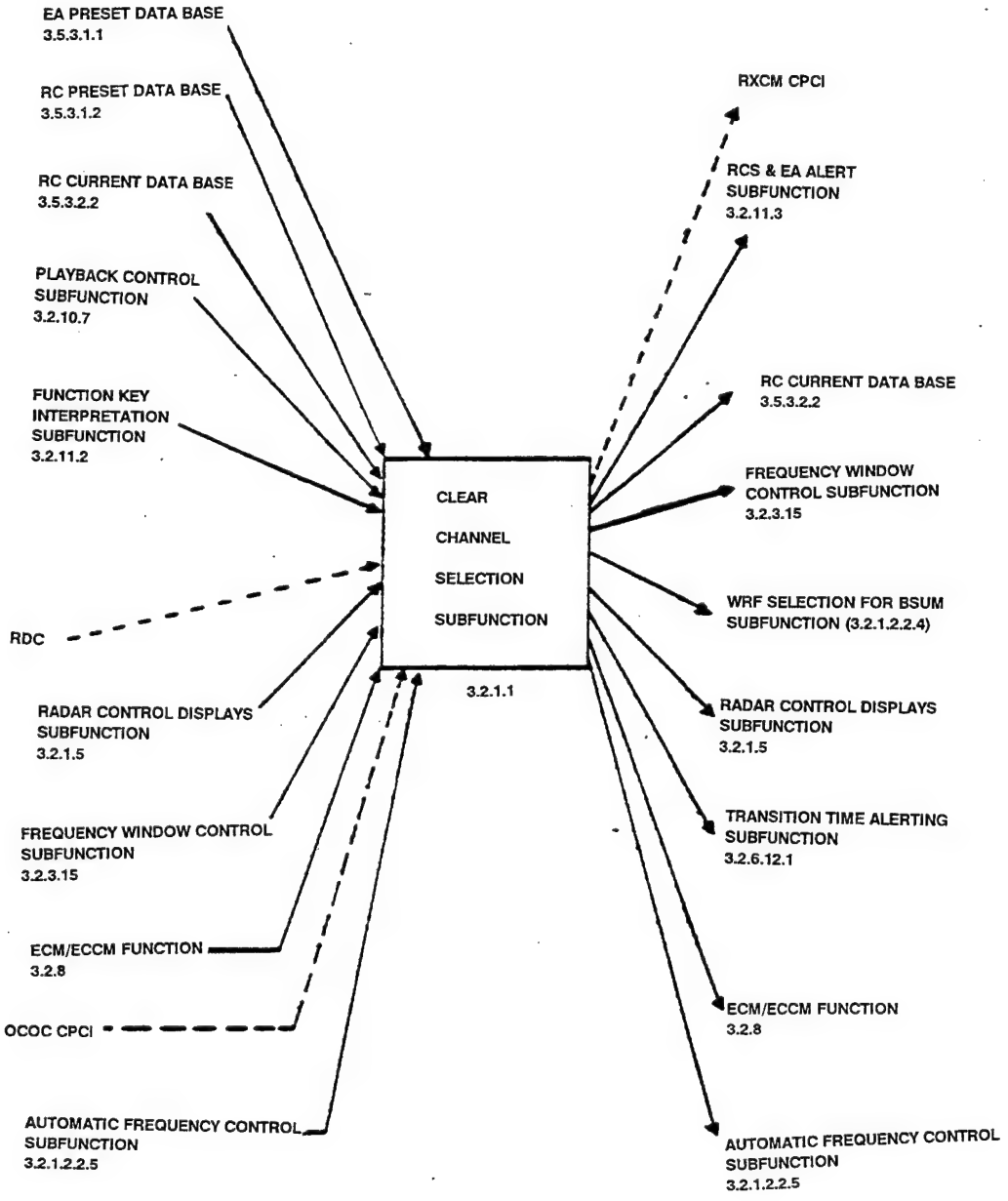

Figure 31. Clear Channel Selection Functional Flow Diagram.

CONSOLE ASSIGNMENT LIST DISPLAY SELECTION

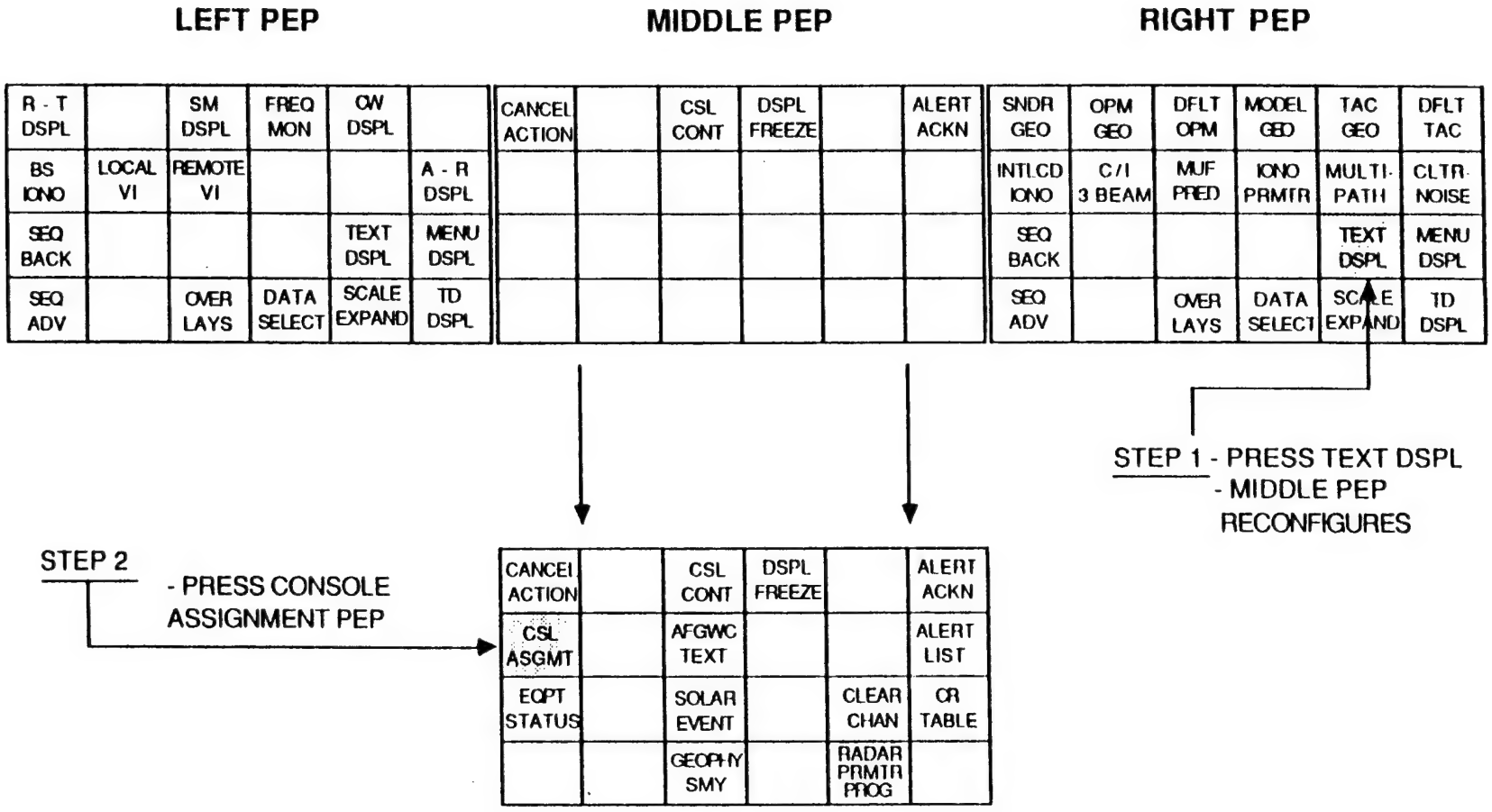

Figure 32. Console assignment List Display Selection.

The displays on the screen can be tables, for example those used for radar operation frequencies, shown in Figure 9, qualitative (gray scale) displays such as the backscatter sounder display in Figure 10, (darker areas indicate better reflection from that range), or a quantitative display of ground clutter, as seen in Figure 16. The radar operator's handbook provides detailed information on using various types of operation consoles. A good example of displays needing keyboard entry is the detection and tracking function, which is discussed in Section 7.

Each control procedure is a sequential set of actions. For example, selecting a radar operating frequency starts with operation of the Vertical Incidence (VI) sounder at the site and of a backscatter sounder for the selected segment-sector. From the backscatter sounder data, a suitable frequency and possible alternate frequencies are determined for illuminating the desired barrier region. Running the clear channel spectrum analysis (some frequencies may have been blocked for other users or some frequency band may be noisy, thus unusable at that time) further limits the frequencies found from the backscatter sounder observations. The process is repeated for every operating sector in all segments. The usable frequencies are entered in the table of operating frequencies. These tabulated frequencies are used for radar operation.

The procedure of updating the Coordinate Registration Tables starts automatically at fixed time intervals (can be manually superseded). The ionospheric model is run. It is updated with real time data available from the remote sites (see Table 2). The updated model is used for computing the elevation-virtual height-range table for the operating frequencies selected as the possible operating frequencies. This table is the basis of the C-R Table. The C-R Table is used in determining the ground location of the mobile target (aircraft).

7. DETECTION AND TRACKING (DT) FUNCTION

7.1 Overview

The principal tasks of the Detection and Tracking (DT) function are to initiate, maintain, and terminate tracks so that verified tracks can be passed to the Correlation -Identification (CI) function for further processing. A simplified block diagram of the DT function is shown in Figure 33. To accomplish this effectively, the function incorporates an automatic track initiation and maintenance algorithm that associates the range, Doppler offset, and beam location of

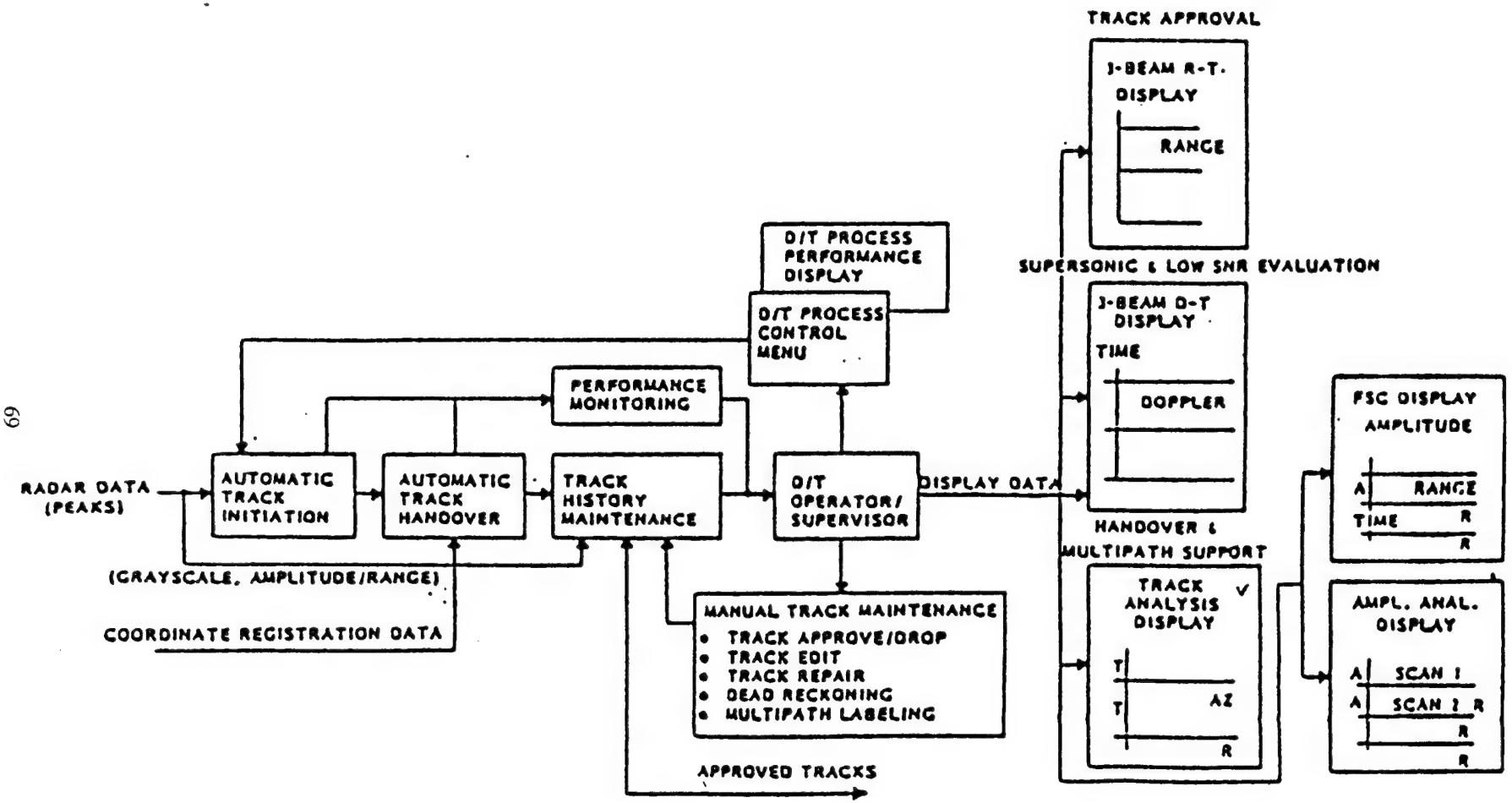

Figure 33. Simplified Block diagram of Detection and Tracking Function.

incoming (current) detections with progressive position for Approved, Established, Potential and New Tracks that are stored in the computer track files. The quality of every track is continually monitored and updated, and poor quality tracks are terminated. This feature reduces the operator load when many tracks with large variances in quality are caused by radar clutter.

Several other features are incorporated into the DT function. For example, tracks are automatically handed over across the sector boundaries, segment boundaries, and between barrier and interrogate beam boundaries. Also, data from a Blind Speed Unmasking Mode (BSUM) can be used to speed up track initiation. Instead of waiting for a target to move out of a radar blind speed, the Waveform Repetition Frequency (WRF) is changed and such targets are observed immediately.

A number of displays are included to aid the operator. It is easier to understand their appearance and usefulness by examining the partial display shown in Figure 34. It is called an Amplitude-Range-Doppler (ARD) or nested Doppler display. It presents the ranges of the contiguous range cells spaced by the range between periodic clutter peaks. The pattern shown around each of the periodic peaks is actually the Doppler distribution or spectrum (amplitude vs. Doppler frequency) of signals in that range bin, and not range. The central peak (clutter line) is the zero-Doppler ground clutter response, which is removed by the digital process. Incoming (positive) and outgoing (negative) target Doppler signals in that range bin appear to the right and left of the central peak respectively. The display is then the juxtaposition of the Doppler spectra for successive range bins and thus the appellation nested Doppler Display. The range resolution (spacing of the ground clutter lines) depends on the bandwidth of the transmitted signal with 5, 10, or 20 kHz typical, corresponding to 16, 8, or 4 nmi respectively. The Doppler resolution depends on the coherent integration time (CIT) with one to a few seconds typical, corresponding to resolution of one, to a fraction of a Hertz, respectively.

A target is manifested by additional peaks in several adjacent cells. It is the processing range sidelobes (Cook and Bernfield[16]) that result in a target's response spreading into range bins. A target response is apparent in the figure and shows the characteristic pattern of multiple peaks (seven in this example). The target location is taken as the range of the maximum amplitude of the curve that is fitted to the target peak distribution. The peaks in adjacent cells all have the

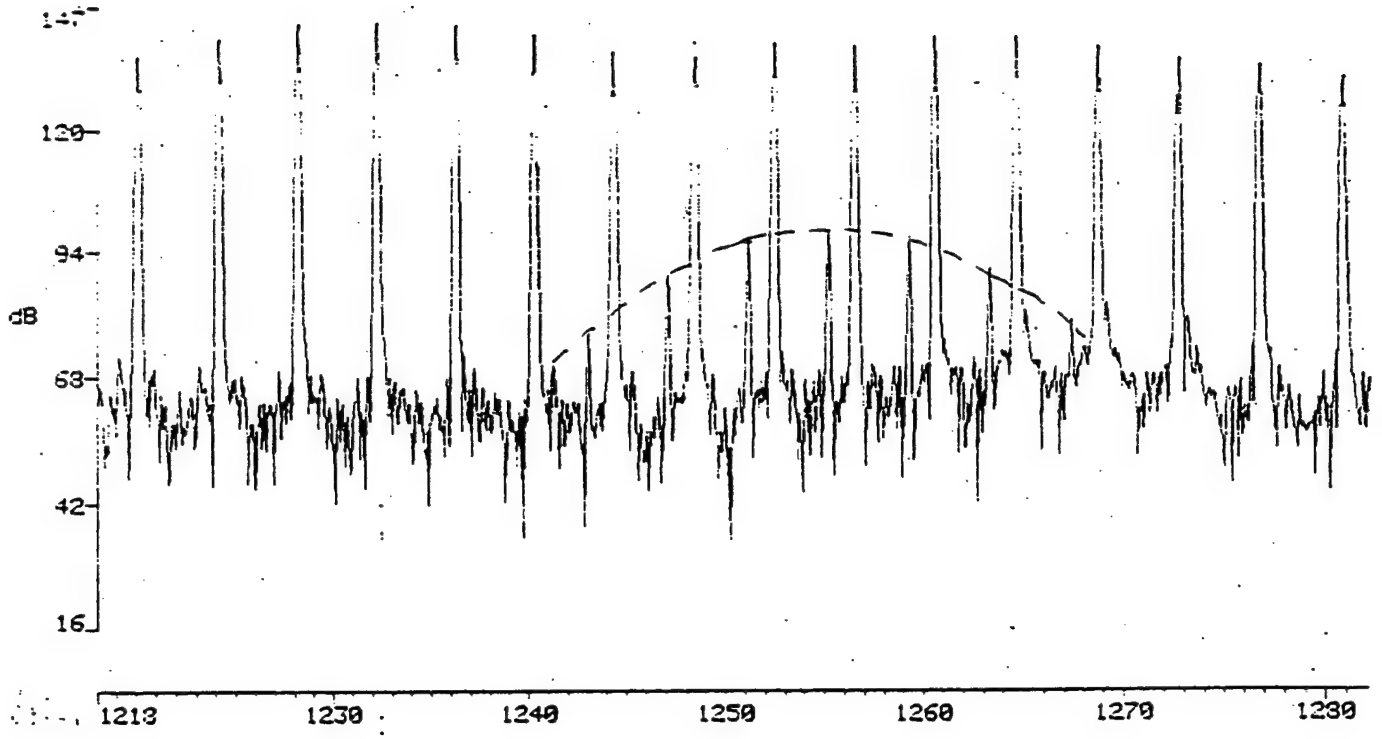

Figure 34. Example of a Single Amplitude-Range-Doppler Display.

same Doppler frequency, that is, the target peaks (for the same target) are all equally displaced from the zero-Doppler clutter line in that range bin. These are the main characteristics by which targets are recognized in the ARD displays. As time progresses, other factors remaining the same, the target pattern moves to the left (incoming target) or to the right (outgoing target) on the display. If the target has a cross range velocity component, it will eventually pass out of one beam and into another. But, as in the range dimension, the target appears simultaneously in adjacent beams because antenna receive beams are overlaid at -2.5dB gain. The amplitude of the response in a beam is proportional to the proximity of the target azimuth to that of the boresight of the beam. The actual target azimuth is estimated by interpolation between adjacent beams.

Another method of displaying the target data, even more useful than the ARD display, shows the range vs. time history of the target. Suppose the clutter lines of the display of Figure 34 are suppressed so that only the target responses remain. This modified signal (amplitude vs. range) is used to control the intensity (gray scale) of a single line of another display so that the greater the target amplitude, the darker the (Doppler-range) pixel corresponding to that target becomes. Data lines of earlier times are shown above the last line to be displayed. Already displaced data lines are scrolled upward one line for each new line inserted at the bottom of the screen. The filled display then is a mosaic that shows the range-time history of a target as a series of tell-tale dark pixel areas that make an easy-to-recognize target pattern. This display is called a Range-Time (RT) display and shows over an hour of target history.

An example of a Three-Beam-Range-Time display is shown in Figure 35. The basic display is constructed as described above, but now the data from three beams are shown, one for each of three adjacent beams in a sector beam. To make display more useful, a number of overlays or templates are available. One shows appropriately labeled tracks that have been initiated (and terminated) as solid lines. This is particularly useful in assessing duplicate tracks on the same target that exist in the overlap region of two beams and multiple tracks of the same target obtained through different radar propagation paths (modes or multipath). Multipath tracks have slight and opposite difference and signal-to-interference ratio as the chief manifestations of multipath propagation. Available to the DT operator is a function that predicts the range

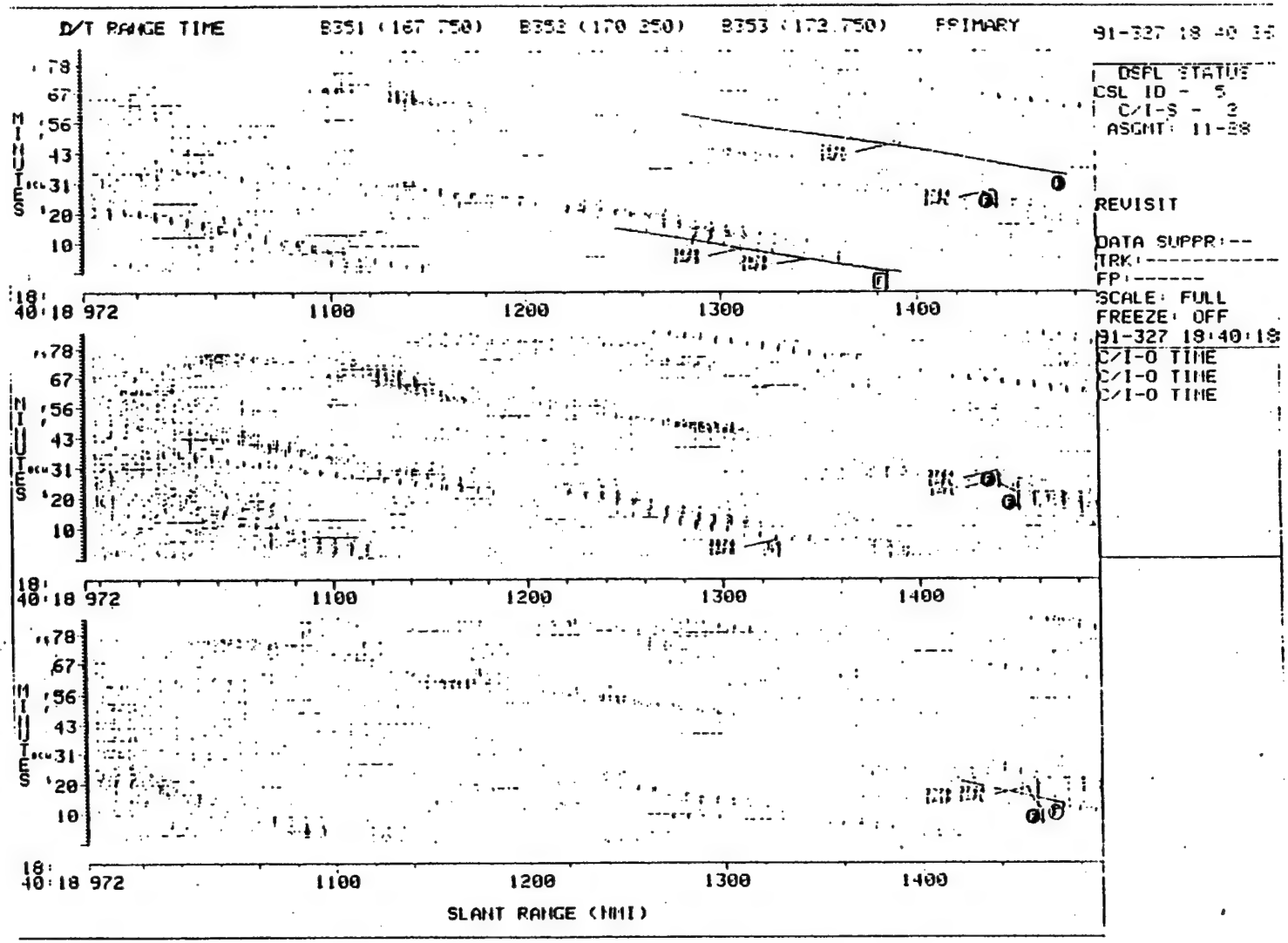

Figure 35. Example of a Three-Beam Range-time Display.

difference between the propagation modes that can be supported by the ionosphere at that time. This algorithm is a part of the coordinate registration (CR) subfunction of the Environmental Assessment (EA) function that was discussed in Section 5.

Another display, the Flight Size Check (FSC) display (not shown) is used to identify the presence of shadowing (closely spaced) targets. This display shows amplitude vs. range for normal and high Doppler resolution and range vs. time for reference. The high Doppler resolution (long CIT) can separate targets within the same range cell and thereby disclose the presence of additional targets that might otherwise be missed.

The Amplitude Analysis display consists of two windows and allows a one to one comparison between target response in the ARD and RT display formats respectively. A reproduction of such a display is shown in Figure 36. Three targets are evident in the (upper) ARD display. They are easily recognized by their characteristic multiple peak patterns explained earlier. The RT display shows the tell-tale multiple intensity pattern with the darkest pixels corresponding to the strongest responses. It is apparent that the targets identified as T_2 and T_3 would be most difficult and easiest to observe, respectively, on an RT display. Also, the track template can show which targets observed in the ARD display, have had tracks initiated. Low amplitude target signals can be missed by the tracker. In such cases, a track can be initiated manually by observing the tell-tale target pattern in the RT display. This display is also useful for identifying, for example, false tracks that are caused by external interference. These can be high quality signals that are accepted by the tracker and subsequently processed. However, their characteristic pattern (in the ARD display) is constant amplitude peaks in all range cells, unlike the target pattern that has peaks that are localized in a few contiguous cells and that fall off in amplitude from the central maximum due to 40 to 60dB range weighting applied.

Not shown is the track analysis display (TA) that provides the azimuth and range history of specific tracks. It is useful in resolving sector and segment ambiguities (duplicate tracks) and in sorting apparent multiple target responses (multiple tracks) that result from multipath phenomena when present.

The Three-Beam Doppler-Time (DT) display is very similar to the Three-Beam RT display. In the latter, the time independent coordinate was range, and Doppler was nested. For

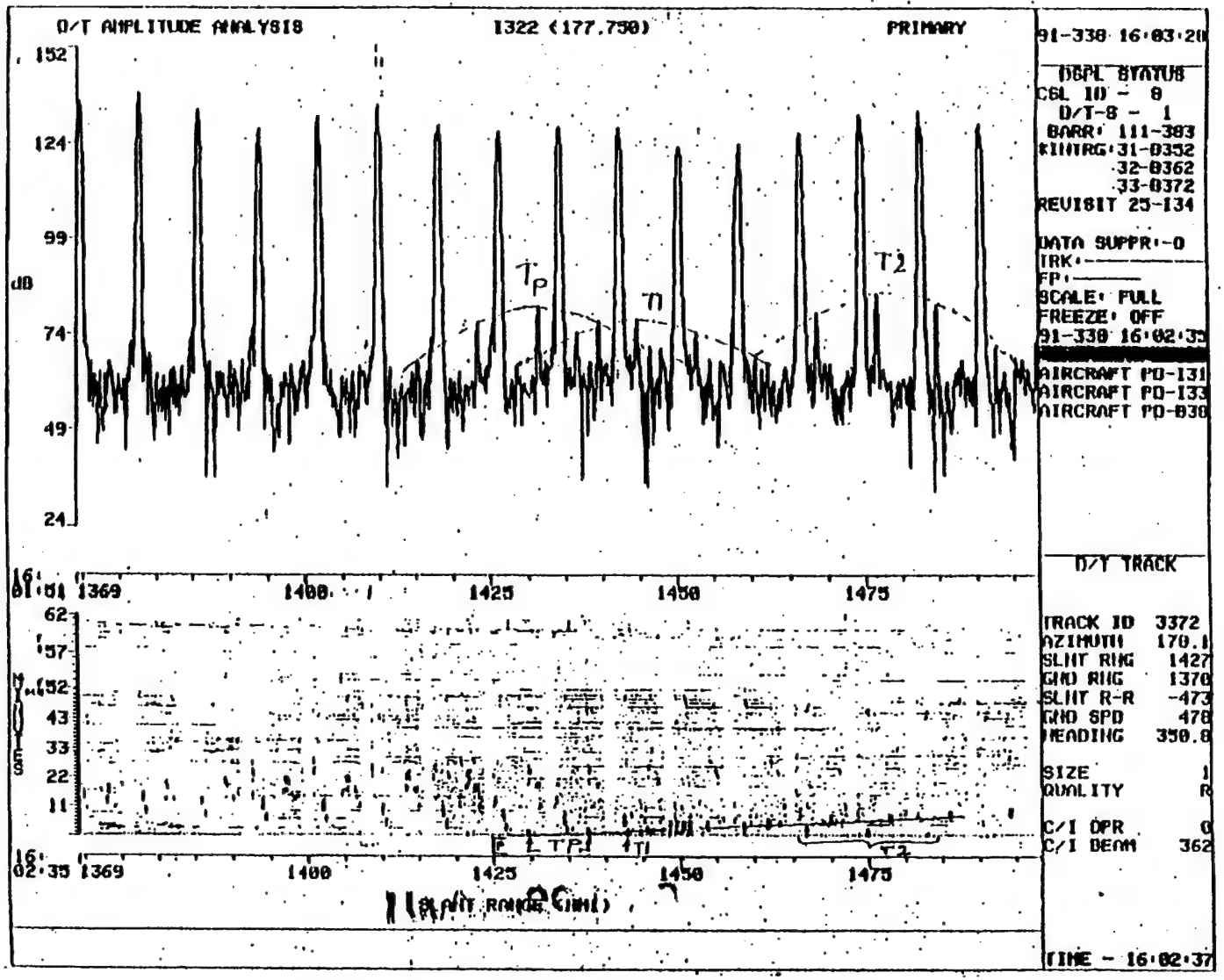

Figure 36. Example of an Amplitude analysis Display.

the DT display the independent variable is frequency, and range is nested. An example of the display is shown in Figure 37. It is built up line by line just like the RT display and is a mosaic with the darkest Doppler-Range pixels corresponding to the highest amplitude signals. Here again, tell-tale patterns may be evident that are useful in identifying specific tracks or in initiating tracks for low amplitude response targets missed by the tracker. For example, supersonic targets would display appropriately high Doppler frequencies for long periods and maneuvering targets would show marked but continuous variations in their Doppler frequency (range rate) as a function of time. Targets too low in amplitude to pass track initiation thresholds may still display a characteristic pixel pattern that could be used to initiate a track manually.

7.2 Signal Processor (SP)

It is instructive to have a clear picture of the signals that the DT system receives from the SP before proceeding with its description. It is in the SP that the received signal energy is sorted into range and Doppler cells on a beam by beam basis. A signal at this stage is represented by its amplitude and three indices that identify the range bin, Doppler cell, and beam (azimuth) with which it is associated. These signal sets are smoothed with a sliding window averaging algorithm that makes the signal values appear to be embedded in a constant noise background. The smoothing is applied across the range extent of each Doppler cell. Within the smoothing process, a number of the greatest amplitude signals may be selected to be removed from the data, the presumption being that they do not represent target signals because of their extremely large amplitude. Additional signals are suppressed that correspond to range-azimuth indices outside the range of interest or inside the selected inhibit zones. An example of the former are signals that originate outside the geographic boundaries of the designated barrier and interrogate sectors. In the latter case, inhibit zones are often set up to exclude areas in which targets are of little interest and their density so high as to compromise radar performance in the balance of the radar's coverage. Inhibit zones are often set up, for example, around busy airports. Signals with Doppler indices that correspond to power line harmonics are also suppressed because they are usually caused by interference from power lines and not target responses.

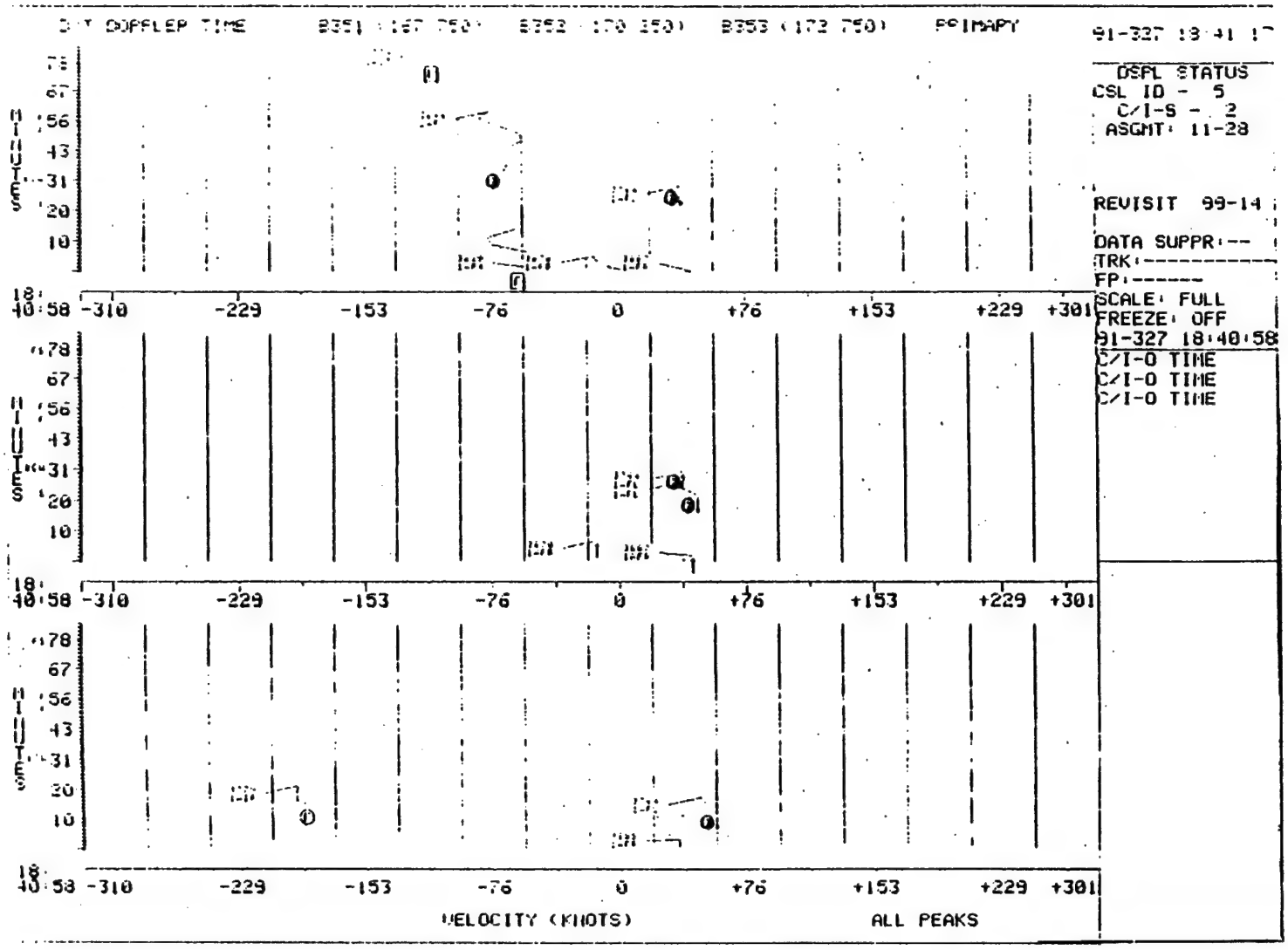

Figure 37. Example of a Three-Beam Doppler-Time Display.

This large set of signals (8192 per beam maximum, that is, 256 cells x 32 Doppler cells) is then analyzed to identify cells in which target-like (cell localized) signals reside. Up to 256 range-Doppler cells, in which the largest amplitude signals are found, are ranked in order of greatest to smallest amplitude.

The threshold for this selection is adaptively adjusted after each CIT to insure that the sample set comes from the entire range-Doppler extent of the input. These samples (256 maximum) for each beam now represent potential target detections that will ultimately be passed to the DT system.

First, however, the signal amplification in adjacent cells and beams are used in appropriate algorithms to establish fine estimates of range, Doppler offset, and azimuth. This is necessary because a target's response occupies several contiguous range and Doppler cells and adjacent receive antenna beams simultaneously. It is these detections with fine location estimates and amplitude ranking that are passed to the DT system over a Wide Band Communications Link.

7.3 Peak Association

The procedure in which the range- Doppler-beam position of a current detection peak is compared to the range-Doppler-position of a target extrapolated from previous detections is called association. The process by which tracks are formed is described in Section 7.4. For now, it suffices to say that a track is formed from a series of detections that establish the range, azimuth, heading, and speed of the target as a function of time. These past data are used to estimate the target's position at the time of current detection. If the target's current position (range, azimuth, range rate) is the same as the target's predicted position then the detection associates with the track and the track is updated to include this current data. To allow for measurement errors, track uncertainties, etc., the target's current and predicted coordinates are not required to be identical but to fall within certain bounds called association gates. The detections (current position) and tracks (predicted position) are tested for association in the range and Doppler dimensions separately so that there is a range association gate and a Doppler association gate.

Before testing for association, the detection peaks in a single beam are range (including the fine range adjustment) ordered. The association algorithm systematically searches for the longest range detection that falls within the maximum range association gate of the longest predicted target (track) range.

All detections (ranges) that fall within the range gate for that track are identified. Because the detections have been range ordered, the algorithm does not test any detections greater in range than the first to fall within the maximum range of the association gate. This offers a tremendous savings in the number of association tests that must be made. The detections that fall within the track range association are then tested in the Doppler dimension. The strongest detection that falls within the Doppler association gate is selected for association.

This process is repeated for the next shorter track range until all tracks in that beam have been tested with the detections for association. Then the detections and tracks in other beams are systematically tested.

The sizes of the range and Doppler association gates are adaptively varied in response to the variance observed in the measured range and Doppler coordinates. Namely, the higher the signal to noise ratio (SNR) of a track and less the variation there is between the coordinates of successive associating detections the smaller are the association gates.

7.4 Initiation, Maintenance, and Termination of Tracks

Several track types defined in Section 7.6 are used within the track initiation/maintenance process, each with an attached quality parameter that is used to upgrade or terminate the track. One type of track is an Established Track. It has an adequately high SNR and Cumulative Track Quality Factor (CTQF) and a sufficiently long history of successful associations. The next lower level of track is Potential Track. It represents a limited series of successful associations whose CTQF is not yet adequately high. When the proper track quality threshold is reached the Potential Tracks become Established Tracks. The most immature track is a New Track, which represents a single high amplitude detection that did not associate with any previous detection. All tracks that have been recently associated with detections are active tracks, and are classified as Current Tracks, and are stored in the Current Track File (CTF).

The relationship among track types and how the DT function operates to initiate, maintain, and terminate tracks is better understood with the simplified block diagram in Figure 38. Established Tracks (1) are smoothed tracks previously obtained from detections and stored in the CTF. The first step in the process is to update the range, Doppler, and beam position of the Established Track to the present time using the range-rate and heading for the track. Now the target's predicted position can be tested against its currently detected position as previously described. If the predicted track position and the current detection associate (2), then the SNR and the CTQF of the track are appropriately adjusted (3) and the current detection is used to update the track in the CTF. If the track (predicted target position, etc.) does not associate (4), the track quality is reduced (5) (its CTQF is decremented) and the track quality is retested(6). If its CTQF is above a threshold, the track is updated in a coast mode and stored in the CTF for the next association test. An Established Track can be maintained in the coast mode for 10 minutes. If decrementing the CTQF results in a track quality that is below a threshold, the track is dropped. That is, if a track is not periodically updated with current data, it is dropped after a coasting period. This is the feature that prevents the track files from being contaminated with old tracks.

Those detections that did not associate with Established tracks (7) are tested against Potential tracks (8) that have been updated to the present time. The SNR and CTQF of tracks that associate (9) with present detections are updated (10) and the track quality is tested (11). If the track quality exceeds the threshold, the Potential Tracks are further tested against New Tracks (12) that have also been updated to the present time. If the detection associates with a New Track (13), its SNR and CTQF are adjusted (14) and the New Track is upgraded to a Potential Track. This is the first step in the track initiation process. Some (N) of the highest amplitude detections that did not associate with New Tracks (15) are updated to New Tracks (16) and stored in the CTF for future association testing. The new tracks that did not associate and the remainder of the detections that did not associate are dropped.

This process is repeated every update or revisit time. Thus, only high quality tracks of sufficiently long duration are identified by the DT function as Established Tracks. The DT operator, after examining each Established Track to insure that it has target-like characteristics

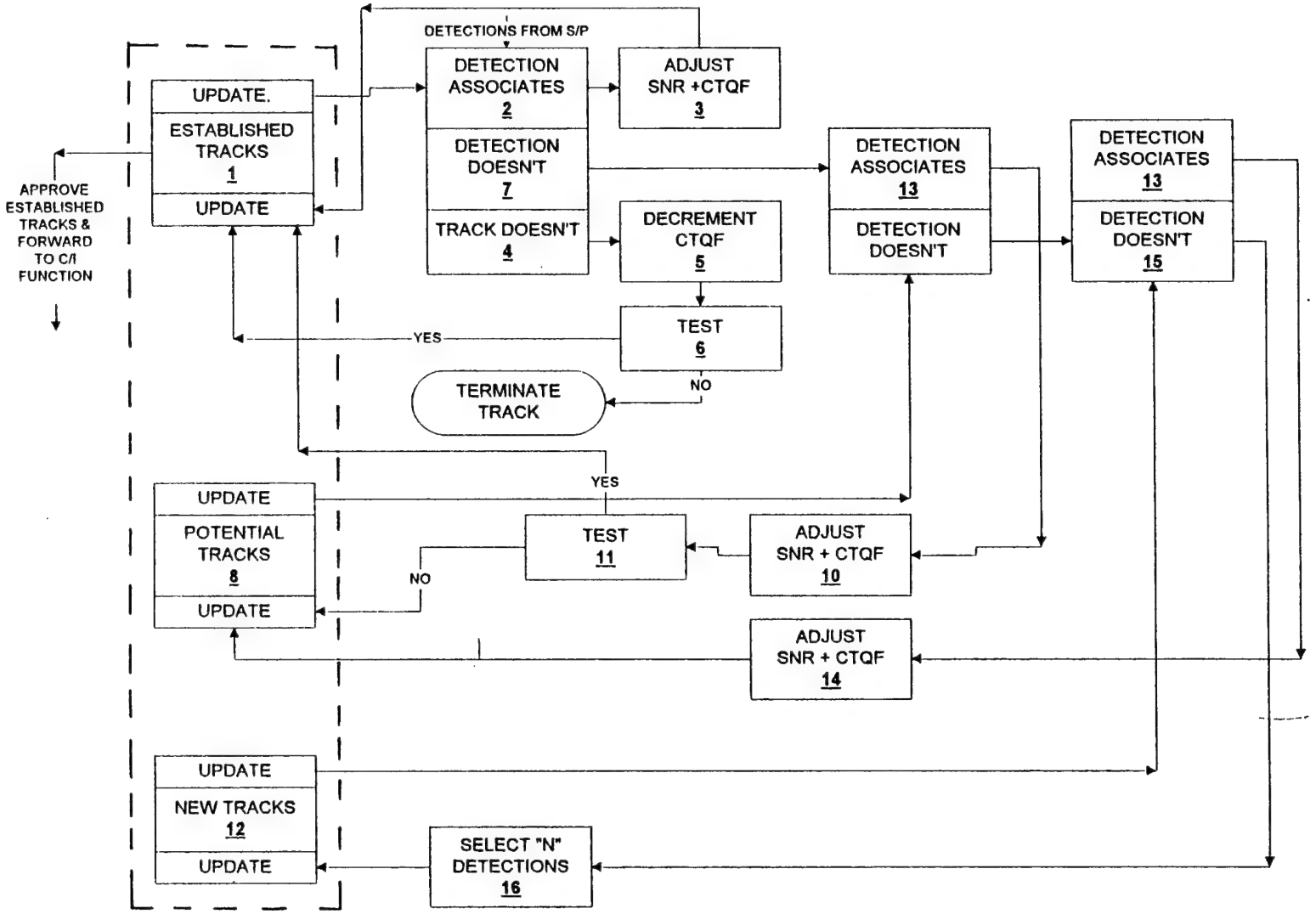

Figure 38. Simplified Block diagram of Procedure for Initiating, Maintaining and Terminating Tracks. The dashed block contains current track files.

(as contrasted to, for example, RF interference), approves the track and it is updated to an Approved Track. The track approval process is quick and direct. The RT display with the Track Overlay shows all current tracks. The DT operator simply places the cursor over the track to be approved, presses the track approve key followed by the Enter key and the Established Track is henceforth processed and labeled as an Approved Track. It is these Approved Tracks that are passed to the CI operator for further processing.

7.5 Other DT Functions

It is probably apparent by now that the radar's automatic tracker initiates tracks that are individually examined by the DT operator and approved as bona fide before they are passed to the Correlation/ Identification operator. In fact, a good way to think about the radar is that in all its operations it makes recommendations to the operators that must be evaluated and then accepted or rejected. For example, the radar may identify multiple tracks caused by multipath and the operator must examine these and ultimately approve or reject these. Algorithms and tabular track data displays help the operator with this assessment. He/she carries out many other track management tasks. Sometimes two or more sequential tracks are formed by the tracker that are in fact segments of the same track. In such cases the DT operator joins the segments together to form a single long track. The operator can also terminate, relabel, and reposition tracks that need action.

Sometimes, however, the radar makes no recommendations. For example if the target signal is too small, the automatic tracker thresholds are not passed and no tracks are established even though a target is present. In these cases the operator uses the RT, DT, and ARD displays to search for the low level characteristic target patterns described in Section 7.1. When one is found, the operator establishes a track manually that will then be processed along with automatically generated tracks.

7.6 Track Definitions

In the above we have referred to various track names. For convenience all these are summarized in the following.

Active Track: A track identifier is assigned to all tracks that fall within the region currently illuminated by the radar. These tracks are maintained in the Current Track File (CTF).

Approved Track: An Established Track that has been approved by the DT operator as representing an aircraft target. This status may also be assigned to a manually established track.

Dropped Track: A track that is cleared from the Current Track File, and the Track History System because it is false. Action can be initiated automatically or manually by the DT operator.

Duplicate Track: An Established or Approved Track that has been automatically generated as a duplicate of an existing track in regions where there is an overlap in coverage, for example, the overlap of two barrier beams or a barrier and interrogate beam.

Established track: An automatic DT status assigned to a Potential track entered into the Current Track File that exceeds the Track Establish Threshold.

Inactive track: A track status assigned to tracks that are not active as defined above. They are not maintained in the Current Track File.

Multiple Track: A track of the same target that has been established because of a different propagation path (multipath) to that target or due to simultaneous detection by tracking in adjacent beams.

New Track: An automatic DT status assigned to a candidate track entered into the Current Track File, based on a single DT peak with sufficiently high amplitude to exceed the Track Initiate Threshold.

Potential Track: An automatic DT status assigned to a candidate track entered into the Current Track File. It is based on two or more DT peaks that provide a CTQF below the Track Establish Threshold but above the Track Drop Threshold.

Terminated Track: A track status assigned to a track a) for which the CTQF falls below threshold, b)that exits the coverage area; c) that is manually terminated by the DT operator; or d)that is merged or combined with another track. These are not maintained in the Current Track File.

8. CORRELATION/IDENTIFICATION

The ultimate task of the radar is to detect and track targets that may present a threat to the Continental United States (CONUS). The difficulty is the separation of this subset of unfriendly threat targets from the large number of friendly targets continually present in the radar's tremendous coverage area. It is the Correlation-Identification (CI) function that performs this separation. The result of the process is a subset of potentially unfriendly and unidentified target tracks. After systematically examining these uncorrelated tracks (recommended by the CI function) to insure that they do not in fact correlate with known flight plans, the CI operator reports them to the Senior Director (SD) who is responsible for the overall operation of the radar. The SD assesses the uncorrelated tracks against such factors as heading, speed, threat profile etc. Those tracks that he identifies as potential threats are forwarded to the Regional Operations Control Center, Sector Operations Control Center, and North American Air Defense Command (NORAD) for further action.

The CI function does not 'identify' a target from its radar signature. Instead, it matches (correlates) Approved tracks with the flight paths of targets in the coverage area inferred from flight plans that are filed for all commercial aircraft and many military aircraft. The flight plans are obtained from the Air Traffic control Centers and Oceanic Control Centers and are updated periodically with pilot position reports. An approved Track that matches a flight path to within certain bounds is deemed correlated and is henceforth identified with that flight plan. Approved tracks that do not correlate form the subset of unfriendly targets that must be reported.

A simplified diagram of the CI function is shown Figure 39. Flight plans for the flights in the coverage area are identified with a Flight Plan Number and entered into the system. These estimated times and positions (latitude-longitude) of each flight plan are adjusted from predictions based on the Flight Plan Data and periodic pilot reports. The Flight Plans are stored in the Track History files and are converted to the more convenient radar centered ground-range azimuth coordinates before testing their correlation with the Approved Tracks. The Approved Tracks are also stored in the Track History files and must similarly be converted before comparison. In this case, the conversion is from the measured slant range-azimuth coordinates to radar centered ground-range azimuth coordinates. The conversion is based on the data stored in

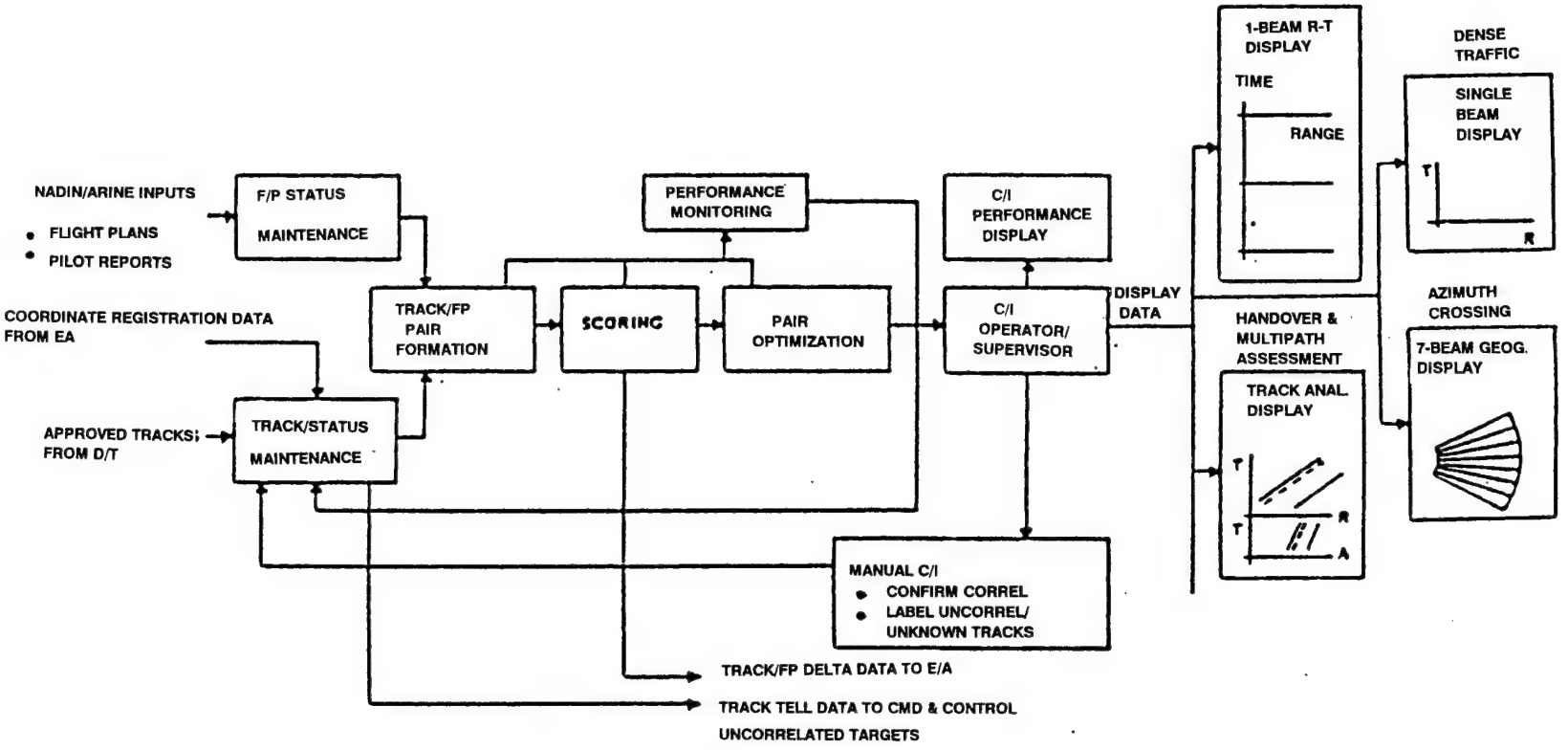

Figure 39. Simplified Block Diagram of the Correlation and Identification Function.

the Coordinate Registration (CR) Tables determined by the Environmental Assessment(EA) System. Essentially, the Coordinate Registration corrects the longer measured actual ray path from the radar up to the refracting layer and down to the target to the shorter range great circle path.

The time synchronized Flight Plans and Approved Tracks are now compared in the Track-Flight Plan Assignment function. This function assigns, on a one-to-one basis, candidate Track-Flight Plan pairs based on their relative closeness in range, direction, azimuth, and range rate. A score is calculated for each possible pair.

Pairs that score sufficiently low (close) are automatically identified by the CI function as correlated. The remaining Approved Tracks and Flight Plans pairings that are sufficiently close are optimized by an efficient algorithm that finally selects the set of pairings, among all possible sets, that yield the lowest overall score. All pairs in this optimal set are also automatically declared correlated by the CI function. Tracks for which no suitably close Flight Plans are found are labeled uncorrelated. The status of all tracks in the Track History files is updated to reflect their current status. This entire process is repeated every 90 seconds. Of course, the CI operator must still confirm the CI function's 'recommendation' of correlated and uncorrelated tracks.

Correlated Track confirmation is accomplished with the CI operator's three beam RT display shown in Figure 40. It shows Approved Tracks and Flight Plans (labeled with their appropriate CI function status) superimposed on the same display. Correlated Track/Flight Plan pairs are confirmed by the CI operator as were the Established Tracks approved by the DT operator.

The CI operator's most important job, however, is not the approval of Correlated Track-Flight Plan pairs, but the assessment of Uncorrelated Tracks so they can, if appropriate, be reported to the Senior Director for further evaluation. The investigation of the Uncorrelated Tracks shown on his three-beam RT display requires the CI operator to work closely with the other radar operators. Among his actions might be consulting with the Flight Plan operator to insure that all Uncorrelated Flight Plans near the track are correct and that Pilot Position Reports have been properly entered into the Track History files. Another reason that a Track and Flight

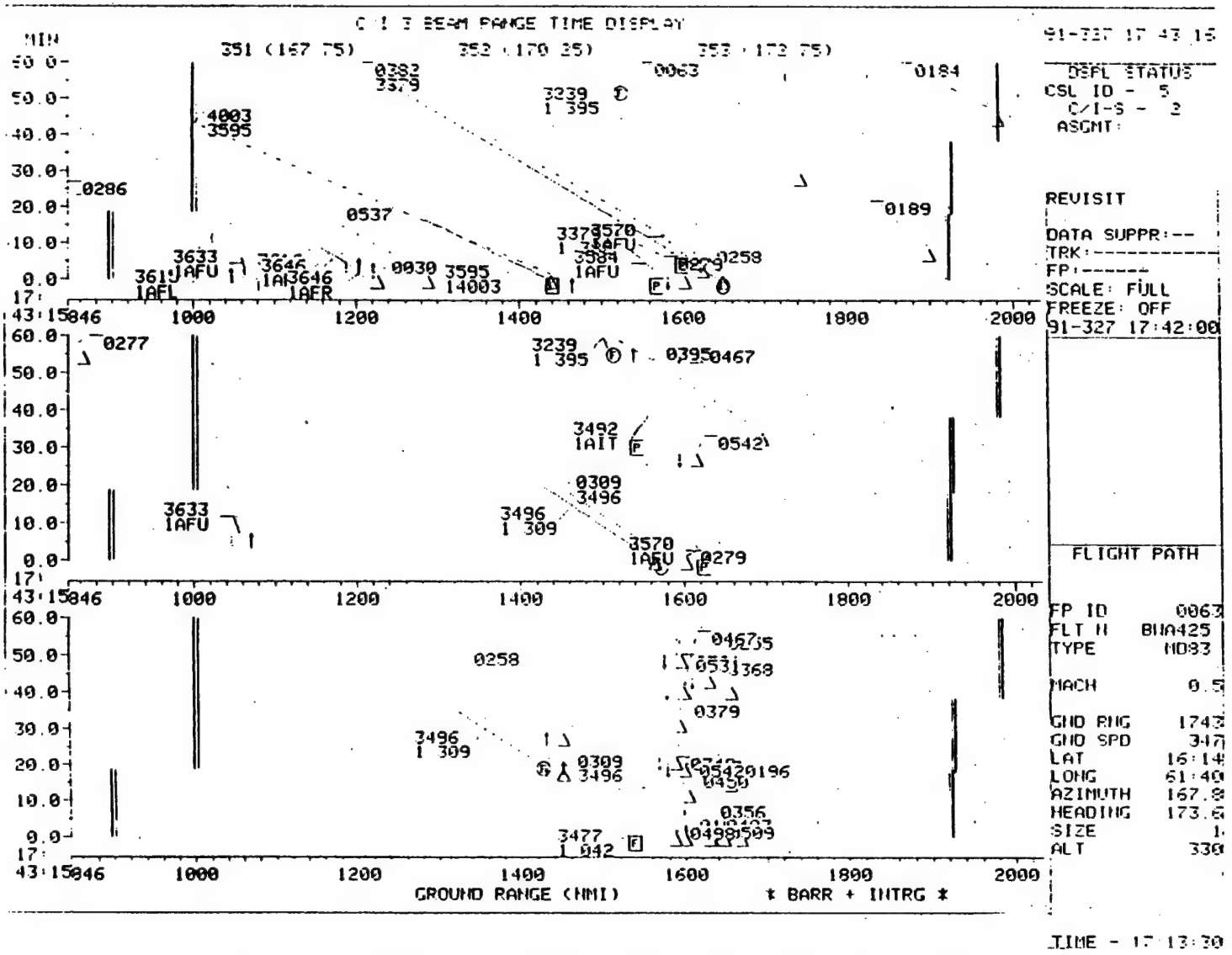

Figure 40. Example of CI Operator's Three-Beam Range-Time Display.

Plan might fail to correlate is an improper Coordinate Registration transformation that would cause a systematic displacement of the track. To preclude this possibility the CI operator would check with EA operator to confirm that the CR tables are still valid.

The Track Analysis Display (not shown) is used to resolve sector boundary handovers. The display shows a single beam RT display in one window and an azimuth-Time display in the other. The power of this display is that it is transparent to beam boundaries so that duplicate (uncorrelated) tracks are easily observed. Uncorrelated multiple tracks caused by multipath are also disclosed by this display. A related display, the single beam RT display in Figure 41, gives an expanded view of Tracks and Flight Plans that is useful in high density areas. Finally, a seven-beam geographic display (not shown) is used to resolve duplicate track problems at boundary crossings.

During the investigation of uncorrelated tracks it may become apparent, for example, that the track is actually correlated with a correct flight plan or that the track is a Duplicate or Multiple track. After this process, tracks that remain uncorrelated are forwarded to the Senior Director for further evaluation.

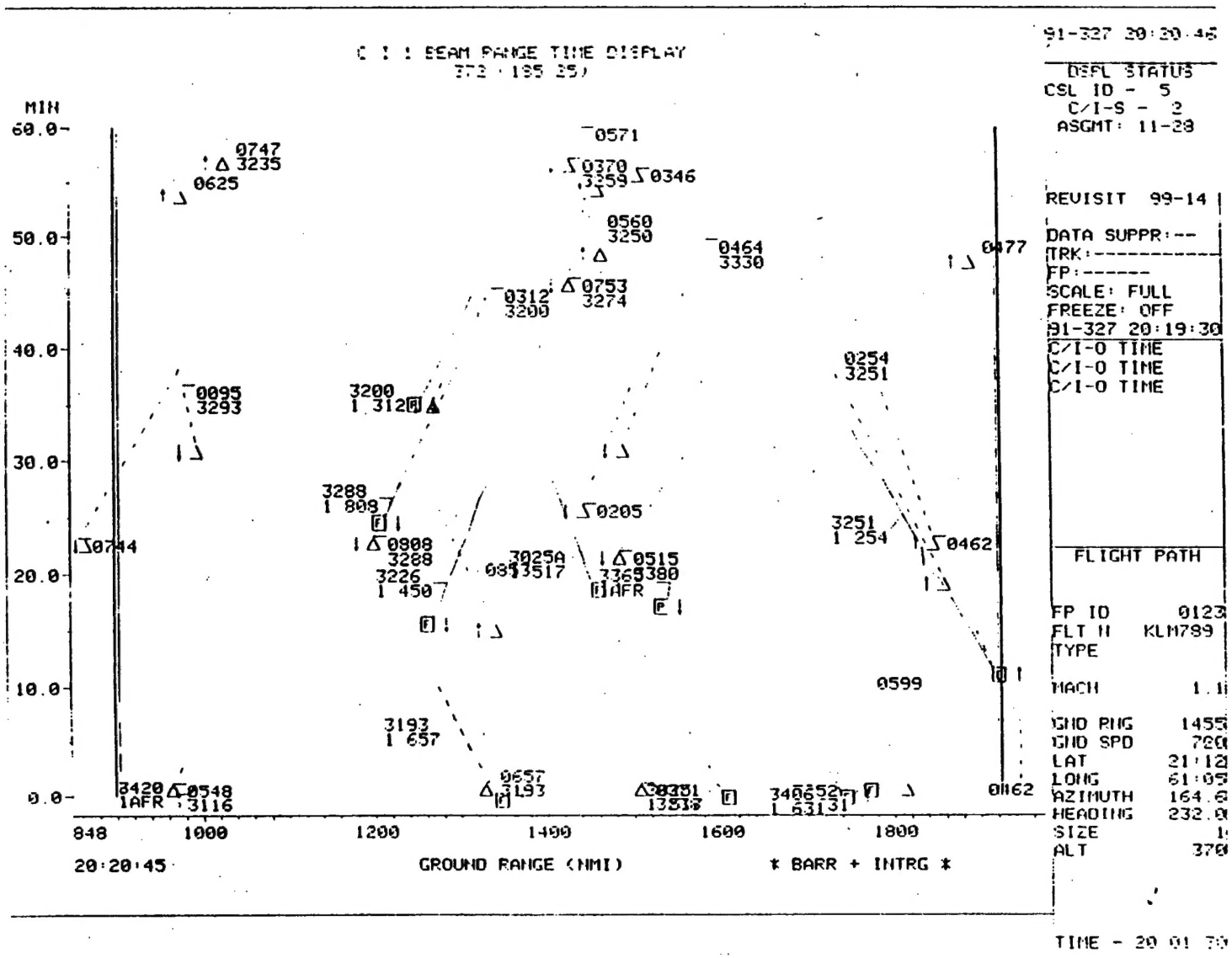

Figure 41. Example of CI operator's Single-Beam Range-time Display.

References

1. Millman, G. H., Bowser, C. A., and Swanson, R. W. (1988) An Ionospheric Model for HF Sky Wave Backscatter Radar, pp 43-1 to 43-15, *AGARD Conference Proceedings No.441, NATO-AGARD Symposium on 'Ionospheric Structure and Variability on a Global Scale and Interactions with Atmosphere, Magnetosphere'*, Munich, Federal Republic of Germany, May 16-20,1988.

2. Reinisch, B. W., Gamache, R. R., Tang, J. S., and Kitrosser, D. F. (1983) *Automatic Real Time Ionogram Scaler With True Height Analysis - ARTIST*, AFGL-TR-83-0209, AD A135174.

3. Jones R. M. and Stephenson J. J. (1975) *A Versatile Three-Dimensional Ray Tracing Computer Program for Radio Waves in the Ionosphere*, OT Report 75-76, US Department of Commerce, Office of Telecommunications.

4. Dandekar, B. S. and Buchau, J. (1986) *Improving f_0F_2 Prediction for the Sunrise Transition Period*, AFGL-TR-86-0028, 1986, ADA170457.

5. Air Force Global Weather Central (1982) *AFGWC Polar Ionospheric Model*, Air Force Global Weather Central, Program Listing.

6. Barghausen, A. F., Finney, J. W., Proctor, L. W. and Schultz, L. D. (1969) *Predicting Long-term Operational Parameters of High Frequency Sky Wave Telecommunication Systems*, ESSA Technical Report ERL 110-ITS-78, Washington, DC.

7. Lloyd, J. L., Haydon, G. W., Lucas, D. L., and Teters, L. R. (1978) *Estimating the Performance of Telecommunication Systems Using the Ionospheric Transmission Channel*, National Telecommunications and Information Administration, Boulder, Colorado.

8. Rush, C. M. and Gibbs, J. (1973) *Predicting the Day-to-Day Variability of the Midlatitude Ionosphere for Application to HF Propagation Predictions*, AFCRL-TR-73-0335, AD764711.

9. Wagner R. A. (1972) *Modeling the Auroral E-layer,* in Arctic Ionospheric Modeling - Five related Papers by Gassman G. E., Buchau J., Wagner R. A., Pike C. A., and Hurwitz M. G,; Air Force Surveys in Geophysics No.241, 1972, AFCRL-72-0305, AD748796.

10. Miller, D. C. and Gibbs, J. (1982) *Ionospheric Modeling and Propagation Analysis*, Final Technical Report RADC-TR-80-29, April 1980, Rome Air Development Center, Air Force Systems Command, Griffiss Air Force Base, New York, 13446.

Preceding Page Blank

11. Dandekar, B. S. (1982) *The Statistical relations Among Q, Kp and the Global Weather Central K-indices*, Environmental Research Papers, No 763, AFGL-TR-82-0010,ADA118734.

12. Dandekar, B. S. (1993) *Determination of the Auroral Oval Q Index from the Air Weather Service K Index*, PL-TR-93-2267, Environmental Research Papers, No. 1136, ADA282764.

13. Dandekar, B. S. (1994) *Assessment of the AN/FPS -118 Ionospheric model and Proposed Improvements,* PL-TR-94-2084, Environmental Research Papers, No. 1148, ADA289439.

14. Croft, T. A., and Hoogasian H. (1968) Exact Ray Calculations in a quasi-parabolic Ionosphere, *Radio Science* **3**:69.

15. Hill, J. R. (1979) Exact ray paths in a multisegment quasi-parabolic ionosphere, *Radio Science*, **14**:855.

16. Cook, C. E., and Bernfield ,M. (1967) "*Radar Signals*", Electrical Science Series, Academic Press.

Bibliography

Sales, G. S. (1992) *High Frequency (HF) Radiowave Propagation*, PL-TR-92-2123, (OTH Handbook Chapter 4), ADA261726.

Sales, G. S. (1992) *OTH-B Radar System: System Summary*, PL-TR-92-2134, (OTH Handbook Chapter 2), ADA261727.

Dandekar, B. S. and Buchau, J. (1995) Editors, *Glossary for Over-the- Horizon Backscatter Radars*, PL-TR-95-2127, (OTH Handbook, Chapter 6).

Dandekar, B. S., Buchau, J., Whalen, J. F., and Fougere, P. (1995) *Physics of the Ionosphere for OTH Operation*, PL-TR-95-2149, (OTH Handbook, Chapter 3).